Book of Abstracts

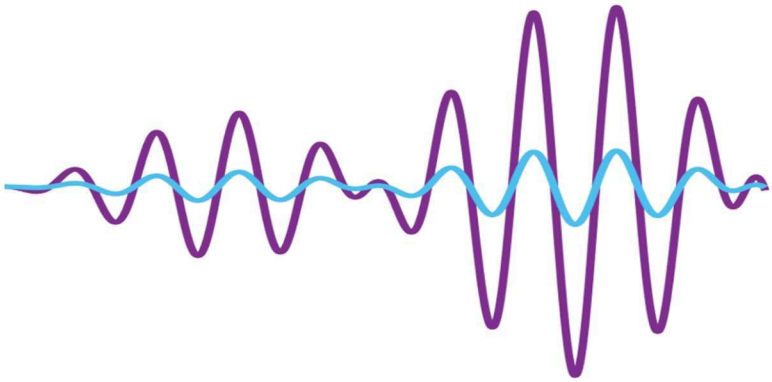

RFI 2024

14-18 October 2024

Bariloche, Argentina

RFI 2024

Index

RFI 2024: Purpose and Vision

Radio spectrum sharing has become challenging due to the ever-growing demand for spectrum access by a wide range of emerging radio services. This in turn leads to an increased risk of Radio Frequency Interference (RFI) between spectrum users. This is particularly true for passive scientific services such as radio astronomy, Earth remote sensing, or meteorology, where sensitive measurements must be carried out in frequency bands defined by the laws of nature.

Protecting the scarce radio spectrum resources for science, while accommodating the needs of other spectrum users, can only be achieved in a joint efort. RFI 2024 ofered the venue to promote interaction, exchange of ideas, and cooperation between researchers, engineers, and users from all radio science disciplines dealing with RFI, uniting them under the common goal of working on solutions to minimize the impact of interference. RFI 2024 was the seventh in a series of workshops focusing on this topic, the first of which took place in Bonn, Germany, in 2001.

After the consistent organization of several workshop editions, focused on scientific services, and growth of the participation, the Scientific Organizing Committee (SOC) of RFI 2024 aimed for expanding the event in the form of a conference and for broadening the scope, stimulating the participation of satellite communication services operators bearing in mind the collaborative spirit required in addressing spectrum management challenges.

PoS(RFI2024)070

RFI 2024: Scientific Organizing Committee

The SOC was established with the view to promote flexibility, agility and gender balance in organizing the conference, while ensuring the solid competence in the areas addressed by the conference, particularly radio astronomy, meteorology, remote sensing and spectrum management. The team is presented below.

Balthasar Indermuehle	General Chair Travel Grants Chair
Willem Baan	Special Advisor
Stephen English	Meteorology Sponsorship Chair
Kirsty McBeath	Meteorology Communication Chair
Alexandra Bringer	Remote Sensing Financial Chair
Flávio Jorge	Remote Sensing Publication Chair
Greg Hellbourg	Radio Astronomy Registration Chair
Haiyan Zhang	Radio Astronomy
Federico Di Vruno	Spectrum Management LOC co-Chair
Ashley Vanderley	Spectrum Management
Paolo de Matthaeis	Remote Sensing
Federico Renolfi	Meteorology LOC Chair

RFI 2024: Venue and Local Organizing Committee

The SOC aimed at promoting geographic distribution of the venue bearing in mind stimulating the scientific communities in parts of the world other than Europe.

The Local Organizing Committee (LOC) has been INVAP in Bariloche, Argentina.

INVAP is known worldwide as a leading company in technological projects actively supporting Argentine development. With more than 40 years of experience, INVAP develops high-end technological systems in the areas of Nuclear; Space; Defense, Security & Environment; and Medical Systems.

RFI 2024: Sponsorship

The RFI 2024 would not be possible without the important support of our sponsors, which we highlight below.

PoS(RFI2024)070

RFI 2024: Publication

The RFI 2024 SOC acknowledged the fact that scientific publications on spectrum management may struggle to find appropriate scientific media of high impact factor. To address that challenge, in addition to organizing the conference proceedings with Proceedings of Science (PoS), the SOC teamed up with the American Geophysical Union (AGU) Radio Science journal to ofer a special collection on RFI 2024 conference.

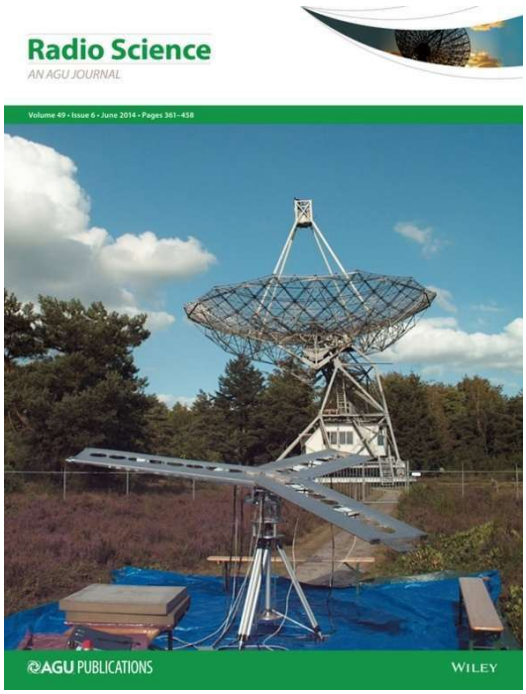

RFI 2024: Abstracts

The RFI 2024 would have not been possible without the active engagement of the targeted scientific communities. Acknowledging the authors making of RFI 2024 a big success, we list the abstracts submitted to the conference in the following pages.

PoS(RFI2024)070

PoS(RFI2024)070

A Novel EMC control method for Actuators in QTT Project

Qi Liu* [(1)], Xiaoyu Dong[(1)], Minghui Cai[(1)], Xiaoming Su[(1)]
[(1)]Xinjiang Astronomical Observatory, Chinese Academy of Science, Urumqi, China, liuqi@xao.ac.cn

Qitai Radio Telescope (QTT), a 110-meter-aperture steerable radio telescope, which is proposed to be built in Qitai County of Xinjiang Uygur Autonomous Region of China. The planned observing frequencies for the QTT cover a wide range from 150 MHz to 115 GHz [1]. QTT will have to cope with many aspects of Radio Frequency Interference （RFI）, such as the actuators in multi-node adjustment system for the main reflector[2] as shown in Figure 1(a). However, as we know that the actuators underneath the panels have to meet very low levels of emissions. The interference level limit of the actuators can be calculated according to the paper [3] as shown in the Fig.1(b), we can see that the limit is about 20dB below the anechoic chamber background noise, moreover, it is hard to test the Shield Effectiveness (SE) of the actuators due to the size and high level of system integration. In the above analysis, it is a challenge to measure and verify the EMC performance of the actuators.

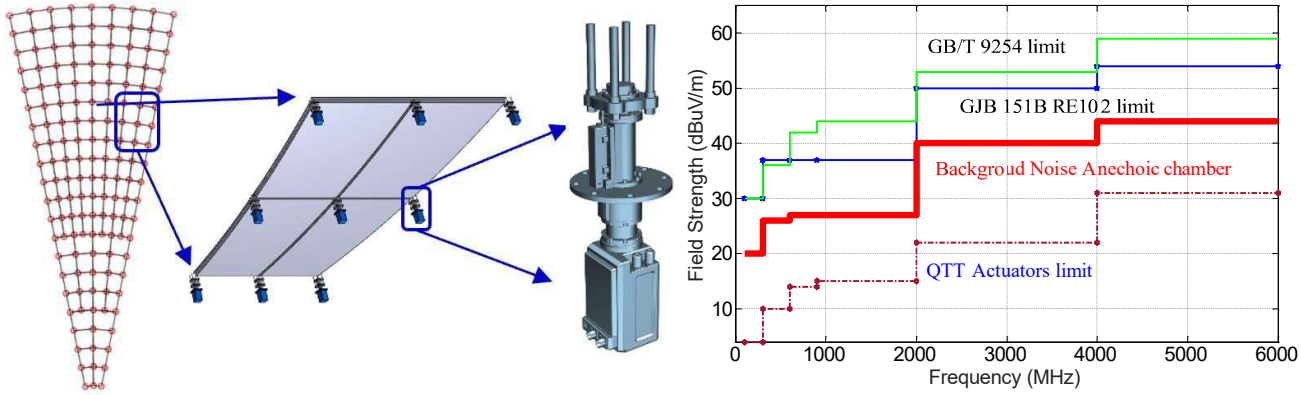

（a）Actuators distribution in the QTT project　　（b）The actuators interference level limit

Figure 1. Actuators distribution and its interference level limit

To solve the issue above, we proposed a novel SE testing method which can evaluate the EMC performance of the actuators effectively. Firstly, the SE requirement was calculated by comparing the radiated emission in unshielded status and the interference level limit of the actuators. In addition, we designed an interface board that all the devices and filters of the actuators can be installed on it, such as the motors, the control board, the power board, the cover, the filters, the waveguide connectors and the shielded gaskets. Furthermore, the interface board can be equipped on the testing windows of the shieled room, that we can measure the SE of the interface board according the measuring standard GB/T 12190[4]. Which means that we can verify the EMC performance by comparing the SE requirements and the SE testing results, and this method was employed in the actuators in the QTT project.

[1] Wang N, “Xinjiang Qitai 110 m radio telescope”, Sci Sin-Phys Mech Astron, 2014, 44: 783 − 794, doi: 10.1360/SSPMA2014-00039.

[2] Na Wang, Qian Xu, Jun Ma, et al., “The Qi tai Radio telescope”, SCIENCE CHINA Physics, Mechanics & Astronomy, 2023, 66(8): 289512, doi:10.1007/s11433-023-2131-1.

[3] Liu Q, Wang N, Liu Y, et al. “An EMC control method for large-diameter radio telescope”, Sci Sin-Phys Mech Astron, 2019, 49: 95−102, dio:10.1360/SSPMA2018-00412.

[4] GB/T 12190, “Method for measurement of the shielding effectiveness for electromagnetic shielding enclosures”, Beijing: China Standard Press, 2021.

Unveiling Human Footprints from Space: Correlating RFI Detected by SMOS with Geopolitical Events and Human Activities

Ekhi Uranga* [1], Álvaro Llorente [1], Judit González [1], and Antonio de la Fuente [2]
[1] ISDEFE, Madrid, Spain; e-mail: ekhi.uranga@ext.esa.int; alvaro.llorente@ext.esa.int; judit.gonzalez.gutierrez@ext.esa.int
[2] ESA-ESRIN, Frascati, Italy; e-mail: antonio.de.la.fuente@esa.int

1. Introduction

Spaceborne missions equipped with advanced sensors have revolutionized our ability to monitor and understand human activities on Earth. Among these missions, the Soil Moisture and Ocean Salinity (SMOS) satellite, initially designed for measuring Earth's soil moisture and ocean salinity for climate and meteorology aims, has unexpectedly unveiled a new feature: detection of L-band transmissions in the protected band of 1400-1472MHz in the form of radio frequency interference (RFI) [1]. Due to the high volume of RFI detected over its operational lifetime of 15 years, SMOS has become instrumental in discerning human activities across the globe. The satellite has detected more than 10,000 persistent RFI sources [2], forming the basis for the data analyzed in this paper. By analyzing RFI patterns, we can unveil the footprints of human presence and activities across different regions of the globe. This paper explores the correlation between RFI detected by SMOS and significant geopolitical events and human activities, ranging from internal conflicts to civil works and urbanization.

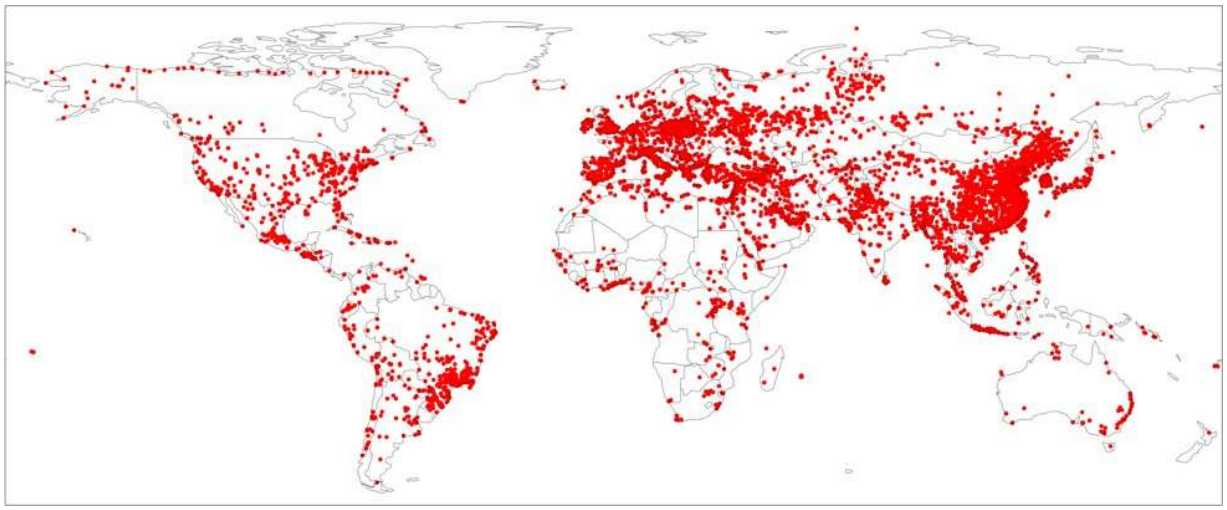

Figure 1: All the persistent [2] RFI sources detected by SMOS (land and coastal areas) from January 2010 to February 2024.

2. Military conflicts

SMOS data can capture anomalous RFI patterns associated with military activities, displacement, and infrastructure disruptions. Monitoring these patterns can provide insights into the dynamics of conflict zones and aid humanitarian efforts.

Also, the “hot borders”, characterized by geopolitical tensions and military activities, are prime areas for RFI detection. SMOS can detect unusual RFI patterns along these borders, reflecting movements of military equipment, surveillance activities, and border infrastructure development.

3. Civil Work

Civil works such as pipeline construction and offshore drilling leave distinctive RFI signatures that can be captured by SMOS. Monitoring RFI associated with projects like Nord Stream and oil platforms in various regions allows for assessing the progress of infrastructure development, environmental impacts, and economic activities.

4. Radars and Airports

Radars, essential for air traffic control and military surveillance, can emit RFI detectable by SMOS. By mapping radar installations and airports, SMOS data can aid in airspace management, aviation safety, and military reconnaissance. Furthermore, analyzing changes in RFI patterns around airports can reveal trends in air traffic volume and urban expansion.

5. Urban Areas

Urban areas exhibit intense RFI emissions due to the concentration of human activities and infrastructure. SMOS data can delineate urban extents, monitor urban growth, and assess the efficiency of urban planning policies. Analyzing RFI patterns in urban areas provides valuable insights into population density, economic activities, and environmental impacts.

Additionally, detailed analysis of the coordinates of all RFI detected by SMOS reveals that a significant percentage of them occur in dense urban areas. This observation highlights that while many interferences stem from militarized zones and active use of the radio frequency spectrum, a substantial portion is generated by the improper use of equipment initially not intended for generating interference. However, given the increasing use of wireless devices, interferences from these sources are becoming more representative. This phenomenon underscores the importance of implementing spectrum management policies and stricter regulations to mitigate interferences and ensure efficient use of the radio frequency spectrum in urban environments.

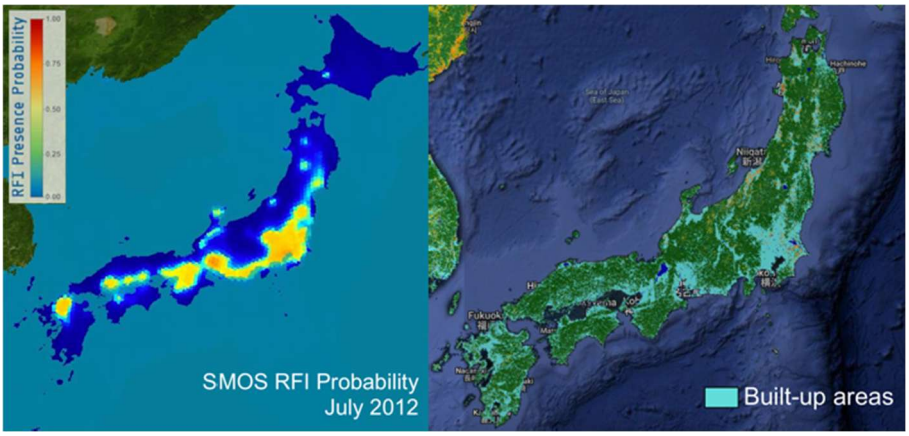

Figure 2: Comparison of the L-band RFI footprint generated by Intermediate Frequency of Satellite Home-TV Receivers [3], with urban areas in Japan [4].

6. Conclusions

The correlation between RFI detected by SMOS and various geopolitical events and human activities offers a unique perspective on understanding human footprints from space. By leveraging SMOS data, policymakers, researchers, and humanitarian organizations can gain valuable insights into conflict dynamics, infrastructure development, and urbanization trends, facilitating informed decision-making and fostering sustainable development efforts globally.

[1] Uranga, E.; Llorente, Á.; González, J.; de la Fuente, A.; Oliva, R.; Soldo, Y.; Jorge, F. SMOS ESA RFI Monitoring and Information Tool: Lessons Learned. Remote Sens. 2022, 14, 5387. https://doi.org/10.3390/rs14215387

[2] Ekhi Uranga, Judit González, Alvaro Llorente, Antonio de la Fuente, "Statistics of Interferent Sources In L-Band Observed by SMOS," RFI 2022 Workshop, ECMWF, Virtual, 14-18 February 2022.

[3] E. Uranga, Á. Llorente, Y. Soldo, F. Jorge, R. Oliva and A. de la Fuente, "SMOS RFI Experience in the 1400-1427Mhz Passive Band Due to Radiations at Intermediate Frequency of Satellite Home-TV Receivers," 2021 XXXIVth General Assembly and Scientific Symposium of the International Union of Radio Science (URSI GASS), Rome, Italy, 2021, pp. 1-3, doi: 10.23919/URSIGASS51995.2021.9560487.

[4] Potapov, P., Hansen, M.C., Pickens, A., Hernandez-Serna, A., Tyukavina, A., Turubanova, S., Zalles, V., Li, X., Khan, A., Stolle, F. and Harris, N., 2022. The global 2000-2020 land cover and land use change dataset derived from the Landsat archive: first results. Front. Remote Sens. 3: 856903. doi: 10.3389/frsen. https://doi.org/10.3389/frsen.2022.856903

RFI 2024

Car radar monitoring campaing at 76-77 GHz

M. Bautista Durán(1), J.A. López Pérez(1), Andrea Martínez(1) , and Dave John(2)
(1) Yebes Observatory (IGN), Yebes Spain, m.bautista@oan.es, jalopezperez@transportes.gob.es, a.martinez@oan.es
(2) Institut de Radioastronomie Millimétrique (IRAM), Granada, Spain, john@iram.es

1 Introduction

The 76-77 GHz frequency band was designated for vehicular and infrastructure radar systems in ERC Recommendation 70-03 [1]. This frequency band is used by long range radar systems which are not compatible with Ultra Wide Band (UWB) Short Range Radar (SRR) systems. Thus a new frequency band of 4 GHz for Automotive UWB SRR was needed within the range 77-81 GHz (ECC DEC(04)03 [2]). In 2004, a Commission Decision was responsible of harmonise radio spectrum to facilitate a coordinated EU introduction of Automotive SRR systems, as shown in 2004/545/EC [3], where the 79 GHz was identified for short range radar devices.

The high cost and complexity of existing automotive radar technology have limited the implementation of such sensors to high end cars only [4]. Today, new vehicles are equipped with 76-77 GHz radar in the front grille of the car for advanced driver assistance systems (ADAS), such as adaptive cruise control (ACC) or automatic emergency braking (AEB). It is expected that in the following years more cars will be equipped with such technology, and future use will include the 77-81 GHz for short range purposes.

Radio Astronomy Service (RAS) is allocated as a primary service in the 76 GHz to 77.5 GHz and 79 to 81 GHz frequency bands, while 77.5-78 GHz is allocated as secondary service. Furthermore, the full frequency range 76-81 GHz is addressed in the footnote RR No. 5.149 [5] because of its scientific interest.

At CEPT level, several compatibility studies has been performed (see ECC Report 350 [6]) showing that several kilometers of separation distances between the cars and the radioastronomy stations are needed to achieve compatibility. As an example, the separation distances needed to achieve compatibility between 77-81 GHz SRR and IRAM 30 meter radiotelecope is around 60-70 km.

During the period of 2020-2021 several RFIs were detected with the IRAM radiotelescope in the range 76-77 GHz. The first hypothesis was that this signal could be generated by automotive radars in cars. To analyse the situation in detail, a monitoring campaign was carried out by Yebes staff in collaboration with IRAM staff using the 72-90 GHz portable RFI receiver available from Yebes Observatory.

The aim of this report is to show the different RFI signals produced by car radars and to highlight the future impact that automotive radars at 79 GHz would have on astronomical observations.

2 Monitoring setup

For this monitoring campaign, the portable receiver designed and built at the Yebes Observatory was used. This equipment consists of two modules, one being the RF part with the W-band horn antenna and LNA, together with the downconverter to shift the 72-90 GHz into the IF range of 1-19.5 GHz. This range matches with the capabilities of our portable spectrum analyser (SA). The second module contains the power supply for this receiver.

Several measurements were made during the monitoring campaign. All of them were performed outdoors, except for the last one where the receiver was placed approximately in the secondary focus (Nasmyth) of the radio telescope.

Firstly, a measurement was carried out with the receiver pointing towards Granada city (20 km in line of sight from the station), but no interference was detected with the receiver and its associated spectrum analyser. Then, some

tests were carried out pointing at one of the station employees' cars (Toyota Corola Hybrid Active Tech - 2021). The test consisted of pointing the receiver at the road leading up to the observatory, while the car was driving along this road, and with the car stopped at some point on the road.

From this set of measurements, it can be concluded that this car model is equipped with a front radar to give the vehicle some assistance options, one of which is the Adaptive Cruise Control (ACC), which is a type of advanced driver assistance system for road vehicles that automatically adjusts the vehicle speed to keep a safe distance from vehicles ahead. In this particular car model, the signal was detected between 76.35 - 76.72 GHz, approximately. The common frequency of this type of radar is between 76 - 77 GHz. It can therefore be concluded that the signal detected by the 30 m radio telescope is from a car radar source.

As can be seen from the graphs above, the signal was only not detected when the car was driving down the road, which means that the front radar was facing away from the RFI receiver. On the other hand, when the car is facing the receiver, regardless of whether the car is moving or stationary, or whether the ACC is on or off, the RFI is perfectly detected by the system. The only moment when the radar is disconnected is when the car is completely switched off.

The results obtained with the spectrum analyser connected to the output of the RFI system measured the vertical polarisation (V-pol) in max hold mode.

To continue the RFI campaign, similar measurements were taken but at different distances on the road. The same car (Toyota Corolla) was driven down the road with the receiver facing the road. The car stopped at two different positions on the road (785 m and 1940 m from the receiver).

At both positions, the radar signal was detected by the RFI receiver. Given the ability to detect signals up to a few kilometres away, the next measurement was made in the direction of a parking lot at 3 km from the station. Several peaks appear at different frequencies and in both polarizations, so no conclusion can be drawn about the polarization of the transmitter.

The final set of measurements was taken with the receiver inside the radio telescope, in the receiver room, in secondary focus (pointing towards the subreflector through the open vertex), while the Toyota car was on the road, pointing towards the radio telescope, with the engine on (ACC on). No great care was taken to align the receiver to the secondary or to correct the receiver's out-of-focus position, due to the near-field conditions of the tests.

The radiotelescope was pointed to different azimuths (230-310) at 0 degrees elevation. The car was placed at 290º azimuth to the telescope and 10º inclination to the vertex of the radiotelescope (the car radar signal should enter through a secondary lobe). The distance from the car to the radio telescope was 120 m. The radar is perfectly detected in this setup and in a wide range of azimuth angles, being the most intense the one from 260º, which is not the direction of the car, so some multipath or bouncing is expected to be the source of this higher level from this direction.

References

[1] Electronic Communication Committee (ECC). Relating to the use of Short Range Devices (SRD). ERC Recommendation 70-03. 11 February 2022.

[2] Electronic Communication Committee (ECC). The frequency bands to be designated for the temporary introduction of Automotive Short Range Radars (SRR). ECC Decision (04)03. 4 March 2022.

[3] Commission. Decision on the harmonisation of radio spectrum in the 79 GHz range for the use of automotive short-range radar equipment in the Community. 2004/545/EC. 8 July 2004

[4] N. Ghassemi, M. Ghassemi, A. Abdellatif, M. . -R. Nezhad-Ahmadi and S. Safavi-Naeini, "Wideband Waveguide to SIW to Microstrip Transition for 79 GHz Automotive Radar Antenna Characterization," 2020 IEEE USNC-CNC-URSI North American Radio Science Meeting (Joint with AP-S Symposium), Montreal, QC, Canada, 2020, pp. 109-110

[5] Radio Regulations Edition 2020.

[6] Electronic Communication Committee (ECC). Radiodetermination equipment for ground based vehicular applications in 77-81 GHz. ECC Report 350. 3 February 2023.

RFI 2024

Hierarchical vision transformers for RFI mitigation in radio astronomy

Xiaowei Ouyang[1], Henk Dreuning[1,2], Michael Mesarcik*[2], and Rob V. van Nieuwpoort[3]
(1) Vrije Universiteit Amsterdam, Amsterdam, The Netherlands,
(2) University of Amsterdam, Amsterdam, The Netherlands,
(3) Leiden University, Leiden, The Netherlands

PoS(RFI2024)070

1 Introduction

Radio Frequency Interference (RFI) is an enormous challenge for radio astronomy due to the increasing scale and sensitivity of modern radio telescopes. Furthermore, the growing number of electronic devices emitting RF signals severely hampers the reliability of radio observations, necessitating advanced methods for RFI mitigation. While machine learning methods have shown promise in this area, most existing approaches rely on Convolutional Neural Networks (CNNs), which carry inherent biases in their assumptions about the inference structure and morphology.

In this paper, we explore an alternative approach using hierarchical vision transformers, specifically the Swin-UnetR [1] architecture, to tackle RFI detection in radio astronomy. Unlike CNNs, transformers do not assume any specific feature morphologies, allowing them to potentially identify RFI more flexibly. This being said, training large transformer models is computationally expensive; often requiring significant resources. To overcome this, we employ pipeline parallelism with CAPSlog [2] as the partitioning strategy, to enable more efficient use of both computational resources and memory to facilitate scalability for future studies as larger datasets become available.

This is the first known application of transformer-based architectures for RFI detection in radio astronomy, representing a shift from traditional methods. Our experiments demonstrate that the Swin-UnetR architecture achieves state-of-the-art performance, outperforming existing methods on three key metrics using data from the LOFAR [3] radio telescope. This novel approach not only advances RFI mitigation but also sets the stage for broader adoption of transformer-based models in radio astronomy.

2 Shifted window vision transformers

The *S*hifted *Win*dow (SWIN) Transformer architecture [1], has gained significant attention for its approach to handling spatial hierarchies in vision tasks. Unlike traditional transformer architectures that maintain a fixed global view, the Swin Transformer operates by gradually merging patches at multiple scales, allowing it to capture both local and global information.

The Swin-UnetR model, which we apply to RFI detection in radio astronomy, combines the down-sampling mechanism of Swin Transformer with the up-sampling architecture of U-Net. The down-sampling stage uses the Swin Transformer's patch-merging technique to reduce the spatial dimensions while extracting essential features. The up-sampling stage, inspired by U-Net, allows the model to generate high-resolution output, which is necessary for accurately identifying RFI patterns within the radio spectrum.

3 Evaluation

The models in this paper are trained and evaluated on the spectrograms from a publicly available dataset generated by the LOFAR telescope [4]. This dataset contains 7,500 training samples labelled by AOFlagger [5] and 109 test samples labelled by human experts. To manage the dataset's size, we down-sample the input spectrograms, reducing them to approximately 10 GB, and then crop them into 512 × 512 pixel images.

We use three configurations of the Swin-UNETR model, each varying a different hyper-parameter of the Swin Transformer architecture. We train each model for 100 epochs using the AdamW optimiser with early stopping, additionally we use 20 cosine warming-up epochs and a learning rate of 10^{-5} and set the decay rate at 0.001. Table 1 presents the number of parameters and the computational resources required for training these configurations.

Model Configuration	# Parameters	Feature size	# Transformer blocks per stage	TFLOPs
Swin-6M	6.5 M	24	(2, 2, 18, 2)	1.105
Swin-100M	102.1 M	96	(2, 2, 18, 2)	12.334
Swin-400M	408.1 M	192	(2, 2, 18, 2)	67.025

Table 1. Parameters and TFLOPs per iteration for each Swin-UnetR configuration

We compare the RFI detection performance of the Swin-UnetR model with existing deep learning solutions, specifically NLN [4] and U-Net [6] as well as AOFlagger [5]. In Table 2 we show the model's detection performance using three metrics: the AUPRC (Area Under Precision–Recall Curve) score, the AUROC (Area Under Receiver Operating Characteristic Curve) score, and the F1-score.

It can be seen that the transformer-based models offers significant improvements across all metrics relative to the other models. Interestingly, the Swin-400M model exhibits higher detection performance compared to both Swin-100M and Swin-6M, suggesting that model size correlates with improved accuracy. Overall, these findings provide insights into the performance dynamics among Swin-UnetR variants and their efficacy against other models.

Metric	AOFlagger[5]	U-Net [6]	NLN [4]	Swin-6M	Swin-100M	Swin-400M
AUROC	0.7883	0.8017	0.8622	0.9711	0.9743	**0.9771**
AUPRC	0.5716	0.5920	0.6216	0.6783	0.6831	**0.6938**
F1-Score	0.5698	0.5876	0.5114	0.6302	0.6281	**0.6401**

Table 2. RFI detection performance in AUROC, AUPRC and F1 score for each model, where bold is best.

4 Conclusion

In this paper we have demonstrated that transformer-based architectures, such as Swin-UnetR, demonstrate notable improvements over traditional architectures for applications in radio astronomy RFI detection. Our findings indicate that model performance tends to improve with the number of parameters in the Swin-UnetR architecture. Larger Swin-UnetR models consistently achieve better performance metrics compared to their smaller counterparts, supporting the notion that increased model capacity allows for the capture of more complex patterns. Additionally, by utilising a parallel method to train these larger architectures, we effectively facilitated more efficient handling of large-scale datasets and potentially reducing training times, which will be further demonstrated in the full paper. This approach could be valuable in broader contexts within radio astronomy, especially for tasks requiring many computational resources. These results not only show the potential of transformer-based models but also open pathways for further research into scalable training techniques and their applicability to RFI detection and other related fields.

References

[1] A. Hatamizadeh, V. Nath, Y. Tang, *et al.*, "Swin UNETR: Swin Transformers for Semantic Segmentation of Brain Tumors in MRI Images," pp. 272–284, 2022.

[2] H. Dreuning, A. B. Liokouras, X. Ouyang, H. E. Bal, and R. V. Van Nieuwpoort, "CAPSlog: Scalable Memory-Centric Partitioning for Pipeline Parallelism," in *2024 32nd Euromicro International Conference on Parallel, Distributed and Network-Based Processing (PDP)*, pp. 17–25, IEEE, 3 2024.

[3] M. P. van Haarlem, M. W. Wise, A. W. Gunst, G. Heald, *et al.*, "LOFAR: The LOw-Frequency ARray," *Astronomy & Astrophysics*, vol. 556, p. A2, 8 2013.

[4] M. Mesarcik, A.-J. Boonstra, E. Ranguelova, and R. V. van Nieuwpoort, "Learning to detect radio frequency interference in radio astronomy without seeing it," *Monthly Notices of the Royal Astronomical Society*, vol. 516, pp. 5367–5378, 9 2022.

[5] A. R. Offringa, J. J. Van De Gronde, and J. B. Roerdink, "A morphological algorithm for improving radio-frequency interference detection," *Astronomy and Astrophysics*, vol. 539, 2012.

[6] J. Akeret, C. Chang, A. Lucchi, and A. Refregier, "Radio frequency interference mitigation using deep convolutional neural networks," *Astronomy and Computing*, vol. 18, pp. 35–39, 2017.

WRC-27 Scientific Agenda Items
The Future of Science Services

Bakaus T.A.(1)
(1) Anatel, Brasília, Brazil, bakaust@anatel.gov.br

1. Introduction

The World Radiocommunication Conference 2023 (WRC-23), held in Dubai, approved Resolution 813 (WRC-23) [1], setting the agenda for the 2027 World Radiocommunication Conference. This agenda includes 19 technical items to be studied in the 2024-2027 cycle and resolved at WRC-27.

Five key scientific items (1.15 to 1.19) focus on Lunar Communications, Radio Astronomy Protection, Space Weather Sensors, Protection of Earth Exploration Services, and Allocation for Earth Exploration. These topics highlight the ITU's commitment to advancing space technologies and protecting scientific services, ensuring innovations benefit both space exploration and Earth observation. This paper explores each topic, detailing strategies to achieve the objectives outlined in the agenda.

2. Study Cicle for WRC-27 (2024-2027)

The study cycle for WRC-27 begins after the conclusion of WRC-23, which set the agenda through Resolution 813. This cycle, spanning from 2024 to 2027, involves the First Session of the Conference Preparatory Meeting (CPM), which assigns the agenda items to the relevant ITU-R study groups. These groups will conduct detailed technical analyses and compatibility studies for the 19 agenda items, including the five scientific topics: Lunar Communications, Radio Astronomy Protection, Space Weather Sensors, Protection of Earth Exploration Services, and Earth Exploration Allocations. This process ensures that each item receives focused attention and that regulatory decisions are well-founded.

Finally, six months before WRC-27, a Second Session of the CPM will be held, where the specific technical and regulatory methods for concluding each agenda item will be established. The administrations will then make decisions on each item at WRC-27.

3. Key Scientific Agenda Items for WRC-27: Significance and Studies Directives

The World Radiocommunication Conference 2023 (WRC), organized by the International Telecommunication Union (ITU), approved Resolution 813, which establishes the agenda for the World Radiocommunication Conference 2027 (WRC-27). This agenda includes 19 technical items, highlighting five key scientific topics that promise significant benefits for the planet, humanity, and individuals. These topics are as follows.

Agenda Item 1.15 (Lunar Communications Development) under Resolution 680 (WRC-23) [2], focuses on enhancing lunar surface and orbit communications to support scientific research and sustained human presence on the Moon. Studies will evaluate spectrum needs for systems in frequency ranges: 390-406.1 MHz, 420-430 MHz, 440-450 MHz, 2 400-2 690 MHz, 3 500-3 800 MHz, 5 150-5 570 MHz, 5 570-5 725 MHz, 5 775-5 925 MHz, 7 190-7 235 MHz, 8 450-8 500 MHz, and 25.25-28.35 GHz. They will consider technical characteristics, protection criteria, and propagation to ensure compatibility with existing services and protect radio astronomy in the Shielded Zone of the Moon (SZM).

Agenda Item 1.16 (Radio Astronomy Protection) under Resolution 681 (WRC-23) [3], focuses on protecting radio astronomy services from interference by non-geostationary satellite systems. Studies will assess the impact of unwanted emissions on RAS frequency bands: 10.6-10.7 GHz, 42.5-43.5 GHz, 76-77.5 GHz, 94.1-95 GHz, 100-102 GHz, 114.25-116 GHz, and 130-134 GHz. The aim is to develop methodologies for separation distances between non-GSO satellite gateways and radio astronomy stations and devise coexistence strategies for Radio Quiet Zones (RQZs). This item also considers formal recognition of RQZs, aiming to integrate such protections into international regulations to minimize interference before satellite operations begin, ensuring astronomers can study cosmic phenomena without interference.

Agenda Item 1.17 (Space Weather Sensors) under Resolution 682 (WRC-23) [4] discusses regulatory measures to protect receive-only space weather sensors for monitoring solar activities affecting satellites, power grids, and aviation. Studies will

focus on frequency bands: 27.5-28.0 MHz, 29.7-30.2 MHz, 32.2-32.6 MHz, 37.5-38.325 MHz, 73.0-74.6 MHz, and 608-614 MHz. The goal is to develop sharing and compatibility criteria, ensuring these sensors operate without interference, and explore their inclusion in the Master International Frequency Register.

Agenda Item 1.18 (EESS and RAS Compatibility) under Resolution 712 (WRC-23) [5], aims to ensure compatibility between the Earth exploration-satellite service (EESS) (passive), the radio astronomy service (RAS), and active services above 76 GHz. Studies will assess the impact of unwanted emissions on EESS and RAS in bands: 86-92 GHz, 92-94 GHz, 114.25-116 GHz, 164-167 GHz, 167-174.5 GHz, 200-209 GHz, and 209-217 GHz. The goal is to set threshold levels for unwanted emissions and update resolutions to protect passive and radio astronomy observations from interference.

Agenda Item 1.19 (Earth Exploration-Satellite Service Allocations) under Resolution 674 (WRC-23) [6] considers new allocations for Earth exploration services to enhance sea surface temperature (SST) measurements. Studies will focus on frequency bands: 4 200-4 400 MHz and 8 400-8 500 MHz, conducting sharing and compatibility analyses. The goal is to ensure these allocations do not interfere with existing services, supporting SST measurement capabilities for climate science.
Collectively, these agenda items promote a safer, more knowledgeable, and sustainable world.

4. Status of discussions and next steps

The status of discussions for all agenda items is at the initial stage of gathering technical characteristics to conduct sharing and compatibility studies necessary for their implementation. Each item is being conducted by its pertinent ITU-R study group, ensuring focused and specialized attention to detail. These studies will lay the groundwork for detailed analyses and regulatory measures to ensure the effective and interference-free operation of various radiocommunication services as outlined in the agenda.

5. Conclusions

The WRC-27 agenda outlines studies on critical issues like lunar communications, radio astronomy protection, space weather sensors, and Earth exploration-satellite service allocations. These efforts aim to enhance scientific research, improve technological capabilities, and ensure sustainable use of radio frequencies. Conducted by ITU-R study groups, these discussions will inform regulatory decisions, fostering a safer, more knowledgeable, and sustainable world, benefiting global radiocommunication services.

Referências

[1]. ITU, "Resolution 813 (WRC-23): Agenda for the 2027 World Radiocommunication Conference," in World Radiocommunication Conference (WRC-23), Dubai, 2023. [Online]. Available: https://www.itu.int/dms_pub/itu-r/oth/0c/0a/R0C0A0000100036PDFE.pdf

[2]. ITU, "Resolution 680 (WRC-23): Studies on frequency-related matters, including possible new or modified space research service (space-to-space) allocations, for future development of communications on the lunar surface and between lunar orbit and the lunar surface," in World Radiocommunication Conference (WRC-23), Dubai, 2023. [Online]. Available: https://www.itu.int/dms_pub/itu-r/oth/0c/0a/R0C0A0000100015PDFE.pdf

[3]. ITU, "Resolution 681 (WRC-23): Studies of technical and regulatory provisions necessary to protect radio astronomy operating in specific Radio Quiet Zones and, in radio astronomy service primary allocated frequency bands globally, from aggregate radio-frequency interference caused by systems in the non-geostationary-satellite orbit," in World Radiocommunication Conference (WRC-23), Dubai, 2023. [Online]. Available: https://www.itu.int/dms_pub/itu-r/oth/0c/0a/R0C0A0000100016PDFE.pdf

[4]. ITU, "Resolution 682 (WRC-23): Consideration of regulatory provisions and potential primary allocations to the meteorological aids service (space weather) to accommodate receive-only space weather sensor applications in the Radio Regulations," in World Radiocommunication Conference (WRC-23), Dubai, 2023. [Online]. Available: https://www.itu.int/dms_pub/itu-r/oth/0c/0a/R0C0A0000100017PDFE.pdf

[5]. ITU, "Resolution 712 (WRC-23): Studies on compatibility between the Earth exploration-satellite service (passive), the radio astronomy service in certain bands above 76 GHz, and active services in adjacent and nearby frequency bands," in World Radiocommunication Conference (WRC-23), Dubai, 2023. [Online]. Available: https://www.itu.int/dms_pub/itu-r/oth/0c/0a/R0C0A0000100018PDFE.pdf

[6]. ITU, "Resolution 674 (WRC-23): Studies on possible allocations to the Earth exploration-satellite service (passive) in the bands 4 200-4 400 MHz and 8 400-8 500 MHz," in World Radiocommunication Conference (WRC-23), Dubai, 2023. [Online]. Available: https://www.itu.int/dms_pub/itu-r/oth/0c/0a/R0C0A0000100019PDFE.pdf

The Importance of Space Sustainability for the Continuity of Scientific Services

Bakaus T.A.[(1)]
[(1)] Anatel, Brasília, Brazil, bakaust@anatel.gov.br

1. Introduction

Since the dawn of the space age, the exploration and utilization of space have provided significant benefits to humanity. Among the many advancements are scientific services that use satellites for Earth exploration, remote sensing, radio astronomy, space weather sensors, and meteorology. However, these services are increasingly vulnerable to the challenges of space sustainability, highlighting the urgent need to adopt responsible practices to ensure their continuity.

2. History of Space Sustainability

The space race between the United States and the Soviet Union in the 1950s and 1960s heralded the dawn of the space age. This era was further defined by the establishment of critical international treaties in the 1970s, notably the 1967 Outer Space Treaty [1], which laid the legal groundwork for the peaceful use of outer space.

As commercial, scientific, and communication satellites proliferated, the space environment became increasingly congested. The accumulation of space debris, arising from decommissioned satellites and rocket fragments, began to present a serious hazard to space operations. This growing concern was highlighted by Kessler and Cour-Palais in their seminal work on collision frequency [2]. Additionally, the deliberate destruction of satellites, such as the 2007 anti-satellite test, intensified the problem, amplifying global awareness about the urgent need for effective space debris mitigation strategies.

3. International Initiatives

International organizations, such as the International Telecommunication Union (ITU), the United Nations Office for Outer Space Affairs (UNOOSA), and the International Academy of Astronautics (IAA), have played crucial roles in promoting space sustainability.

The ITU has been notable through specific resolutions, such as Resolutions 218 and 219 from the 2022 Plenipotentiary Conference and Resolution 74 from the 2023 Radiocommunication Assembly [3], [4], [5]. These resolutions establish standards and recommended practices for mitigating space debris and promoting safe and sustainable operations in space.

UNOOSA promotes international cooperation and the development of guidelines to mitigate space debris and ensure the sustainable use of space [6], [7]. The IAA, in turn, organizes conferences and studies, providing an important platform for discussing sustainable practices and publishing reports on space debris management and operational sustainability [8].

4. Importance of Space Sustainability for Scientific Services

Earth Exploration by Satellite: Earth observation satellites are essential for monitoring environmental changes, natural disasters, and human activities. Space sustainability is crucial to ensure these satellites can operate safely and provide accurate and continuous data.

Remote Sensing: Used in a wide range of applications, from precision agriculture to natural resource management, remote sensing relies on the integrity of satellites in orbit. Mitigating space debris and implementing sustainable practices ensure that these satellites continue to provide vital information.

Radio Astronomy: Radio astronomy uses radio telescopes to study the universe. Interference from space debris and radio pollution can hinder astronomical observations. Sustainable space practices help minimize these interferences, ensuring the quality of research.

Space Weather Sensors: These sensors monitor and predict space weather events, allowing mitigation of their adverse effects. Space sustainability is essential to keep these sensors operational and effective, protecting other satellites and terrestrial infrastructure.

Meteorology: Meteorological satellites provide essential data for weather forecasts and climate monitoring. The integrity and functionality of these satellites depend on a safe and sustainable space environment, free of debris that could cause damage or interference.

5. Space Sustainability and the Future of Scientific Services

To ensure the continuity and effectiveness of scientific services, it is vital to adopt space sustainability practices. The international community is working to develop guidelines and technologies that mitigate the risks associated with space debris.

Space Debris Mitigation: Implementing technologies to remove or avoid the creation of space debris is essential. This includes developing deorbiting systems for satellites at the end of their life cycle and promoting responsible launch practices.

Strengthening Satellite Resilience: Designing satellites with greater resistance to space weather and debris perturbations is crucial. This can include using more robust materials, system redundancy, and the ability to perform evasive maneuvers.

International Cooperation: Collaboration between countries and international organizations is fundamental to monitor space weather and develop coordinated responses to adverse events. Initiatives like the International Charter on Space and Major Disasters [9] and ITU projects are important examples of joint efforts.

6. Conclusions

The importance of space sustainability for the continuity of scientific services cannot be overstated. Earth exploration by satellite, remote sensing, radio astronomy, space weather sensors, and meteorology depend on the integrity and functionality of satellites in orbit. Adopting sustainable practices and cooperating internationally are essential steps to protect these vital services and ensure they continue to benefit humanity safely and efficiently.

The scientific community must remain vigilant and proactive in implementing and promoting space sustainability practices, collaborating with international organizations, and adopting technological innovations that mitigate risks. The future of scientific services, and by extension, global knowledge and well-being, depends on our actions today.

Referências

[1].United Nations Office for Outer Space Affairs. (1967). Outer Space Treaty. [Online]. Available: https://www.unoosa.org/oosa/en/ourwork/spacelaw/treaties/introouterspacetreaty.html

[2].D. J. Kessler and B. G. Cour-Palais, "Collision Frequency of Artificial Satellites: The Creation of a Debris Belt," Journal of Geophysical Research, vol. 83, no. A6, pp. 2637-2646, 1978.

[3].International Telecommunication Union, "Resolution 218 (PP-22)," [Online]. Available: https://www.itu.int/dms_pub/itu-s/opb/conf/S-CONF-ACTF-2022-PDF-E.pdf

[4].International Telecommunication Union, "Resolution 219 (PP-22)," [Online]. Available: https://www.itu.int/dms_pub/itu-s/opb/conf/S-CONF-ACTF-2022-PDF-E.pdf

[5].International Telecommunication Union, "Resolution 74 (Assembleia de Rádio 2023 da ITU)," [Online]. Available: https://www.itu.int/dms_pub/itu-r/opb/act/R-ACT-RES-074-2023-PDF-E.pdf

[6].United Nations, "Vienna Declaration on Space and Human Development," 1999. [Online]. Available: https://www.unoosa.org/pdf/reports/unispace/viennadeclE.pdf

[7].United Nations Office for Outer Space Affairs, "Guidelines for the Long-term Sustainability of Outer Space Activities," 2019. [Online]. Available: https://www.unoosa.org/res/oosadoc/data/documents/2018/aac_1052018crp/aac_1052018crp_20_0_html/AC105_2018_CRP20E.pdf

[8].International Academy of Astronautics, [Online]. Available: https://iaaweb.org/

[9].International Charter Space and Major Disasters. Available: https://disasterscharter.org

RFI 2024

Protecting radio astronomy from interference: The role and activities of CRAF

M. Lindqvist(1)
(1) Department of Space, Earth and Environment, Chalmers University of Technology, Onsala Space Observatory, 439 92 Onsala, Sweden; e-mail: Michael.Lindqvist@chalmers.se

Radio astronomy is crucial for advancing our understanding of the universe. However, safeguarding radio astronomy from radio interference is becoming increasingly challenging as spectrum usage grows for both terrestrial and space-based services. On behalf of European radio astronomers, the Committee on Radio Astronomy Frequencies of the European Science Foundation (CRAF) coordinates activities to keep the frequency bands used by radio astronomy and space sciences free from interference. It aims to provide a cost-effective single voice on frequency protection issues for European radio astronomy observatories and research institutes, achieving a significantly greater impact than that achievable by individual national institutions. By working together, European observatories and institutes can profit from synergy effects, cover many more topics and learn from each other. In recent years, work in CRAF has been allocated to small teams, so-called Work Item teams, which deal with well-defined topics such as satellite services, international Mobile Telecommunications Service, or questions of spectrum engineering. This presentation will provide an overview of CRAF's initiatives at both national and international levels, highlighting our preparations for the World Radio Conference 2027.

PoS(RFI2024)070

RFI 2024

Antenna allocation technique to analyze self-generated interference

Raúl Tomás Horst(1), Sebastián Chiocchetti*(2), Nahuel Alincastro*(2), and Daniel Lipuma(2)
(1) Balseiro Institute, San Carlos de Bariloche, Argentina, raul.horst@ib.edu.ar
(2) INVAP S.E., San Carlos de Bariloche, Argentina, {schiocchetti,nalincastro,dlipuma}@invap.com.ar

1. Introduction

This study focuses on the potential degradation of receivers caused by nearby transmitters, both in terms of distance and frequency, due to coupling between antennas mounted on large electrical structures. In environments where transmitters and receivers must coexist, the goal is to find methods to position antennas in such a way that prevents self-generated interference from their own transmissions. As a specific case study, this paper examines a communications satellite and its Telemetry, Command, and Ranging (TCR) service in the Ka band. Beyond addressing the specific technical issue, the proposed strategy aims to develop a systematic analytical process that minimizes computational resources and engineering hours. This work presents results from simulations using CST Studio Suite 2021 software and validation through measurements.

2. Modelling of large electrical structures in Ka Band

The strategies considered when simulating structures with dimensions much larger than the operational wavelength on conventional computers, rather than on a more powerful computing cluster, involve simplifying the structure. These simplifications include avoiding small-scale details, using Perfect Electric Conductor (PEC) as the material for conductive structures (assuming zero thickness), and simulating antennas separately. Additionally, it is analyzed whether it is appropriate to import simulated antennas as far-field sources or near-field sources (files usually provided by suppliers in the case of commercial antennas) depending on the regions of the radiation pattern[1]. The integral and optical methods accept these imports, discarding the use of other methods[2].

3. Validation

The coupling between a horn antenna and a waveguide transition in the Ka-band mounted on a structural satellite model with a maximum dimension of 4.4 m (292 λ) was measured. The horn antenna was fed through an RF generator, and the power received in the waveguide transition was measured using a spectrum analyzer, with RF absorbers being used to reduce measurement errors due to unwanted reflections. Measurements were taken on the front face of the platform at a height of 16.2 cm from the antennas at an elevation angle of 0° (aligned) as a function of the distance between antennas, as shown in Figure 1, and at a height of 23.2 cm with an elevation angle of 90°.

The coupling with the waveguide on the top face of the platform was then measured in two positions, referred to as case A and case B. In case A, the simulated value was -47.5 dB, and the measured value was -49.9 dB. In case B, the simulated value was -62.7 dB, while the measured value was -65.2 dB.

Different simulation methods were compared against the measurements to determine the preferred values to report. Percentage summations (in times) of simulation errors for each method were performed, contributing to total errors when the simulation value was below the measurement range. In this way, simulating a value lower than the measured one was penalized, whereas simulating a higher coupling value than the measured one (a false positive) was not penalized.

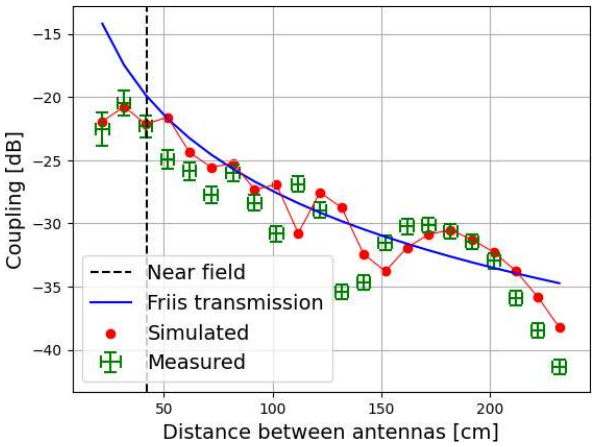

Figure 1. Coupling between the horn antenna and waveguide transition on the satellite platform was measured as a function of the distance between them at 20.1 GHz. The antenna height was 16.2 cm, with an elevation angle of 0°. In the near field, the integral method was used with near-field sources, while in the Fresnel zone and far field, the optical method with far-field sources was employed.

4. Results for a typical TCR

The TCR system transmits sensor data and the operational status of a geostationary satellite, enabling the measurement of the Earth-satellite distance and the satellite's location to determine orbit parameters. It also receives control commands from the ground.

The frequencies of interest analyzed are 20.1 GHz, where the transmitter operates with higher power and has an interference immunity of -25 dBm, and 28.7 GHz, where the receiver has the highest sensitivity and an interference immunity of -142 dBm. The CAD model of the satellite and the far-field sources of the antennas were available, so the coupling between the antennas mounted on the satellite was simulated to analyze whether the received powers at the receiver comply with the interference immunity values with a safety margin of 6 dB[3].

5. Conclusions

A criterion was established to simplify the modeling of large electrical structures from an electromagnetic perspective and to define whether far-field or near-field sources are required when introducing antennas into the platform. Additionally, information on the most appropriate simulation method was provided.

The interference between the reception and transmission subsystems of a commercial TCR mounted on a geostationary satellite was analyzed by simulating the coupling between antennas to evaluate the power levels in the RF chain, concluding that the receiver will not suffer EMI from the transmitter. Furthermore, a coupling limit was identified for a typical TCR system in the Ka-band, avoiding the need for detailed analysis, ensuring that there will be no EMI with fewer requirements.

The analysis was optimized by providing recommendations for future work, covering the CAD modeling of structures and simulation configuration, aiming to reduce engineering hours and computational resources when analyzing antenna coupling on electrically large structures, such as a geostationary satellite operating in the Ka-band, but also extrapolating this approach to analyze any large platform (in terms of wavelengths) where transmitters and receivers coexist.

References

[1] Trevor S. Bird, *Mutual Coupling Between Antennas.* 2021.

[2] Dassault Systems, *CST Studio Suite - Workflow & Solver Overview.* 2020.

[3] Department of Defense, USA, *MIL-STD-464C - 5.1 Margins.* 2010.

RFI 2024

A Fast Implementation of the Algorithm GMAP-TD for Clutter Interference Mitigation

M.E. Amoia*(1)(2)(3), M. Hurtado(1)(4), J.I. Fernández Michelli(1)(2)(3), F. Renolfi(4)
(1) National University of La Plata (UNLP), Argentina
(2) National Scientific and Technical Research Council (CONICET), Argentina
(3) Research Institute of Electronics, Control and Signal Processing (LEICI)
(4) INVAP, Argentina

1 Introduction

Coherent pulsed radars measure the Doppler frequency shift due to the movement of a target. Thereby, Doppler weather radars leverage this principle to estimate the Doppler spectrum of the hydrometeors [1]. The power spectral density provides insight about the nature of the weather phenomena (snow, rain, or hail) and helps to forecast severe storms.

Typically modeled as a Gaussian function [2], the Doppler spectrum for single-channel radars is characterized by power, mean frequency, and spectrum width. Nevertheless, the signal of interest is contaminated by internal and external noise and ground clutter. While noise presents as a flat spectrum, ground clutter exhibits a zero-centered Gaussian spectrum with a narrower width compared to the weather signal. Ground clutter is often the strongest component of the radar signal, overwhelming the signal of interest by tens of decibels. Figure 1 shows an example of a typical weather radar spectrum.

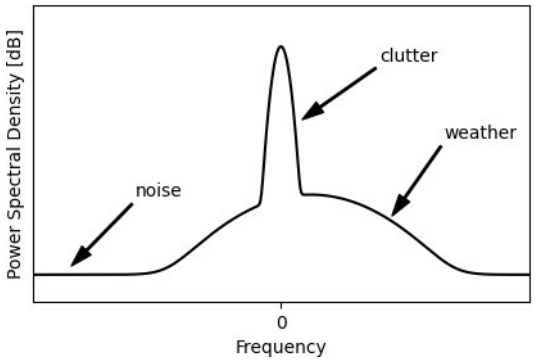

Figure 1. Sketch of the weather radar spectrum.

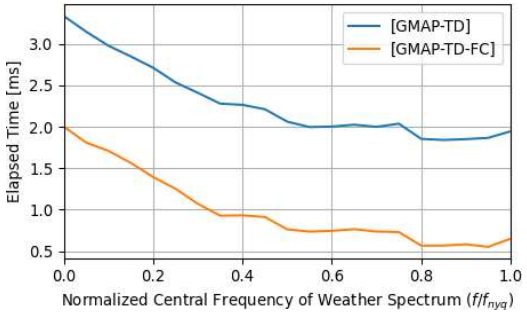

Figure 2. Computation time of GMAP-TD and GMAP-TD-FC.

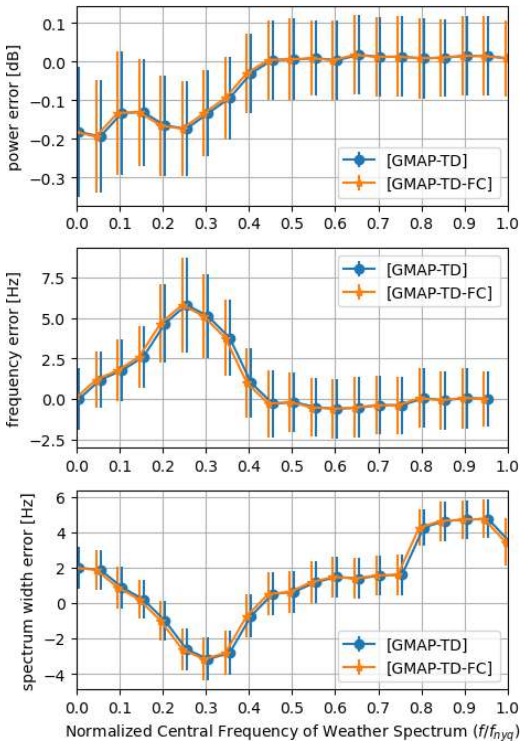

Figure 3. Bias and standard deviation in the estimation of weather parameters.

In weather radars, the clutter spectrum competes with the spectrum of the signal of interest, masking the weather echos from possible detection. Therefore, efficient signal processing techniques are crucial to mitigate clutter

interference while the impact on the weather spectrum is minimized. Simple solutions, such as moving target indicator (MTI) techniques and notch filters, are ineffective for weather radars. Owing to the spectral overlap, these filters remove clutter but also shear the weather spectrum, leading to biased weather parameter estimates. The Gaussian Model Adaptive Processing (GMAP) algorithm addresses this drawback by first filtering out clutter and then attempting to recover the removed section of the weather spectrum [3]. However, GMAP operates in the frequency domain, suffering from energy spillover from strong clutter into the weather spectrum as a consequence of the use of finite series. In order to mitigate this, GMAP employs aggressive tapering windows that reduce spectral leakage but also decrease the operational SNR and increase the uncertainty of weather parameter estimates.

Adaptive time domain filtering methods, like the parametric time domain method (PTDM), offer superior performance to GMAP but are computationally expensive [4]. On the other hand, the algorithm GMAP in the time domain (GMAP-TD) has improved performance than GMAP by operating the filtering stage in time domain [5]. Moreover, it can be applied to staggered pulse repetition intervals.

In this paper, we present the Fast Computation GMAP-TD (GMAP-TD-FC) algorithm. The proposed algorithm does not alter the fundamentals of the original GMAP-TD, achieving identical estimation performance. However, it reduces the computation time, at the expense of larger memory requirement. The faster computation makes GMAP-TD more suitable for real time applications.

2 Preliminary Results

To assess the performance of the proposed GMAP-TD-FC algorithm, simulated weather radar data was processed using both GMAP-TD and GMAP-TD-FC. The complete article will detail the mathematical development of GMAP-TD-FC and evaluate its performance using real weather radar data.

2.1 Computation Time Reduction

Figure 2 illustrates the significant reduction in computation time (around 50%) achieved by the GMAP-TD-FC algorithm compared to the original GMAP-TD method. It is worth noting that for frequencies close to 0, the computation time of both algorithm is slightly higher. This behavior reflects the requirement for more iterations to reconstruct the Gaussian shape of the spectrum due to the greater overlap between the weather spectrum and the clutter spectrum in that region.

2.2 Estimation accuracy

Figure 3 shows the mean and standard deviation in the estimation of the parameters of interest for both algorithms. The results indicate that there is no degradation in the estimation accuracy of the parameters when using the GMAP-TD-FC, verifying that the reduction in computation time does not compromise the estimation quality.

3 Acknowledgement

This work is supported by UNLP (Grant 11-I-257), CONICET (Grant PIP-1515), and INVAP.

References

[1] R.J. Doviak, D.S. Zrnic, D.S. Sirmans, “Doppler weather radar,” *Proceedings of the IEEE*, **67**, 11, pp. 1522–1553, 1979.

[2] V.N. Bringi, V. Chandrasekar, Polarimetric Doppler Weather Radar: Principles and Applications, Cambridge University Press, 2001.

[3] A.D. Siggia, R.E. Passarelli, “Gaussian model adaptive processing (GMAP) for improved ground clutter cancellation and moment calculation,” *Proceedings of ERAD*, **2**, pp. 421–424, Apr. 2004.

[4] C.M. Nguyen, D.N. Moisseev, V. Chandrasekar, “A parametric time domain method for spectral moment estimation and clutter mitigation for weather radars,” *Journal of Atmospheric and Oceanic Technology*, **25**, 1, pp. 83–92, 2008.

[5] C.M. Nguyen, V. Chandrasekar, “Gaussian model adaptive processing in time domain (GMAP-TD) for weather radars,” *Journal of Atmospheric and Oceanic Technology*, **30**, 11, pp. 138–139, 2013.

Radio Frequency Interference Survey Analysis in most passive Earth Observation Frequency Channels using the Earth Observation RFI Scanner (EORFISCAN)

R. Onrubia[(1)], R. Oliva [(1)], D. Duncan[(2)], N. Bormann[(2)], J. Barbosa[(3)], I. Nestoras[(3)], A. Jordao[(3)] , Y. Soldo[(4)], F. Jorge[(4)]
[(1)] Zenithal Blue Technologies, Barcelona, Spain
[(2)] European Center for Medium-Range Weather Forecasts (ECMWF), United Kingdom
[(3)] Research and Development in Aerospace (RDA) GmbH, Switzerland
[(3)] European Space Agency (ESA)

1. Introduction

Radio Frequency Interference (RFI) is a growing threat for Earth Observation (EO) sensors, in particular for passive microwave sensors. Since these instruments measure the natural electromagnetic emissions from ground, any unnatural emission will affect negatively the observations. If RFI-affected data is used to feed Numerical Weather Prediction (NWP) models, it could lead to weather forecast errors. This data needs to be flagged as contaminated, and these RFI sources reported to the authorities.

The Earth Observation RFI Scanner (EORFISCAN) is an ESA project to assess the presence of RFI in most EO frequency bands. EORFISCAN is the natural continuation of the Ground RFI Detection System (GRDS) [1], developed by ZenithalBlue Technologies in collaboration with Research and Development in Aerospace GmbH. EORFISCAN reads EO products, applies a combination of multiple RFI detection techniques (such as intensity, cross-polarization, kurtosis, spatial variability or the generalized RFI Index [2]), and flags the data according to three different threshold levels. These thresholds are different for each terrain type, depend on the incidence angle, azimuth angle, and latitude, and are statistically determined. The system adjusts the thresholds according to a database of previous RFI detections to make the thresholds stricter in regions prone to RFI. Once processed, the EO input products can be modified to include these results without modifying the product structure, so the products can still be read by the users with their normal software.

2. Results

Previously, the software was validated for the SMOS mission in collaboration with ECMWF. Now this partnership has extended to validate most of passive EO frequency channels for a full survey of the RFI presence in passive sensors. To this goal, observations of AMSR2, AMSU-A, MWHS-II, and AMR-C sensors were selected to be fed to the EORFISCAN. The combination of these 4 sensors covers a survey of all passive microwave Earth Observation bands as shown in Table 1.

Table 1 Sensors used to cover the main passive microwave Earth Observation bands

Freq. (GHz) / Sensor	6.4-7.7	10.6-10.7	18.6-18.8	23.6-24	31.3-31.8	33.5-34.5	36-37	50.2-50.4	52.6-59.3	86-92	114.25-122.25
AMSR2	X	X	X	X			X			X	
AMSU-A			X	X	X	X					
MWHS-II						X					
AMR-C				X							

Only surveys of the first three frequency bands from **¡Error! No se encuentra el origen de la referencia.** can be found in the literature; there little or no information on the rest of the bands. Besides, the analyses are conducted with different RFI detection techniques between studies. On the contrary, EORFISCAN analyzes all bands with the same techniques, although the thresholds depend on each instrument, allowing a fair intercomparison between bands or sensors.

The first three AMSR2 frequencies show more contamination than the typical found in literature [2], or that is more extensive, as seen in Figure 1. New contamination is found in the North Sea and the Yellow Sea at 6.9 GHz, and over land at the very tip of South of Africa. At 7.3 GHz, reflections from satellites [3] not only have a larger extension such as in Japan, but also can be seen near the Arabian sea, the Gulf of Mexico, and the US west coast. At 10.65 GHz, the reflection from geosynchronous satellites, typical in Europe, can be also seen in the coast of the Bay of Bengal.

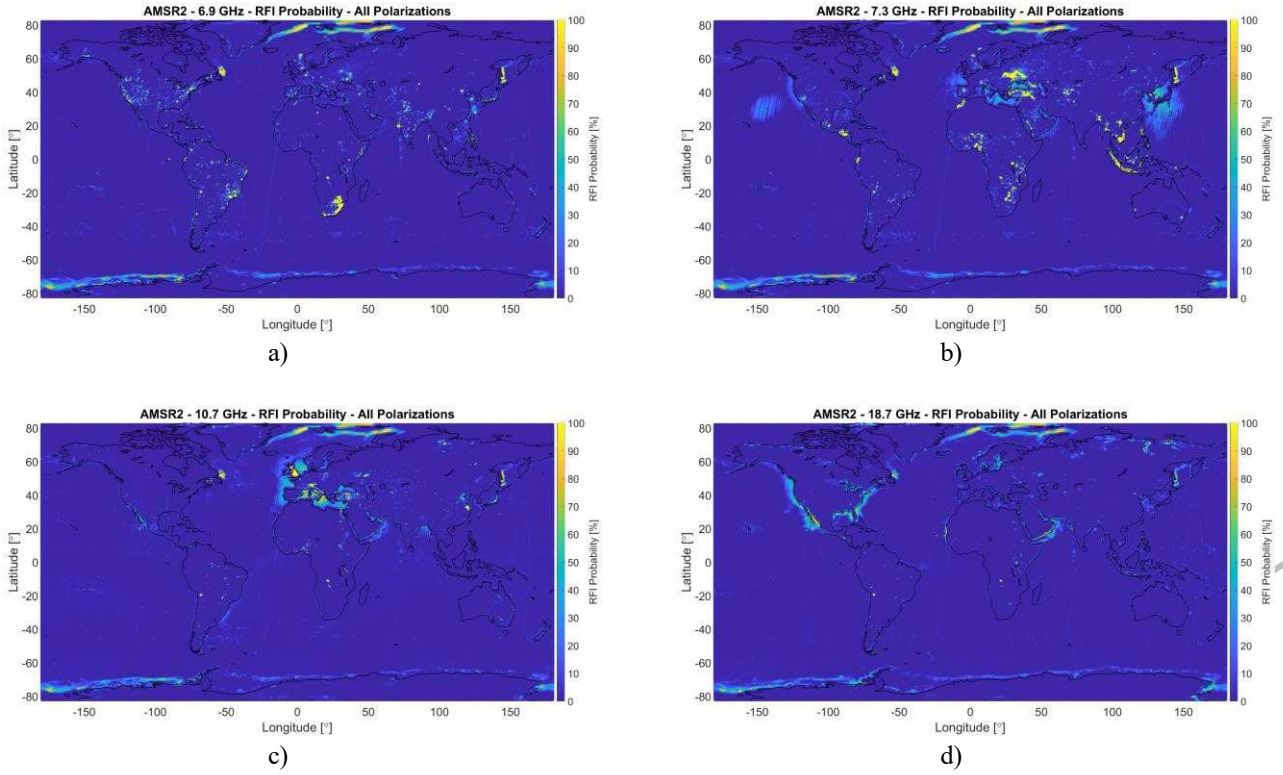

Figure 1 RFI Probability in AMSR2 in a) 6.9 GHz, b) 7.3 GHz, c) 10.7 GHz, and d) 18.7 GHz, for March 2022.

Note some false positives in all bands due to the sea ice edge misclassification (e.g., northeast from Greenland, near the Antarctica coastline, in the Ojotsk Sea, and near Terranova coastline).

The results at higher bands, where less RFI is expected, are still under assessment and will be presented at the conference.

In collaboration with ECMWF, the flagged data from AMSR2 and AMSU-A were assessed via all-sky radiance departures using their NWP model. The majority of flagged points exhibit positive departures, indicative of skillful RFI detection. This corroboration of the RFI identification methods demonstrates good skill in C-band in particular, where the removal of contaminated observations leads to a much more symmetric PDF of departures over sea, for example. There was no clear signal of interference corroborated at AMSU-A frequencies.

[1] R. Onrubia, R. Oliva, P. Weston, P. de Rosnay, S. English, J. Barbosa, I. Nestoras, "The Ground RFI Detection System (GRDS), a New Concept for RFI Detection in Earth Observation Missions", ESA Living Planet Symposium 2022, Bonn (Germany), 2022.

[2] D. W. Draper, "Radio Frequency Environment for Earth-Observing Passive Microwave Imagers," IEEE Journal of Selected Topics in Applied Earth Observations and Remote Sensing, vol. 11, no. 6. Institute of Electrical and Electronics Engineers (IEEE), pp. 1913–1922, Jun. 2018. doi: 10.1109/jstars.2018.2801019.

[3] Y. Wu, M. Li, Y. Bao, and G. P. Petropoulos, "Cross-Validation of Radio-Frequency-Interference Signature in Satellite Microwave Radiometer Observations over the Ocean," Remote Sensing, vol. 12, no. 20. MDPI AG, p. 3433, Oct. 19, 2020. doi: 10.3390/rs12203433.

Passive Instrument RFI above 10 GHz: Past, Present and Future

Otto W. Bruegman[(1)], David G. Lubar* [(2)], and David B. Kunkee[(2)]
(1) NOAA Office of LEO Observations, Lanham, MD USA, Otto.Bruegman@noaa.gov
(2) The Aerospace Corporation, El Segundo, CA USA David.G.Lubar@aero.org, David.B.Kunkee@aero.org

1. Introduction

There are thousands of satellites in planning by the end of the decade. Depending on the source, the estimated numbers of satellites to reach orbit by the next decade range from 20,000 to 65,000 satellites. Considering the planet has approximately 25% - 30% of the most conservative number listed above (i.e., 20,000) of satellites currently in orbit, these numbers represent unprecedented growth. The demands on the radio spectrum to communicate with these constellations, are driving usage higher and higher in frequency, often in proximity to the passive bands where no radio frequency transmissions occur.

The paper will discuss the history of using microwave sounders for temperature and humidity measurements and how growth in spectrum use increases the potential risk for adjacent band interference. Scientists performing data assimilation for numerical weather prediction in support of weather forecasting depend on passive bands that are not affected by out-of-band emissions from nearby sources to detect critical features of the atmosphere.

Frequency allocations for transmissions in proximity of the 50.2 – 50.4 GHz vertical temperature passive band, terrestrial broadband near the 23.6-24.0 GHz passive band, among others, and future regulatory actions proposed in the International Telecommunications Union (ITU) are discussed with a description of satellite instruments in those passive bands.

Due to increased utilization of frequency bands adjacent to Earth Exploration Satellite Service (EESS) allocated bands and, in some cases, increased in-band (shared) use of EESS bands, there have been increasing instances of RFI contamination of EESS measurements. New and proposed use of spectrum in EESS adjacent bands includes space-to-Earth satellite links adjacent to the 10.6 – 10.7 GHz EESS band, proposed new Earth-to-space links near 50.3 GHz that will operate in bands adjacent to EESS allocations in the 50.2 – 50.4 GHz and 52.3 – 55.5 GHz bands, and Earth-to-space links in the 81 – 86 GHz band that is adjacent to the EESS band 86 – 92 GHz. What is different for the current vs. past proposals for new utilization is the global nature of the proposed radio service, and the high volume of radio transmitters and satellites planned to realize the global service. The global extent of new systems and the level of traffic proposed results in increased risk of contamination to existing EESS.

Other examples where the trend to increase spectral utilization may impact EESS include the band segment 36 – 37 GHz EESS band where an adjacent band segment, 37 – 37.6 GHz currently allocated for Government systems use, is being considered for re-allocation for commercial use and with dense radio systems. If this change is approved, there will be increased risk of contamination to EESS measurements in this region. There is also the case of the EESS band segment 18.6 – 18.8 GHz that is shared with Fixed Satellite Service (FSS), where space-to-Earth transmissions reflected from oceans and lakes routinely interfere with EESS measurements near the coasts of North and South America, Australia and many other regions of the ocean that are close to populated areas. Expansion of FSS services both in-band and adjacent to the 18.6 – 18.8 GHz band are likely to increase the current impact to global EESS observations in this band.

Other non-satellite applications near passive bands include broadband connectivity to aircraft in flight and ships at sea.

Specifically for NOAA's Advanced Technology Microwave Sounder (ATMS) instrument, Channels 1, 3, 4 and 16 appear to be at risk for interference, both over land and over ocean areas from these new spectrum users. Regulators appear to agree that the passive sensing missions from scientific satellites are important, but there are concerns about adequate protection from harmful interference as more and more systems are approved for operation.

2. Satellite Constellations and Adjacent Passive Band Usage

As Dr. Stephen English of ECMWF summarized after RFI2022, "<the speakers confirmed> the observations between 20 and 200 GHz have the largest impact on the skill of NWP of any observation type." Temperature profiles in portions of the 50 – 63

GHz band and precipitation data acquired in the 86 – 92 GHz segment, are likely to join a list of lower frequency passive bands potentially or significantly impacted by unwanted emissions.

A subset of planned or proposed or licensed satellite constellations are shown in Table 1 below:

Table 1. Selected Satellite Systems, adjacent to the 50.2-50.4 GHz or 81 – 86 GHz Passive Bands

System Name	No. of Satellites	Lifetime	24.25 – 27.5 GHz	47.2 – 50.2 GHz	50.4 – 51.4 GHz	81 – 86 GHz	Other	Comment
60Starlink (CHN)	1296 expanding to 12,000	Unkn.		X	X		TBD	Sponsored by Shanghai government in Ku, Q and V-band
Athena-5 (USA: EMTECH)	120	12 yrs.		X	X		X	Originally known as Theia
Kuiper (USA: Amazon)	3232 to 7774	7 yrs.		X	X		X	System filed for V-band
One Web (Europe: EUTELSAT)	Up To 6372	10 yrs.		X	X		X	
Starlink Gen2 (USA: SpaceX)	7500 granted 29988 requested			X	X	X	X	Gateway Uplinks have temporary authorization now
ViaSat (USA)	20	20 yrs.		X	X		X	
Multiple GEOs	More than 12	15 yrs.		X	X			
Broadband Terrestrial	Multiple Countries	Permanent	X					Roll out varies. Subject to ITU Res 750 (WRC-19)

For commercial systems that are authorized in the United States, some bands do not have formally established service rules which can impact out-of-band emission (OOBE) requirements levied upon the systems. The combined effects of multiple sources of OOBE and the worldwide nature of the ground uplinks for non-geostationary satellite constellations have the potential to create unwanted interference over portions of land areas on multiple continents.

Contamination of EESS measurement is exacerbated by the trend of EESS systems to utilize adjacent spectrum to the primary EESS band segment allocations in order to improve the radiometric performance of space-based systems. In Low Earth Orbit (LEO) the satellite ground track speed is determined by the orbital dynamics which in turn limits the dwell time of the scanning instrument. To improve sensitivity without increasing the complexity of the instrument, wider bandwidths are sometimes utilized to improve the radiometric sensitivity (Noise Equivalent Difference Temperature) and improve the sensor's environmental parameter retrieval capability. However, with increased use of adjacent bands, globally, this technique to improve radiometric sensitivity results in significantly increased impacts from Radio Frequency Interference even though usage of adjacent bands for the radiometer receiver has no impact on the radio service utilizing the adjacent bands. As a result, increased utilization of adjacent bands also limits the ability of EESS sensors to utilize extra bandwidth to improve their performance – even in areas of the globe that are sparely populated such as open ocean areas.

Due in part to increased spectral utilization, it becomes even more important to effectively determine when a measurement has contamination due to RFI. However, modern communications waveforms are often spread over wide-band frequency channels which tend to mimic the characteristics of naturally occurring Gaussian background noise. As a result, it becomes increasingly difficult to determine the level of contamination using Kurtosis-type tests which depend on a waveforms departure from Gaussian characteristics to identify contamination of the naturally occurring upwelling energy received at the radiometer in orbit.

This paper will discuss these factors and urge better coordination of how we advocate for protecting these passive bands.

Integrated RF Attenuation Maps for RFI Impact Assessments

Johan Havenga[1] and Abraham J. Otto[2]
(1) South African Radio Astronomy Observatory, Cape Town, South Africa, jhavenga@sarao.ac.za
(2) Jacobs, Wellington, New Zealand, braam.otto@jacobs.com

Radio Frequency Interference (RFI), Radio Frequency (RF) Attenuation Maps, Propagation Modelling, Square Kilometre Array (SKA)

1 Introduction

The SKA Observatory's mid-frequency radio telescope (SKA-MID) will consist of 197 15 m-diameter dishes operating between 350 MHz and 15.4 GHz. Construction of SKA-MID is currently underway in the Northern Cape of South Africa and will eventually integrate the existing 64-element MeerKAT array. The pristine radio-quiet MeerKAT National Park in the Karoo is home to a number of operational telescopes. Therefore, the management and control of RFI during the SKA-MID construction phase are critical. This paper proposes the use of pre-generated integrated RF attenuation maps to streamline interference impact assessments of large, complex telescope sites.

2 RFI Controls Process

The South African Radio Astronomy Observatory (SARAO) RFI team is responsible for establishing controls to minimise interference and maximise the scientific return of the radio astronomy telescopes in the national park. One such RFI control is the issuing of valid RFI permits or Certificates of Compliance (CoC) for temporary or permanent equipment to be installed on the observatory site. Interference management is done through RFI impact assessments that make use of RF propagation modelling to determine path loss between an interference source and a sensitive telescope receiver. Eligibility of RFI permits, or CoCs, is dependent on whether the levels of characterised radiated emissions from the devices in question are below the telescope protection thresholds [1, 2]. This is determined by evaluating the path loss available at a device's intended location toward any telescope receiver. With several operational radio telescopes in the MeerKAT National Park, and more set to be built in the near future, the required number of RFI impact assessments and path losses calculated drastically increase as construction continues. Pre-calculated integrated RF attenuation maps (Section 3) provide a much faster way of determining where a device is likely to interfere with surrounding sensitive receivers.

3 Integrated RF Attenuation Maps

The attenuation maps are based on the principle of RF propagation reciprocity. Rather than running point-to-point predictions for every unique interference assessment case (i.e., transmitting devices to the nearest receiving telescope), the maps use the various radio telescopes as "transmitters" in the propagation modelling point-to-point calculations for a fixed, meshed grid area. The point-to-point predictions for each radio telescope are generated using the Longley-Rice irregular terrain model (ITM) in SPLAT-RF! [3] with Shuttle Radar Topography Mission (SRTM) 1-arc second Digital Elevation Model (DEM) data for a radius of 20 km and a receiver height of 1.5 meters around each telescope. This leads to a data file, per emitter height, with path loss entries in decibels for every 30 meters in a grid with the telescope in question at the centre. This is done for every element in the array (i.e., 64 for MeerKAT or 197 for SKA-MID) and saved as individual attenuation maps. The individual receiver maps are integrated into a single map for a complete telescope array, and are produced over a range of frequencies between 50 MHz and 26 GHz. The aggregation is done by taking the minimum attenuation available in a grid block between all the individual maps. The result is a 3D dataset that is a function of longitude, latitude, and attenuation per frequency that can be interpolated per coordinates and frequency to determine the attenuation budget for that location. An example of an integrated attenuation map for the SKA-MID array at a frequency of 6 GHz is shown in Figure 1.

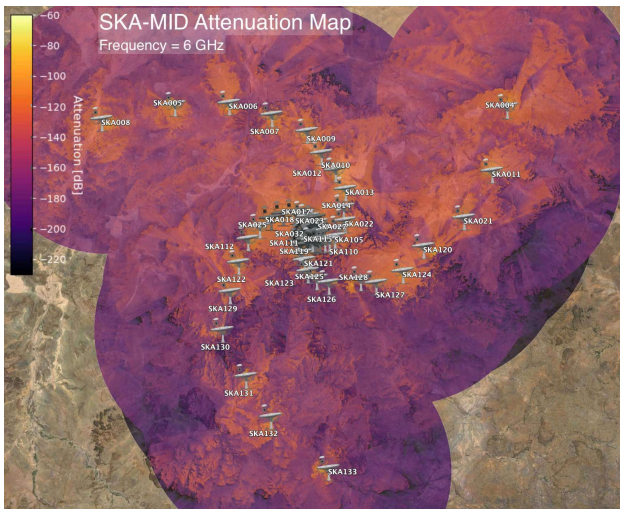

Figure 1. SKA-MID integrated attenuation map at a frequency of 6 GHz.

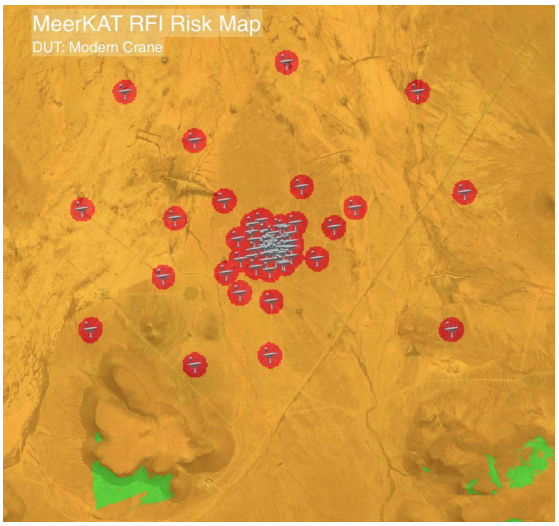

Figure 2. Zoomed in MeerKAT RFI risk map for a modern crane.

4 RFI Risk Assessment

Risk assessment tools were developed by both SARAO and the SKA Observatory [4] to reduce analysis time in determining where, and to what extent, devices might interfere with the operational telescopes. The input is an Effective Isotropic Radiated Power (EIRP) measurement file, or commercial/military EMC standards radiated compliance limits, and the output is a KMZ file that can be used in a GIS application. These tools use the pre-generated RF attenuation maps to quickly interpolate the path loss profiles, given the intended location of use, and produce RFI risk maps. The attenuation profile calculated is a list of attenuations applicable for various frequencies for that location. The RFI risk map in Figure 2 shows where an example temporary device will likely cause interference levels higher than the telescope protection thresholds (shown as yellow), as well as where it might exceed the radio telescope digital saturation levels (shown as red). When a location is highlighted as medium or high risk, a more detailed propagation analysis can be considered.

5 Conclusions

This paper highlighted the use of integrated RF attenuation maps to streamline interference impact assessments of large, complex telescope sites. The attenuation maps are based on the principle of RF propagation reciprocity. The maps are pre-generated by considering the radio telescopes as "transmitters" in the propagation modelling whilst determining point-to-point path loss calculations for a meshed grid surrounding the telescope receivers. An overview of risk assessment tools developed by both SARAO and the SKA Observatory was provided. The tools reduce analysis time in determining where devices are likely to interfere with the operational telescopes, thereby shortening turnaround time for RFI impact assessments. When a device at a specific location is highlighted as a medium or high risk, a more detailed propagation analysis can be considered to ensure compliance to the telescope protection levels.

References

[1] *Regulations on Radio Astronomy Protection Levels in Astronomy Advantage Areas declared for the purposes of Radio Astronomy*, Government Gazette, Republic of South Africa, No. 35007, pp. 31-34, 10 February 2012.

[2] A. J. Otto, F. Di Vruno, T. Nkawu, P. Dewdney, G-H Tan, H. Smith, T. Tzioumis and J. Jonas, *SKA RFI/EMC Standard*, Document Number SKA-TEL-SKO-0000202, Rev 4, SKA Observatory, Jodrell Bank, Macclesfield, UK, 2021-05-01.

[3] *RF Signal, Propagation, Loss And Terrain (SPLAT!) Analysis Software*, https://www.qsl.net/kd2bd/splat.html, Last accessed 28/06/2024.

[4] *SKAO RFI/EMC Standards*, https://emc-standards.skatelescope.org/, Last accessed 28/06/2024.

The Xbox ("EXperiment Box"): A Reconfigurable Test Setup for the Investigation of the EMI Shielding Properties of Materials and Interfaces within a Reverberation Chamber

Aneshka Bothma*(1), Jason Fynn*(1), and Jacobus Christiaan Visser (2)
(1) SARAO, Observatory, Cape Town, Western Cape, South Africa
e-mail: abothma@sarao.ac.za; jfynn@sarao.ac.za; cvisser@sarao.ac.za

1. Introduction

Across the industry, EMI hardened enclosures and interfaces are imperative to ensuring compliance with various EMI/RFI standards for radiated emissions and susceptibility. The application of such enclosures and interfaces are broad and often require further investigation once implemented into a final design to confirm their theoretical achievable shielding effectiveness through empirical measurements. The reconfigurable test setup XBox ("EXperiment Box") aims to aid the design process by providing a method to test and qualify subsystem level components during the prototyping stage before a final system design is assembled for compliance testing. This paper presents the results of different test methods using the XBox and their advantages and disadvantages.

2. Reconfigurable test setup

The XBox was derived from a method "fields in a single-fed partially loaded rectangular multimode cavity" [1] and a nested Reverberation Chamber (RC) measurement technique. The Xbox is fitted with an interface panel, which provides conductive continuity between the enclosure and an N-type RF connector. The N-type connector has a probe connected on the inside acting as a loop antenna, exciting magnetic fields which have perpendicular EM waves. The setup is seen as a two-port system measuring the scattering parameters between the two ports, with port 1 connected to the antenna in the RC and Port 2 connected to the Xbox's probe on the outside. The attenuation values of the open and closed Xbox can be subtracted to determine the shielding of the material. Initial investigations were done to ensure measurement efficiency and indicated that different probe locations excited several modes, but the typical attenuation difference was similar. That indicated that each of the probe locations excited sufficient modal distributions for a valid measurement to be made with one probe in one orientation.

(a) Xbox inside RC with Antenna

(b) Loop antenna on inside of XBox

Figure 1. Xbox two-port system setup

2. Investigations

Copper gland and braided cable.

A shielding prototype such as a copper gland and braided cable was measured using the **two-port Xbox system**. First the s-parameters of the two-port system were captured with the XBox open as the baseline to use in shielding calculation. Then the s-parameters of the two-port system were captured with the Xbox closed with the original solid metal plate as a reference for shielding comparison. Lastly the s-parameters of the two-port system were captured with the new metal plate with a braided cable going through a gland interface. The raw s-parameter data were processed to define the attenuation values between the open box and closed Xbox. This was used to compare the difference in attenuation (shielding) between the solid metal plate and the metal plate with the interface, which showed similar results, concluding good shielding on the interface. But because

of the use of a loaded multimode cavity technique with the two-port system, it is important to understand that the screened test box had modal excitation frequencies where resonant modes are excited according to the size of the test box. Therefore, the same measured values were plotted for the modal excitation frequencies to clearly see the attenuation comparison between the two different test setups.

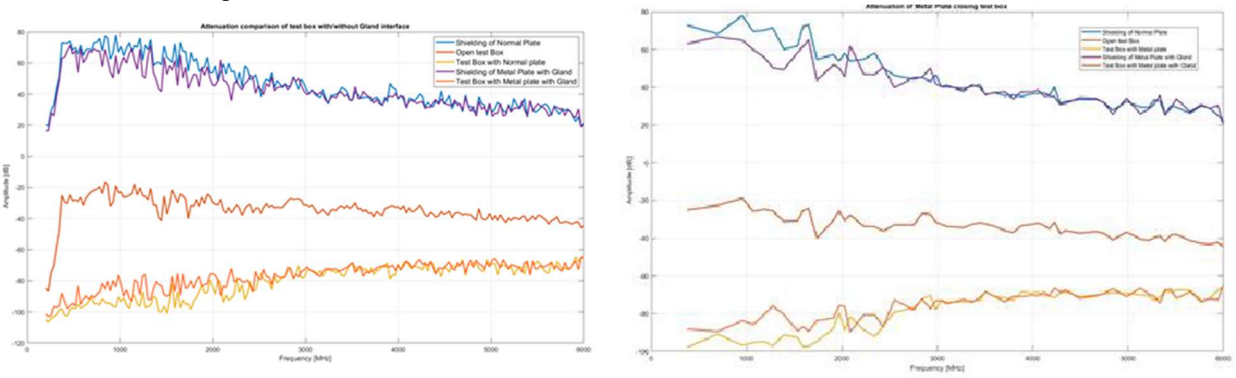

(a)Shielding attenuation (b) Shielding attenuation at modal excitation frequencies

Figure 2. Shieling results using the Xbox with the two-port system.

The advantage of the test setup is the exact known source projected in at port 2, however the disadvantage of this setup is that the system creates modal resonances due to not being able to stir the modal excitations within the enclosure, the enclosure size limits the test frequency range and needs calibration of the two-port system before measurement can be started.

Rotary gasket

Another shielding measurement method with the Xbox is to use a reference RF source. In this case a comb generator is used to test the SE of a copper rotary gasket. The **comb generator is placed inside of the Xbox**. The RC antenna measures the max emissions from the comb generator when Xbox is open as well as closed with the interface plate in place. The shielding of the interface plate is calculated by deducting the max emissions received of the two setups seen below. The example below shows the shielding properties of an EMI rotary gasket with and without a penetrating shaft.

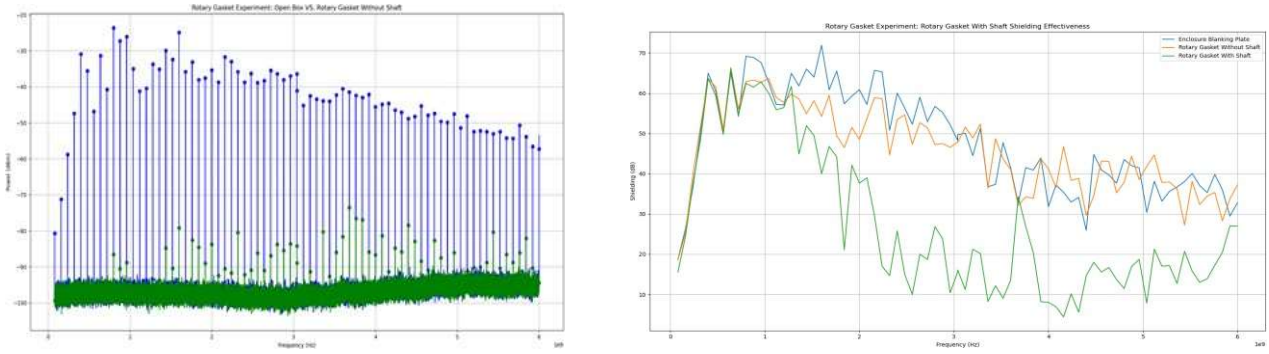

(a) Measured Power Delta (b) Calculated Shielding Effectiveness

Figure 1. Xbox comb generator setup

The above-mentioned method has proven to be less time consuming as there is no need for VNA calibration. It must be noted that this method has the disadvantage of loading the comb generator's antenna by placing it in the Xbox resulting in the actual radiated power being ambiguous. Further work is required to improve the field uniformity within the Xbox with this setup.

3. Summary and Conclusion

The investigations show that both methods with the Xbox works efficiently in determining the shielding value of a particular interface or material. This is valuable as more mitigation methods and materials have been needed to avoid EMI/RFI. The SARAO team evaluate shielding properties of many RFI mitigation solutions before implementation. It is recognized that future measurements are needed such as comparing the two methods results on the same interface, stirring and unstirring operation inside of the Xbox and orientation changes of the comb generator to conclude the investigation properly.

[1] Tse V. C. T. Chan and H.C. Reader, "Understanding Microwave Heating cavities" *Artech House*, 2000, pp. 102-105, ISBN 1-58053-094-X.

Wi-Fi Interference Removal in Córdoba: a stepping stone for better data quality on urban C-band Weather Radars

Matías E. Suárez* [1,2,3], Ignacio A. Montamat [1], Denis A. Poffo[1,2,3], Raúl A. Comes[1,2,3] and Andrés Rodríguez[2,3]
[1] Radar and Remote Sensors Laboratory (LRSR), Faculty of Mathematics, Astronomy, Physics and Computer Science (FaMAF), Córdoba, Argentina
[2] Hydrometeorological Observatory of Córdoba (OHMC), Ministry of Public Services, Córdoba, Argentina, info@ohmc.ar
[3] Hydrometeorology Laboratory (LHM), Faculty of Exact, Physical and Natural Sciences (FCEFyN), Córdoba, Argentina

1. Abstract

The present work shows Córdoba province's experience on Wi-Fi interference removal and mitigation for the RMA series weather radars, manufactured by INVAP SE. Specifically, the RMA-1 case is elaborated as it best illustrates how a heavily contaminated weather radar can become one of the cleanest in the network provided proper resource management and inter-institution collaboration. Materials and methods for detecting and removing/mitigating Wi-Fi interference are presented, as well as the necessary procedures to avoid incidence repetition. Finally, historical radar images are compared against actual ones in order to illustrate the implemented mechanism's performance.

2. Introduction

Argentina's weather radar network, known as SiNaRaMe, is one of the most advanced technologies for large-domain nowcasting in Latin America and the first network, south of the United States, to integrate both C-band and S-band weather radars along with other remote sensing instruments (e.g. disdrometers or automatic weather stations) [1]. By far, the most prominent sensors in this network are the C-band RMA series weather radars, manufactured by INVAP SE.
The RMA weather radar series represent more than 90% of the existing radars in the network. Deployed over 20 provinces, these systems provide hydrometeorological service for more than 95% of Argentina's population. Due to its operating frequency, nowadays point to point Wi-Fi signals represent an important threat to the radar's performance capabilities, especially under severe weather conditions [2].
Since its installation in 2015, the RMA-1 weather radar has been largely affected by Wi-Fi interference as it is deployed in the very core of Córdoba's capital, the second most populated city in the country. Taking this into account, two faculties from the National University of Córdoba (UNC) decided to join efforts and collaborate in overcoming this difficulty: the Faculty of Mathematics, Astronomy, Physics and Computer Science (FaMAF) and the Faculty of Exact, Physical and Natural Sciences (FCEFyN).

3. Material and Methods

In order to be able to detect and measure these unwanted Wi-Fi signals, the aforementioned academic units decided to invest in dedicated equipment from the ANRITSU brand: a portable vector network analyzer (VNA MS2038C) and an interference hunter equipped with a directional antenna (MA2700A). Additionally, a protocol for interference removal and mitigation was developed by the Radar and Remote Sensors Laboratory at FaMAF, and an assessment of the RMA series pointing accuracy and receiver's performance and selectiveness was carried out in collaboration with INVAP SE.
In parallel, the necessary permits and authorizations were requested and subsequently obtained from the competent authority (ENACOM, formerly CNC) to establish a regulatory framework for weather radars in Argentina, allowing its use as a radio frequency device and reserving its corresponding operating bandwidth. Furthermore, a job position was created for RMA-1's health status monitoring and a corresponding radar engineer was designated. This professional also acted as a contact point for the ENACOM's staff in order to coordinate actions for better effectiveness and smoother cooperation in the detection and neutralization of interference sources on a daily basis. All these measures allowed for the inclusion of the weather radar into ENACOM's operational work agenda as a priority asset.
Regarding the actual method for detecting and neutralizing an interference source, the main steps involved are the following: firstly, the direction of the interference source is estimated, at a broad level, by inspecting the radar's L2 imagery. The relevant images are then georeferenced on a GIS software (i.e. Google Earth) and radial traces are drawn over the interference line for finner direction detail. Subsequently, the interference is classified as being either near or far away from the radar based on its

characteristics and taking into account the radar's antenna specifications (i.e. directionality, location and secondary lobes gain). This procedure defines a potential geographic area for the location of the interference source. At this point, a vehicle campaign is initiated, equipped with detection tools (VNA and interference hunter) with the objective of assessing the area. Once the source of the interference has been identified, the owner or person in charge of the transmitting device is contacted and instructed to correct the issue immediately or else proceed with the equipment's deactivation and confiscation by the ENACOM.

4. Results

Since the RMA-1 became operational, a number of campaigns have been conducted with the objective of detecting and neutralizing a variety of sources of interference. As a result, the RMA-1 is now considered to be one of the cleanest weather radars in the network in terms of interference and it is continuously monitored. Figure 1 illustrates the last recorded event where intense interference was registered (mainly at the south-west of the radar) in May 2022 (left panel) and the resulting status after several campaigns implementing the protocol over a two-month period (right panel).

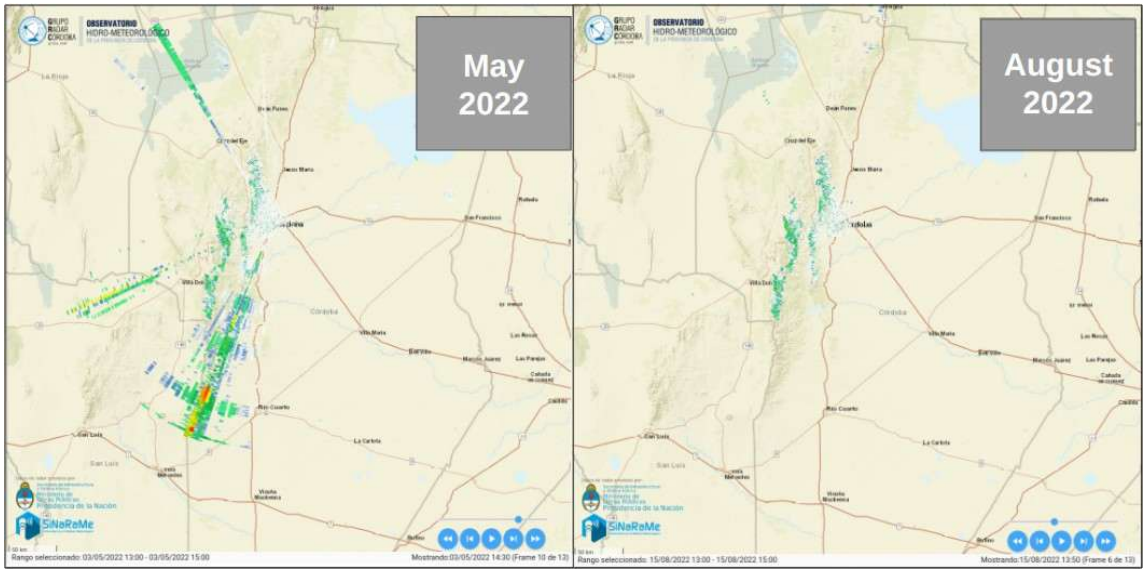

Figure 1. Before and after L2 Radar Reflectivity Factor COLMAX.

Currently, the RMA-1's health is being continuously monitored by the Radar and Remote Sensors Laboratory personnel as C-band communications are increasingly dense and the allocated bandwidth gets interfered every now and then by illegal unregistered transmitters.

5. Conclusions

The present work shows Córdoba province's experience on Wi-Fi interference mitigation for the RMA series weather radars manufactured by INVAP SE. This series represents more than 90% of the existing radars in the network. Deployed over 20 provinces, these weather radars provide hydrometeorological service for more than 95% of Argentina's population.
Due to its operating frequency, nowadays point to point Wi-Fi signals represent an important threat to the radar's performance capabilities. This work shows how inter-institution collaboration and proper resource management make possible the removal or mitigation of Wi-Fi interference on C-band weather radars. As a result of Cordoba Province's effort and state policies, the RMA-1 is nowadays one of the cleanest and most interference-free weather radars in Argentina and the developed know-how is available for replication across the RMA series and other weather radars in the region.

6. References

[1] A. Rodríguez, C. Lacunza, J. Serra, A. C. Saulo, H. H. Ciappesoni, et al., "SiNaRaMe: El Primer Sistema Integrado de Radares Hidro-Meteorológicos de Latinoamérica," *Revista de la Facultad de Ciencias Exactas Físicas y Naturales, Universidad Nacional de Córdoba*, 4; 1; 3-2017; 41-48, http://hdl.handle.net/11336/77624.
[2] E. Saltikoff, J.Y. Cho, P. Tristant, A. Huuskonen, L. Allmon, R. Cook, E. Becker and P. Joe, The threat to weather radars by wireless technology. Bulletin of the American Meteorological Society, 97(7), 2016, pp.1159-1167, https://doi.org/10.1175/BAMS-D-15-00048.1.

Impact of RFI on Numerical Weather Prediction and Climate Reanalysis

Stephen English, Tracy Scanlon, David Duncan, Alan Geer, Patricia de Rosnay, Pete Weston, Niels Bormann, Bill Bell, Mohamed Dahoui

ECMWF, stephen.english@ecmwf.int

1. Introduction

Weather forecasting beyond a few hours into the future relies on accurate computer simulations known as Numerical Weather Prediction (NWP). NWP in turn relies on millions of accurate observations to create the initial state for these computer projections. In the past these were primarily atmospheric weather observations and satellite measurements sensitive to weather parameters, but NWP now adopts an Earth System approach where observations of the earth's surface (e.g. land, snow, sea ice, ocean) and atmospheric composition (e.g. ozone, aerosol) are equally important. These observations rely on a number of narrow discrete spectral bands, each with unique properties, from 1.4 GHz to 190 GHz, with in the very near future additional bands up to 670 GHz. Many of these bands are afforded protection under footnote 5.340 of the Radio Regulations. However as pressure grows on some of these bands, efforts both to demonstrate their value and to monitor the status of RFI are vital. This abstract will describe current approaches and results from NWP centres, and will highlight the need to further develop enhanced bespoke RFI monitoring.

2. Current value of bands

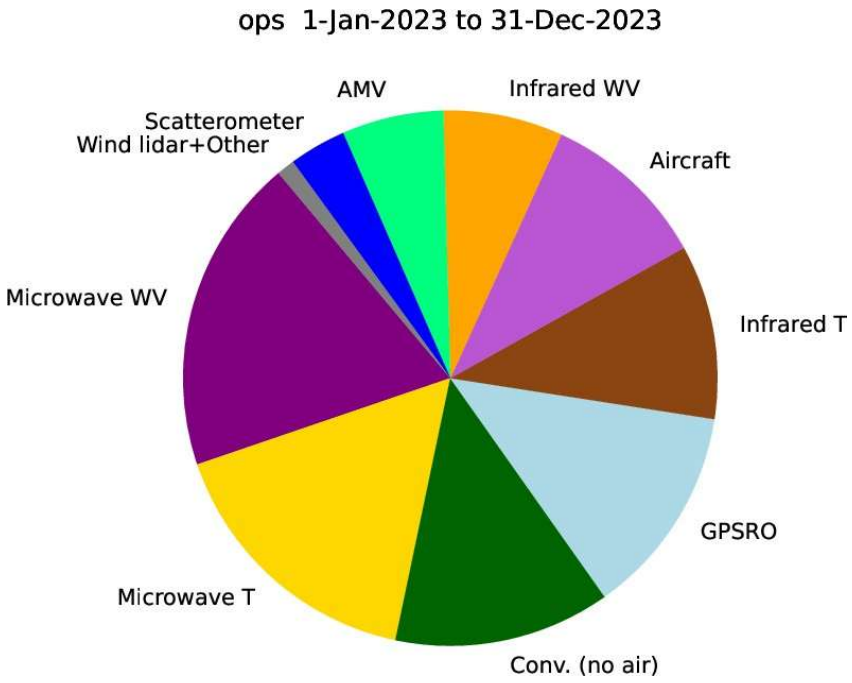

Figure 1. Current impact of main observing systems at ECMWF in 2023 (averaged over the whole year).

Figure 1 shows the latest contributions of different observation types at ECMWF to the skill of short-range weather forecasts through a technique known as Forecast Sensitivity Observation Impact, FSOI (Baker and Langland, 2004). Passive microwave observations account for around 36% of impact and active microwave around 17%, so 53% of the impact of observations on short range forecast skill came from microwave observations at ECMWF in 2023. Infrared satellite observations contribute

around 18%, surface and aircraft data 13% and 10% respectively and feature tracking in satellite images around 7%. This shows very clearly how important microwave observations are to numerical weather prediction, and thus the high societal and economic benefit of these observations.

Discussions concerning bands generally consider one band at a time. But in practice operational systems need a set of bands to uniquely separate different signals, from changes in temperature, water vapour, liquid water, precipitation, and changes in the earth's surface. The simplest way to consider this is if you have ten unknown quantities, you need ten independent observations. If you lose one, then the problem becomes mathematically ill-posed. This is a simplification but gives a general idea. It is challenging to isolate the value and impact of a single band, as it's loss or degradation will impact the correct interpretation of other bands, making the analysis more dependent on other prior information to solve the ill-posed inversion. However, in the broadest terms the bands between 50 and 58 GHz and between 175 and 192 GHz are the most critical, because they provide three-dimensional temperature and humidity information respectively. However, bands close to 10, 18, 24, 31, 89 and 150 (or 166) GHz are critical to correctly allow for the impact of clouds and rain on the signals. The bands close to 1, 7, 10 and 18 and 31 GHz are also critical for allowing for changes in the earth's surface. The loss of any one band undermines the integrity of the system that delivers the impacts described in the previous paragraph.

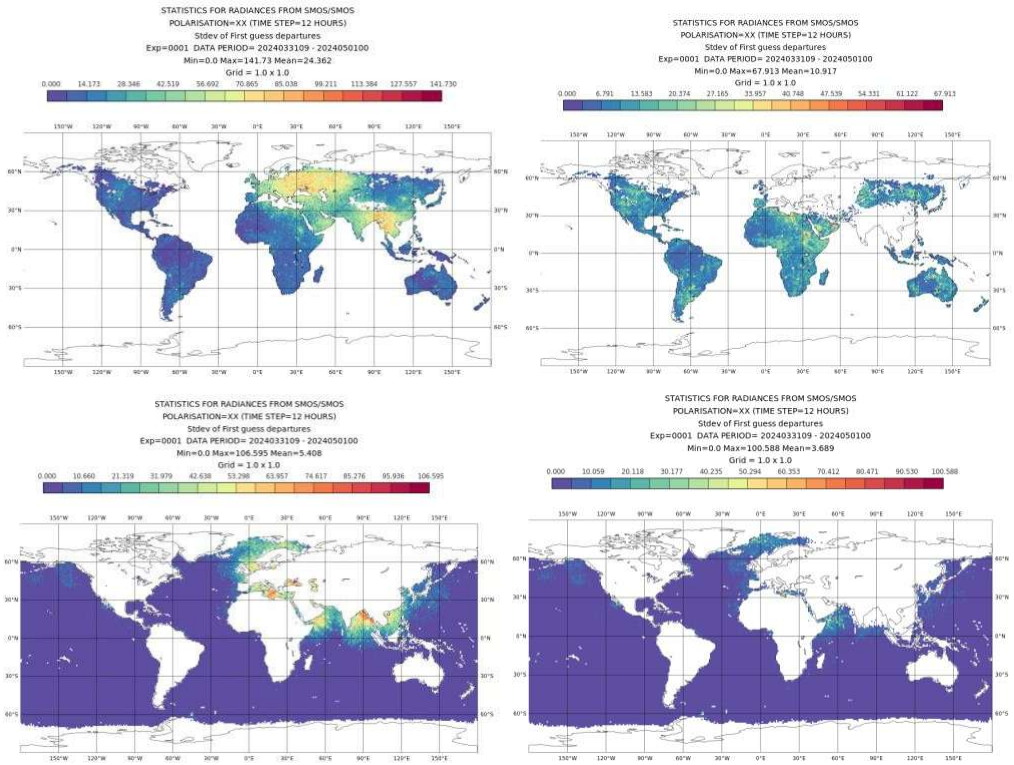

Figure 2. Impact of RFI on L-band (SMOS) 1.400-1.427 GHz in ECMWF NWP system shown as standard deviation of SMOS brightness temperature (in K), at 30 degrees incidance angle, x polarisation), before (left) and after (right) filtering, for land (top) and ocean surfaces (bottom), for April 2024.

The DA component of the NWP system is also used to produce a high-quality historical reanalysis datasets e.g. ERA-5 (Hersbach *et al*. 2020). Any impact of RFI on data used by reanalysis makes the assessment of climate trends more difficult especially if the level of RFI is changing with time. The impact of RFI on current reanalysis products is considered to be negligible. However, if there is a future increase in RFI in key bands, this could undermine their interpretation and our ability to accurately monitor climate change. This can occur both through sampling changes due to screening out some data and also the impact of undetected RFI.

3. Monitoring and detection

As shown in Weston and de Rosnay (2021) RFI screening of SMOS L-band data has been significantly improved in recent years but remains sub-optimal and fails to screen all SMOS observations which are affected by RFI (Figure 2). ECMWF was part of the ESA RFI4EO project led by Zenithal Blue Technologies aiming at using various statistical and pattern recognition algorithms (ground RFI detection system - GRDS) to improve the RFI screening (Oliva et al., 2021). Results using a month of

SMOS data indicated that the GRDS system demonstrates significant improvements. Standard NWP monitoring and ML enhancement.

4. Attribution

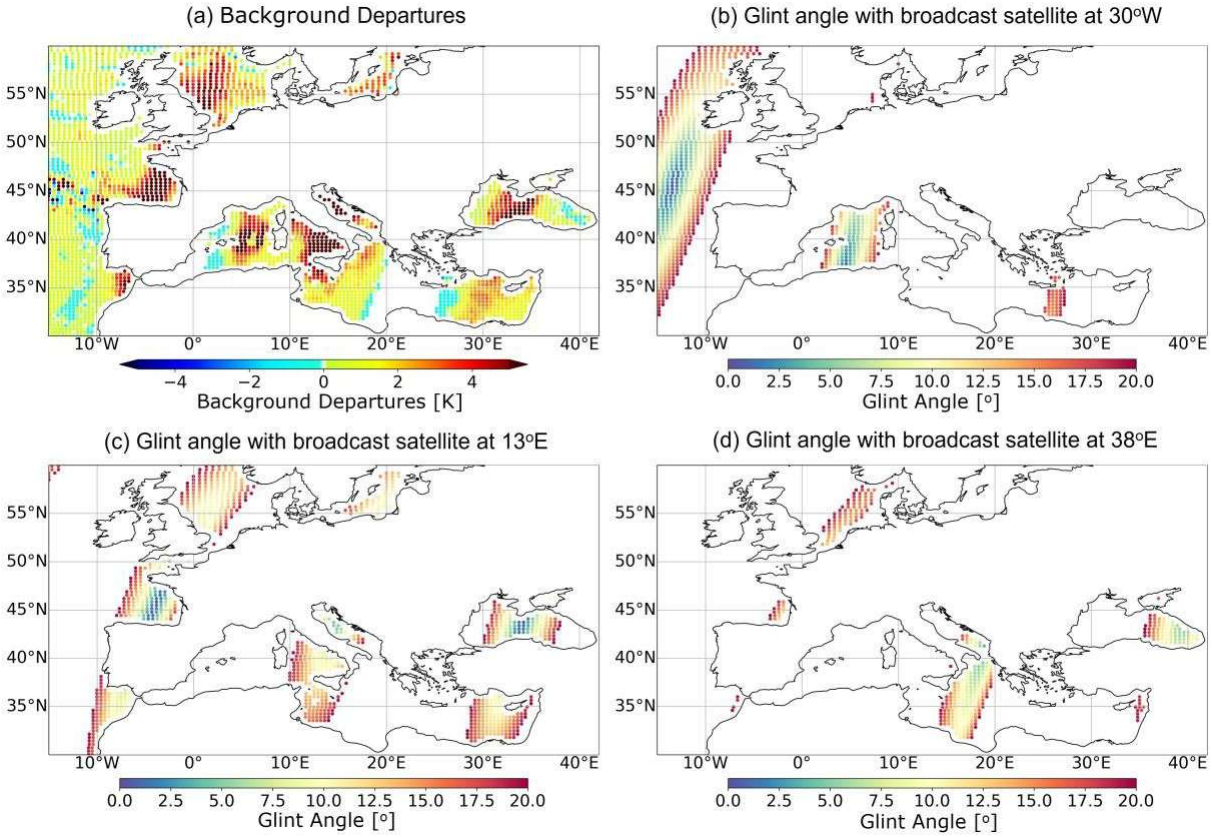

Figure 3: Maps for 2022-07-15T00 for (a) background departures due to RFI contamination and the glint angles of the observations with geostationary satellites placed at (b) 30°W, (b) 13°E and (c) 38°E.

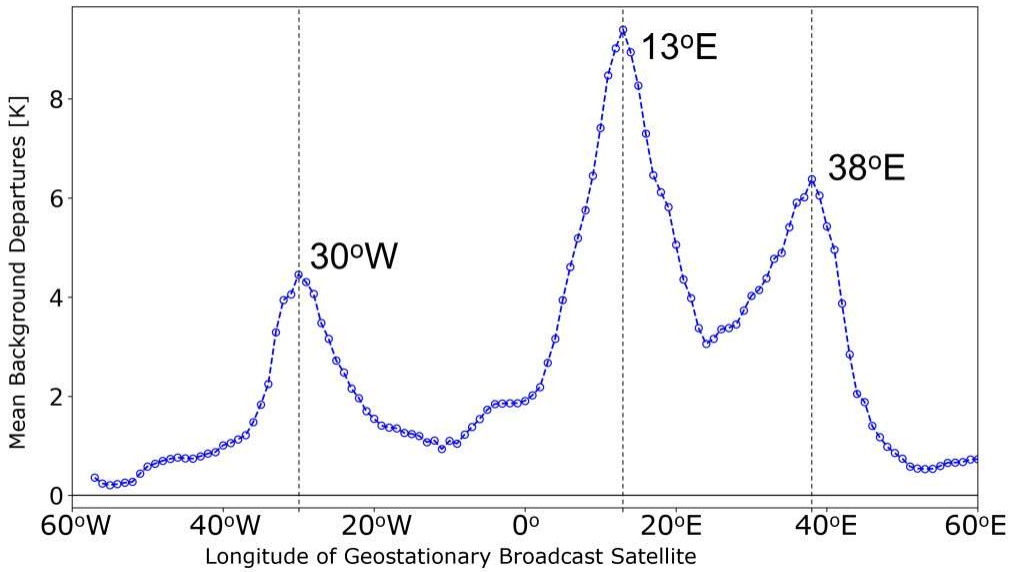

Figure 4: With geostationary satellites placed at 1°longitude spacings (at the equator), the mean of the background departures over Europe is calculated for the locations where the corresponding glint angle is less than or equal to 3°.

With the recent introduction of low frequency MW channels to support ocean analysis, it has been seen that the 10.65v GHz channel on AMSR2 suffers from large positive background departures over Europe (Figure 3a) in the descending node which

are suspected signals from broadcast satellites being reflected off the ocean. These departures align with low glint angles (below 3 degrees) between AMSR2 and specific theoretical geostationary satellites placed at 1 degree spacings around the equator. Figure 4 shows the peaks in the background departures relating to specific theoretical geostationary satellite locations with the related glint patterns shown in Figure 3 (b to d).

5. Summary

Clean spectrum in critical bands underpins the performance of modern NWP systems, which in turn underpin the reliability and accuracy of warnings, resulting in saving of life and property, in addition to day-to-day socioeconomic benefits. This clean spectrum cannot be taken for granted and enhanced monitoring of interference is being developed. This is showing increased occurrence of RFI in bands below 20 GHz, and in some cases it is possible to identify the likely source. However enhanced monitoring and on flight filtering need to be backed up by strong and effective regulation based on international agreement, at the World Radiocommunication Conferences.

[1] H. Hersbach, Bell B, Berrisford P, et al. The ERA5 global reanalysis. *Q J R Meteorol Soc*. 2020; 146: 1999–2049. https://doi.org/10.1002/qj.3803

[2] R. H. Langland, and N. Baker, "Estimation of observation impact using the NRL atmospheric variational data assimilation adjoint system," 2004 *Tellus*, 56A, 189–201.

[3] R. Oliva *et al*., "Results from the Ground RFI Detection System for Passive Microwave Earth Observation Data," *2021 IEEE International Geoscience and Remote Sensing Symposium IGARSS*, Brussels, Belgium, 2021, pp. 1827-1830, doi: 10.1109/IGARSS47720.2021.9553636.

[4] P. Weston and P. de Rosnay. "SMOS Brightness Temperature Monitoring Quality Control Review and Enhancements" *Remote Sensing 13, no. 20* (2021) doi: 10.3390/rs13204081

RFI 2024

SigCLR: A contrastive learning approach to unsupervised modulation recognition and novelty detection

Nicholas Bruce*(1), Belaid Moa(2), Stephen Harrison(1) and Peter Driessen(2)
(1) Dominion Radio Astrophysical Observatory, Herzberg Astronomy and Astrophysics Research Centre, National Research Council Canada, Penticton, BC, Canada
(2) Department of Electrical and Computer Engineering, University of Victoria, Victoria, BC, Canada

1 Introduction

As radio environments become more occupied, and radio frequency interference (RFI) monitoring efforts increase to wider bandwidths, there is a huge amount of RFI data being collected. At the Dominion Radio Astrophysical Observatory (DRAO), a progression of work has led from building a wideband RFI monitor [1], to finding a method for detecting signals in wideband spectra [2], and finally extracting baseband time series of these detected signals [3] while discarding the rest of the wideband spectra. This process not only reduces the data volume, it recovers the time-domain characteristics of the interfering signals. These time-domain characteristics are lost in other common stored data types like integrated power spectra and occupancy.

Collecting data in this way enables rich RFI science, such as RF site characterization and signal identification, to be done without storing large data volumes. However, a major challenge posed by this type of dataset is that it lacks labels, which makes tasks such as modulation recognition, feature vector extraction, and novelty detection difficult.

2 This work

In this work we demonstrate a method of both modulation detection and novelty detection on an unlabelled dataset. The dataset contains 53 modulations and more than one million unique signals. It was generated using TorchSig [4]. This large signal count is necessary for self-supervised deep learning methods. One such method is called contrastive learning, which is renowned for its excellent performance and ability to accurately detect and label objects in images [5]. This method is more accurate than state-of-the-art supervised methods such as ResNet-50, but requires a far larger training set.

We introduce our model architecture, SigCLR, in which we adapt and apply the image-based contrastive learning method to complex-valued radio time-series data from the TorchSig dataset.

Figure 1 shows the architecture and training process for the model. Each time-series signal $s(t)$ is duplicated and a different RF-specific augmentation, a_i and a_j such as gain drift, clipping, or spectral inversion are selected from the same family of augmentations A. The now differently augmented copies $s_1(t)$ and $s_2(t)$ are passed through identical encoders, and projection heads. The resulting representations z_1 and z_2 are compared at the output of the projection heads using a cross-entropy function which teaches the network that the signals should be identical. Once trained, the augmentation pipeline is removed from the start of the network and the projection head is removed from the end of the network, leaving the encoder. The encoder is used alone as the input to downsteam tasks. Some downstream tasks we show include SigCLR's ability to cluster similar types of signals, which results in a modulation detector, and identify anomalous signals which weren't well represented in the training data.

We intend to show SigCLR working on real signals collected at DRAO, and eventually integrate it into our operational RFI monitor where it will be used to help characterize the sites RF environment as well as alert site operators to anomalous signals in real-time.

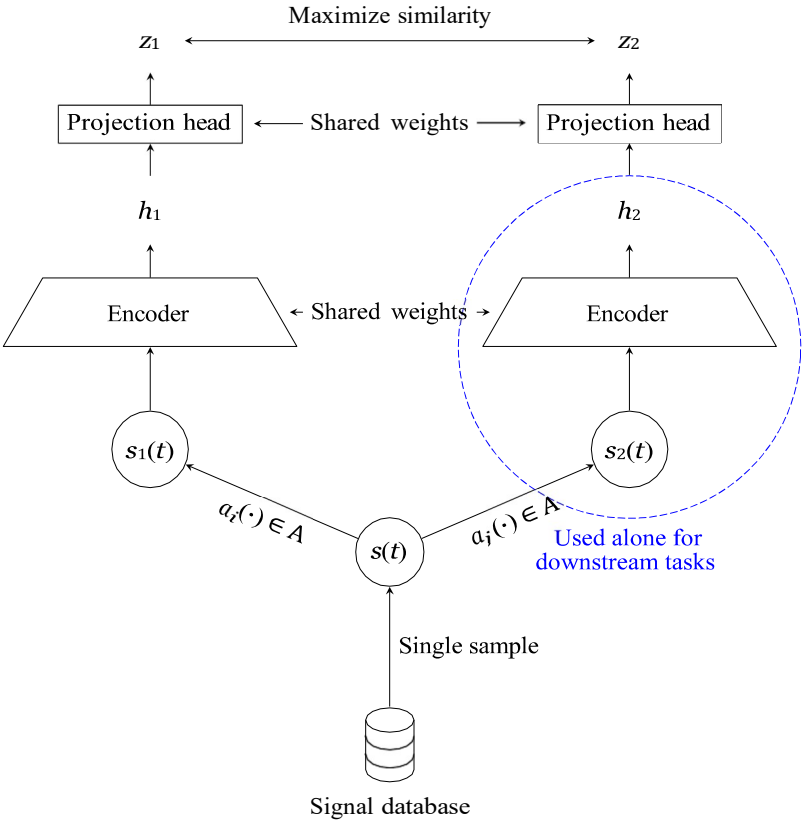

Figure 1. SigCLR model architecture

References

[1] S. Harrison, A. Lakhani, J.-P. Lavigne, *et al.*, "RFI monitor system design for the Dominion Radio Astrophysical Observatory," in *XXXIV General Assembly and Scientific Symposium of the International Union of Radio Science*, 2021.

[2] S. Harrison, R. Coles, T. Robishaw, and D. Del Rizzo, "RFI novelty detection using machine learning techniques," in *RFI2019: Coexisting with Radio Frequency Interference*, 2019.

[3] N. Bruce, S. Harrison, and P. Driessen, "DDC Pool: Efficient down-conversion of signals for RFI monitoring," in *Proceedings for RFI 2022*, 2022. [Online]. Available: https://www.ursi.org/proceedings/2022/rfi2022/RFI22PaperDDCPoolEfficientdownconversionofsignalsforRFImonitoring.pdf (visited on 11/18/2023).

[4] L. Boegner, M. Gulati, G. Vanhoy, *et al.*, *Large scale radio frequency signal classification*, arXiv:2207.09918, 2022. arXiv: 2207.09918 [cs-LG]. [Online]. Available: https://arxiv.org/abs/2207.09918.

[5] T. Chen, S. Kornblith, M. Norouzi, and G. Hinton, *A Simple Framework for Contrastive Learning of Visual Representations*, en, arXiv:2002.05709 [cs, stat], Jun. 2020. [Online]. Available: http://arxiv.org/abs/2002.05709 (visited on 02/02/2024).

Evaluating Low-Precision Floating-Point Formats for Next-Generation Radio Telescope Correlators and Beamformers: A Quantitative Analysis of Linearity and Dynamic Range

Thushara Kanchana Gunaratne [(1)], and Nicholas Bruce*[(1)]
[(1)] Herzberg Astronomy and Astrophysics Research Center, National Research Council Canada, Penticton, British Columbia, Canada, Thushara.Gunaratne@nrc-cnrc.gc.ca

1. Introduction

The global Radio Frequency Interference (RFI) environment is deteriorating, affecting even the most remote and sparsely populated regions that were prime candidates for radio telescopes [1]. This decline is largely due to the proliferation of ubiquitous terrestrial wireless communications systems and thousands of satellites providing communication, broadcasting, sensing, and navigation services [2]. Recently, the wireless communication industry has been pushing for the allocation of spectrum frequencies beyond 100 GHz, which were traditionally reserved for radio astronomy and other passive observations, for both terrestrial and space communications [3-4]. This will further exacerbate the impact of RFI for existing and future radio telescopes. Historically, astronomers humorously suggested placing highly sensitive radio astronomical observatories on the far side of the moon to shield those from Earth's RFI. This idea, once a mere jest, is becoming a reality with plans to launch telescopes such as the Lunar Crater Radio Telescope (LCRT) [5] and LuSEE-Night [6] projects to the moon's far side in the near future. However, these facilities will still require a communication system with satellites orbiting the moon to relay observed data back to Earth. Also, there is the risk of self-interference from the electronics and power systems of the radio telescope itself. Moreover, the moon risks becoming crowded with RFI as additional lunar exploration missions, such as those planning to establish communication networks like Nokia's proposed 4G lunar network [7], move forward. Given these challenges, it is crucial to explore other RFI mitigation strategies that can be applied for Earth-based radio telescopes. The following study focuses on maintaining the linearity of the signal processing chain to prevent strong RFI from contaminating the spectral ranges critical for key radio astronomical experiments.

2. Maintaining the Linearity of the Signal Chain

One of the primary goals of radio telescopes is to achieve high dynamic range observations across a wider spectrum. The forthcoming 2030 Wideband Sensitivity Upgrade (WSU) for the Atacama Large Millimeter/sub-millimeter Array (ALMA) is set to significantly enhance its capabilities. This upgrade will double the instantaneous bandwidth processed by the telescope to 16 GHz, and later increase it to 32 GHz, while also achieving an imaging dynamic range of approximately 42 dB (15,000:1) [8]. Similarly, the next-generation Very Large Array (ngVLA) telescope, an advanced and expanded version of the existing Very Large Array (VLA) in New Mexico, USA, plans to introduce a new frequency band (Band 6) covering 70 – 116 GHz [9]. The ngVLA aims for a dynamic range of 45 dB across its full operational frequency range from 1.2 GHz to 116 GHz [9]. For these advanced radio telescopes, the current development efforts are concentrated on enhancing antennas, feeds, receivers, clock distribution networks, and digitizers to capture celestial signals with high fidelity. The following sections will delve into the processing of these digitized signals, focusing on the generation of visibilities and beams with high dynamic range.

Achieving a high dynamic range in visibilities and beams is crucial along with high linearity throughout the signal chain of the correlator and the beamformer [10]. A highly linear signal chain not only ensures that visibilities and beams accurately reflect the signal strengths of celestial phenomena but also helps to avoid spectral confusion from harmonics and intermodulation products. This is particularly important when strong RFI signals are present, as non-linearities in the signal chain can create spectral artifacts that obscure faint celestial signals, thereby reducing dynamic range and leading to false detections [10]. Traditionally, the digital signal chain of a correlator or a beamformer is implemented with fixed-point arithmetic [11] that offers deterministic precision and simple hardware implementation [10]. To maintain linearity with fixed-point arithmetic, especially when the signal bandwidth changes significantly, it is essential to increase the resolution and/or scale the signal appropriately at each stage [11]. This often involves extending the bit width to accommodate the full dynamic range of the signal without overflow or underflow, and carefully applying scaling to preserve precision [10]. Therefore, designing fixed-point signal chains requires extensive analysis and verification to balance precision, dynamic range, resource utilization and power dissipation.

On the other hand floating-point number representation offers a way to achieve a higher dynamic range using a fixed bit-word size, though it can compromise linearity to some extent along with higher hardware complexity [11]. Low precision floating-point formats such as Float16, bFloat16, TensorFloat32, and Float32 are increasingly used in deep-learning neural network implementations and are supported natively by major Graphics Processing Unit (GPU) vendors like NVIDIA, Intel, and AMD [12]. For Field Programmable Gate Arrays (FPGAs), Intel-Altera has also integrated native support for addition, subtraction, and multiplication operations in Float16 and Float32 formats within the DSP blocks of their Agilex-7 series FPGAs [13]. AMD-Xilinx has followed through with the support for Float16 and Float32 formats in their Versal devices [14]. We hypothesize that the signal chain for the correlator beamformer in next-generation radio telescopes could be efficiently implemented using these low-precision floating-point numbers, potentially reducing resource consumption and power dissipation while still meeting the requirements for linearity and dynamic range. To this end, we have initiated a quantitative study to assess the linearity and dynamic range of a correlator beamformer implemented with Float16, TensorFloat32, and Float32 formats along with fixed-point formats of the same length 16-, 19- and 32-bits under various RFI conditions. In this study, test vectors representing expected RFI levels at a remote site at the 10th, 50th, and 90th percentiles are used. These vectors are processed with a typical 'FX' type correlator [10] that has been designed to achieve a dynamic range of 50 dB using the proposed floating-point formats, and the resulting visibilities are compared with those from a 'golden reference' model using Float64 format. Similarly, an end-to-end simulation of a 'phase-delay' beamformer using the candidate floating-point formats and related fixed-point formats will be conducted to compare the generated beams against the golden reference.

[1] I. Sihlangu, N. Oozeer, and B. A. Bassett, "Nature and Evolution of UHF and L-band Radio Frequency Interference at the MeerKAT Radio Telescope," in Proceedings of RFI Workshop 2022 [Online], Feb. 2022.

[2] C. G. De Pree, C. R. Anderson, and M. Zheleva, "Astronomy is under threat by radio interference from satellites – here's what can be done about it," World Economic Forum, Mar. 07, 2023. Available: https://www.weforum.org/agenda/2023/03/astronomy-radio-interference-satellites-technology/. [Accessed: Jun. 26, 2024]

[3] T. S. Rappaport et al., "Wireless Communications and Applications Above 100 GHz: Opportunities and Challenges for 6G and Beyond," in IEEE Access, vol. 7, pp. 78729-78757, 2019, doi: 10.1109/ACCESS.2019.2921522.

[4] "Preferred frequency bands for radio astronomical measurements below 1 THz," International Telecommunication Union - Radiocommunication Sector, Recommendation ITU-R RA.314-11, 2023. Available: https://www.itu.int/dms_pubrec/itu-r/rec/ra/R-REC-RA.314-11-202312-I!!PDF-E.pdf. [Accessed: Jun. 26, 2024]

[5] S. Bandyopadhyay et al., "Conceptual Design of the Lunar Crater Radio Telescope (LCRT) on the Far Side of the Moon," 2021 IEEE Aerospace Conference (50100), Big Sky, MT, USA, 2021, pp. 1-25, doi: 10.1109/AERO50100.2021.9438165.

[6] S. D. Bale et al., "LuSEE 'Night': The Lunar Surface Electromagnetics Experiment." arXiv, Jan. 24, 2023. doi: 10.48550/arXiv.2301.10345. Available: http://arxiv.org/abs/2301.10345. [Accessed: Jun. 26, 2024]

[7] "Nokia aims for the Moon with LTE/4G | Nokia." Available: https://www.nokia.com/about-us/newsroom/articles/nokia-aims-for-the-moon-with-lte4g/. [Accessed: Jun. 26, 2024]

[8] J. Carpenter, C. Brogan, D. Iono, and T. Mroczkowski, "The ALMA2030 Wideband Sensitivity Upgrade," ALMA Memo 621, Oct. 2022. Available: https://library.nrao.edu/public/memos/alma/main/memo621.pdf. [Accessed: Jun. 26, 2024]

[9] "ngVLA Performance Estimates", (December 2021) Available: https://ngvla.nrao.edu/page/performance. [Accessed: Jun. 26, 2024]

[10] A. R. Thompson, J. M. Moran, and G. W. S. Jr, Interferometry and Synthesis in Radio Astronomy, 3rd edition. New York, NY: Springer/Sci-Tech/Trade, 2017.

[11] M. D. Ercegovac and T. Lang, Digital Arithmetic. Morgan Kaufmann Publishers, 2004.

[12] NVIDIA Corporation, NVIDIA Tesla P100 GPU architecture, WP-08019-001 v01.1, (2016). Available: https://images.nvidia.com/content/pdf/tesla/whitepaper/pascal-architecture-whitepaper.pdf. [Accessed: Jun. 26, 2024]

[13] "Intel Agilex® 7 Variable Precision DSP Blocks User Guide," Intel. Available: https://www.intel.com/content/www/us/en/docs/programmable/683037/23-3/variable-precision-dsp-blocks-overview.html. [Accessed: Jun. 26, 2024]

[14] "Versal ACAP DSP Engine Architecture Manual", AMD-Xilinx. (AM004), 2022-09-11. Available: https://docs.amd.com/r/en-US/am004-versal-dsp-engine/Floating-Point-Time-Interleaved-Dot-Product-Engine. [Accessed: Jun. 26, 2024]

RFI 2024

RFI mitigation filter for CHIME/FRB data based on the Karhunen–Loève (KL) transform

Shion Andrew*(1) and Juan Mena-Parra (2)
(1) MIT Kavli Institute for Astrophysics and Space Research, Massachusetts Institute of Technology, USA
(2) Dunlap Institute for Astronomy & Astrophysics, University of Toronto, Canada

PoS(RFI2024)070

1 Introduction

Extragalactic fast radio bursts (FRBs) are bright (1-100Jy) millisecond-duration radio pulses of unknown astrophysical origins. Thanks to its large field of view (~ 200 sq. deg.) the Canadian Hydrogen Intensity Mapping Experiment (CHIME) telescope has emerged as the world's leading detector of FRBs. CHIME is a phased radio interferomter operating from 400-800MHz, making it a powerful instrument for measuring frb morphology, polarimetry, and more recently angular positions with very long baseline interferometry (VLBI) [1]. However, a broad range of RFI sources typically renders ~ 40% of the band unusable, limiting the accuracy of measurements that require broad band information such as VLBI fringe fits and rotation measure fits.

One type of RFI mitigation strategy permitted by phased antenna array radio telescopes such as CHIME is spatial filtering of RFI from the desired signal through adaptive beamforming. The primary advantage of adaptive beamformers is that they are non-parametric–no a priori knowledge about the RFI source is required, which is particularly useful for types of RFI that are unpredictable in time and frequency.

Here we present one type of spatial filter based on the Karhunen–Loève (KL) transform and demonstrate its performance on CHIME/FRB channelized raw voltage data.

2 Implementation

Suppose we have voltage data measured over N antennas represented by the vector $\boldsymbol{d}$. This dataset consists of the desired astrophysical signal $\boldsymbol{s}$ as well as signals from interfering sources $\boldsymbol{f}$. Assuming the signal to be uncorrelated with the noise, the full array covariance of the dataset $\hat{D}$ is then

$$\hat{D} = \langle \boldsymbol{d}\boldsymbol{d}^{\dagger} \rangle = \hat{S} + \hat{F},$$

where $\hat{S}$ and $\hat{F}$ denote the array covariance of the desired signal and unwanted interference, respectively. In most cases, the principal components of these constituent signals occupy different vector subspaces. For instance, in the case that the desired signal is from a a single point source in the sky, $\hat{S}$ will be rank 1. So long as the source of interference does not exhibit a spatial signature identical to the desired signal, the eigenvectors corresponding to the largest eigenvalues of $\hat{F}$ will occupy a subspace that is distinct from the subspace occupied by $\hat{S}$.

The KL filter rotates the data into a vector space where $\hat{S}$ and $\hat{F}$ are simultaneously diagonalized such that diagonal elements of the total covariance matrix, which we will denote as Λ, are a direct measurement of the signal-to-contaminant ratio of a given mode. The corresponding change of basis matrix R can be obtained from the generalized eigenvalue equation

$$\hat{S}\hat{R} = \hat{F}\hat{R}\hat{\Lambda}. \tag{1}$$

Thus the full KL filter operation on the voltage data can be expressed as

$$\boldsymbol{d}_{\text{filtered}} = \hat{R}\hat{X}\hat{R}^{-1}\boldsymbol{d} \tag{2}$$

where $\hat{X}$ is a diagonal matrix with zeroes corresponding to the modes we wish to remove.

For CHIME/FRB data, we make two important notes. First–because all our sources of interest are point sources, we only require a single mode from our data. In this case the filter operation can be re-cast as a beamformer:

$$b(t) = \boldsymbol{s}^{\dagger}\boldsymbol{d}_{\text{filtered}} \tag{3}$$

$$= \boldsymbol{s}^{\dagger}\hat{R}\hat{X}\hat{R}^{-1}\boldsymbol{d} \tag{4}$$

$$\propto R^{-1}\boldsymbol{d} \tag{5}$$

where $\boldsymbol{s}^{\dagger}\hat{R}\hat{X}$ reduces to a constant in the case that X is rank 1. This is another form of the well-known maximum signal-to-noise beamformer or MVDR beamformer where the constant is set by the desired normalization of the beam[2]. Second—we note that this filter requires a model for $\hat{S}$ and an estimate for $\hat{F}$. $\hat{S}$ is well modeled for CHIME as long as the steering vector of the beam is specified. For frequency channels that are heavily RFI contaminated, the eigenvalues characterizing all contaminants will be much larger than those characterizing the desired signal, in which case $\hat{F}$ can be obtained from the sample covariance of the data. In the case of transients where the expected arrival time of the astrophysical pulse is already known, $\hat{F}$ can be obtained for *any* frequency channel by computing the sample covariance immediately before or after the pulse (typically ~ 10ms long), under the assumption that $\hat{F}$ is stationary under short timescales.

3 Results and Conclusions

Figure 1 shows a comparison between the sensitivity of an FRB observation obtained from conventionally beam-forming to the observation obtained after applying the KL filter over the frequency range 730-750MHz, a portion of the CHIME band where RFI is typically ~ 20 – 30dB stronger than the sky. While the observation without the filter is completely corrupted by rfi interference, the data post-cleaning recovers a measurement of the FRB pulse that otherwise would have been un-observable in this part of the band.

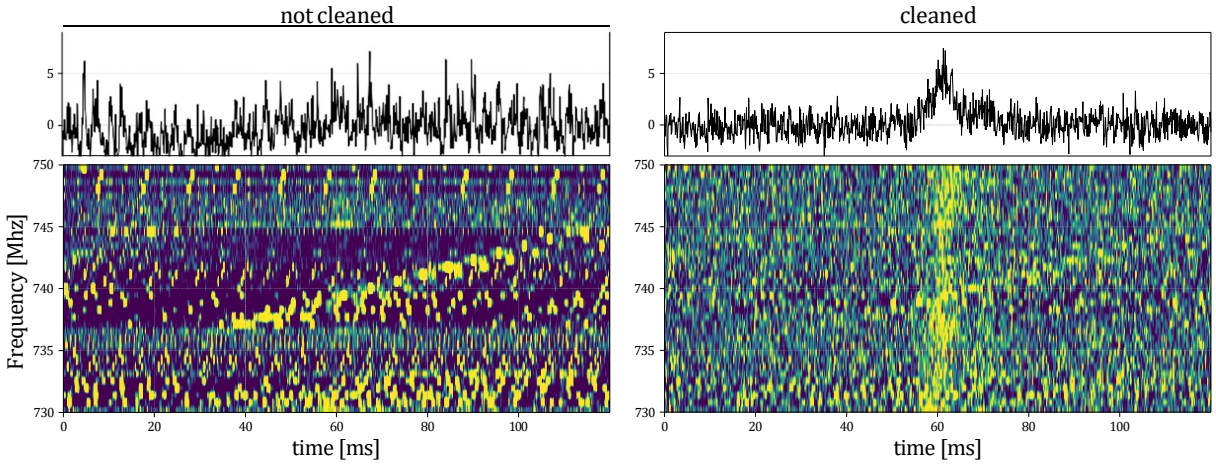

Figure 1. Waterfall plot of the power measured by CHIME post-beamforming towards the fast radio burst FRB20191219F without applying the KL-filter (left) and after applying the filter (right) for RFI contaminated channels.

This example demonstrates the potential for our KL-based RFI mitigation technique for observing transients with the CHIME instrument, as well as next-generation radio inteferometers for transients more broadly such as CHORD, BURSTT, and CHARTS. Finally, while the example provided demonstrated the recovery of pulse morphology, this filter can be applied to a broad range of applications that require broad band information, including polarimetry, scintillometry, and VLBI.

References

[1] Lanman, A. E., "CHIME/FRB Outriggers: KKO Station System and Commissioning Results", *arXiv e-prints*, 2024. doi:10.48550/arXiv.2402.07898.

[2] Capon, K., "High-resolution frequency-wavenumber spectrum analysis", *Proceedings of the IEEE*, vol. 57, no. 8, pp. 1408-1418, Aug. 1969, doi: 10.1109/PROC.1969.7278.

COPERNICUS IMAGING MICROWAVE RADIOMETER SATELLITE RADIO FREQUENCY INTERFERENCE PROCESSOR

Steen Savstrup Kristensen[(1)], Jan E. Balling[(1)], Sten Schmidl Søbjærg[(1)], Niels Skou[(1)], Tiziano Botticchio[(2)], Valerio Tocca[(2)], and Lorenzo Forgia[(2)],

(1) National Space Institute, B 348, Technical University of Denmark
DK-2800 Kgs. Lyngby, Denmark
e-mail: ssk@space.dtu.dk

(2) Thales Alenia Space Italy
Via Saccomuro, 24 – 00131, Rome, Italy

The Copernicus Imaging Microwave Radiometer (CIMR) satellite with its on-board Radio Frequency Interference (RFI) processor has been under design, development and manufacturing for some years now. Compared to previous microwave imaging satellites CIMR has significantly increased requirements for both spatial and radiometric resolution in order to improve monitoring of a large number of geophysical parameters. This has led to a significantly larger analogue input bandwidth, and with the growing amount of RFI within the microwave frequency bands used by CIMR, RFI detection and filtering is paramount.

Algorithms for detection and filtering of RFI in radiometer data have been developed for at least two decades. These algorithms require Analogue to Digital Converter (ADC) sampling of the full radiometer bandwidth without aliasing as well as digital processing at the sampling data rate. This has to be done on-board as it is impossible to downlink the number of raw ADC samples needed to hold the full analogue bandwidth. On-board processing can be done using modern high-speed ADCs and the large Field Programmable Gate Arrays (FPGA) available today.

The first ESA effort to perform in-flight on-board RFI detection and filtering will be done at Ku-band on the meteorological satellite MetOp-SG-B which comprises a microwave imager that includes Ku-band. This satellite is now expected to be launched in 2026 so unfortunately no in-flight experience is available yet. The CIMR satellite, a high priority Copernicus mission satellite, comprises L-, C- X-, Ku- and Ka-band radiometers with a total of 25 fully polarimetric radiometers as shown in *Table 1*. Additionally, the total analogue bandwidth that needs to be processed for RFI is approximately 17 GHz for CIMR compared to 400 MHz for MetOp-SG-B, so CIMR represents major increase in complexity even though it is expected to be launched just a few years after MetOP-SG-B.

Table 1: CIMR radiometer bands and channels.

Band	Center Freq. (GHz)	Band-width (MHz)	Channels	Spatial Resolution [km]
L	1.4135	25	1	<60
C	6.925	400	4	≤15
X	10.65	100	4	≤15
K	18.7	200	8	≤5.5
Ka	36.5	300	8	≤4

Using modern high speed ADCs it is possible to digitize multiple analogue stacked radiometer bands in one ADC input thus reducing the number of ADCs required, and with large FPGAs, hardware is reduced to a reasonable amount. Additionally, modern high-speed ADCs often have two parallel analogue inputs sampled by the same clock. Using these features, multiple polarimetric radiometer bands are merged into one wideband digital input that is on-board processed into separate radiometer bands.

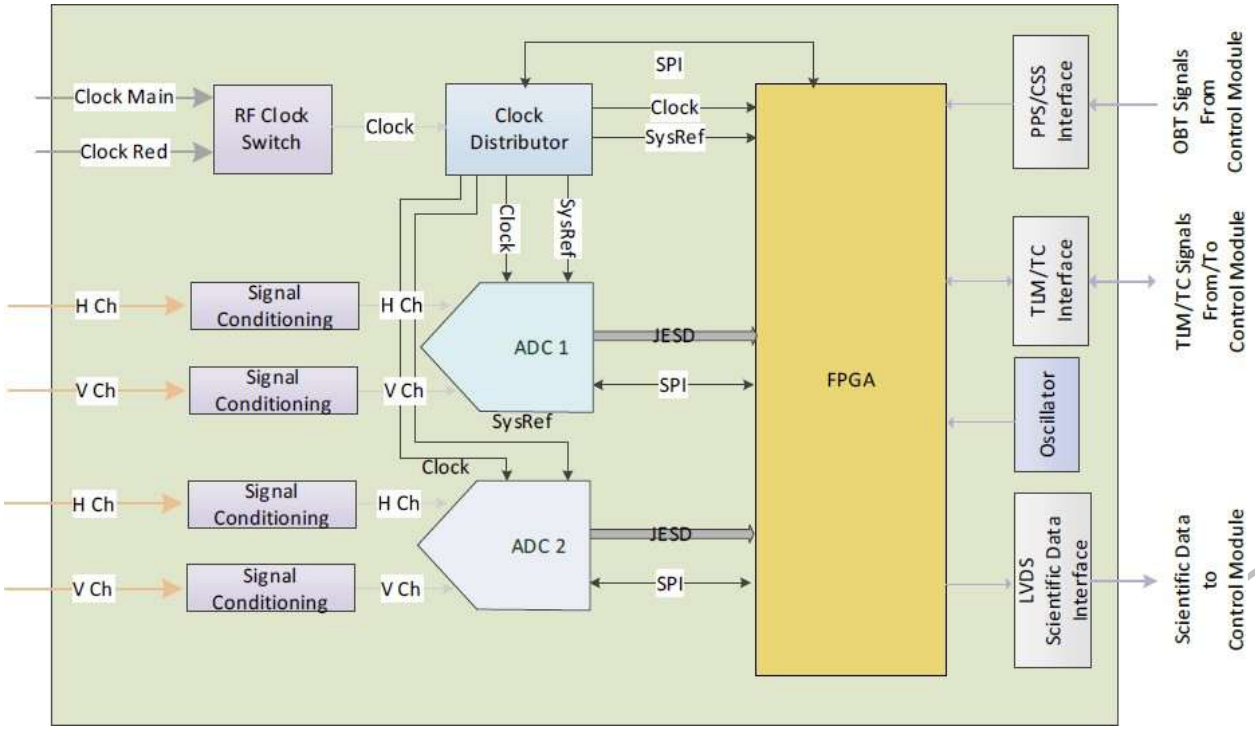

Figure 1: The block diagram of an RFI processor board (Thales Alenia Space Italy).

Figure 1 shows the CIMR RFI processing board implementation block diagram. Two dual input ADCs operating at 1430 MSamples/s having H- and V-polarization as their respective inputs can digitize two 715 MHz wide polarimetric inputs. This bandwidth enables analogue stacking of two polarimetric radiometer bands in each ADC. The FPGA performs RFI detection and filtering of the digital input from the two ADCs thus handling four polarimetric radiometer bands. The 25 radiometer channels in Table 1 can therefore be processed by seven boards. Six boards would have been sufficient if analogue stacking of three radiometer bands were applied, however, this would provide very little redundancy. The digital processing architecture for the FPGA has been developed and is being tested at the time of writing. Design, implementation and test results will be presented.

Index Terms – Radiometer, RFI, detection, filtering, mitigation, CIMR

Programme of the European Union Copernicus co-funded with esa

Radiometry in C-band – current and expected RFI, and possible long-term solution

Yan Soldo* [1], Flávio Jorge[2], Josep Roselló[1] and Craig Donlon[1]

[1] ESA/ESTEC, Noordwijk, The Netherlands
[2] Akkodis for ESA/ESTEC, Noordwijk, The Netherlands

Sea Surface Temperature (SST) is a critical parameter for the prediction on tropical cyclones, fishery resources, and more. Radiometry in C-band, i.e., near 7 GHz is needed for measurements of SST. In fact, SST can only be measured in the infra-red domain (but only during clear-sky conditions, which occur globally around 40% of the time) or in C-band (in all-weather conditions).

Given the importance of SST measurements, it is one of the longest-observed variables, dating back to the late 1970's (and much earlier if we consider measurements made from the surface).

Despite their importance, passive EO measurements near 7 GHz are affected by Radio Frequency Interference (RFI), as documented extensively in the scientific literature. Furthermore, a significant increase in RFI in this band is expected in the coming years due to:

- The WRC-23 decision of identifying the 6.425-7.125 GHz range for International Mobile Telecommunications (IMT) in several countries
- The progressive adoption, in several countries, of new Wi-Fi systems in the range 5.925-7.125 GHz

One of the reasons why RFI is increasing in this band is that Earth Observation (EO) sensors have poor regulatory protection in this portion of the spectrum: there is no formal allocation for them, and the Radio Regulations (RR) simply acknowledges their presence.

Therefore, stakeholders of EO sensors near 7 GHz have two issues to address: 1) coping with more widespread RFI in the measurements; 2) improve the regulatory protection for EO sensors in that band.

ESA is one of these stakeholders, since it plans to launch the Copernicus Imaging Microwave Radiometer (CIMR), who will feature a channel near 7 GHz.
To address 1), ESA has worked on a sophisticated approach to detect and report RFI in all the CIMR channels. To address 2), ESA has supported efforts the inclusion, in the agenda for the World Radiocommunication Conference 2027 (WRC-27), of an item on two potential new primary allocations for EO sensors.

This new Agenda Item (AI 1.19) considers potential new bands at 4.2-4.4 GHz and 8.4-8.5 GHz. These new bands, which are quite narrow when compared with the bandwidths needed by modern radiometers, would need to be used in conjunction with the traditional channel near 7 GHz. The combined measured in the three bands is expected to provide benefits in terms of:

- Better scientific retrievals (i.e. multi-spectral approach)
- Improved capability to detect RFI (i.e. cross-frequency detection)

To study these aspects, and therefore to start assessing the usefulness of the potential new bands, ESA is starting to develop plans for an experimental campaign in which water bodies will be observed simultaneously in the three bands.

This paper will discuss the current status of RFI near 7 GHz, the expected impact of new RFI (from IMT and WiFi), and it will present the discussions and the possible outcomes of AI 1.19.
It will also describe what has been done within ESA to cope with RFI in CIMR and to plan the experimental campaigns to start observing water bodies at the new bands.

WRC and Earth observation – Impact of WRC-23 and work ongoing for WRC-27

Yan Soldo* [(1)], Flávio Jorge[(2)] and Josep Roselló[(1)]

[(1)] ESA/ESTEC, Noordwijk, The Netherlands, yan.soldo@esa.int
[(2)] Akkodis for ESA/ESTEC, Noordwijk, The Netherlands, flavio.jorge@ext.esa.int

1. Introduction

The electromagnetic spectrum is an irreplaceable resource for EO. Remote sensing instruments are special users of the spectrum in the sense that their ability to function properly is heavily dependent on the availability of usable specific portions of the electromagnetic spectrum, which is determined by the geophysical characteristics and interactions that they aim to observe. Naturally, there is a variety of other users of the spectrum, for example mobile networks, TV broadcasts, radio amateurs just to name a few. Therefore, there are rules to coordinate how the spectrum should be used and thus reduce the risk of Radio-Frequency Interference (RFI). The Radio Regulations (RR) is the international treaty describing the rules for use of the electromagnetic spectrum. The RR are revised approximately every four years during the World Radiocommunication Conferences (WRCs). The last WRC, WRC-23 deliberated on several topics which have direct consequences for Earth Observation (EO). This contribution gives an overview of the relevant WRC-23 decisions for EO.

2. Changes to the Radio Regulations

For the Earth Observation community, the agenda of WRC-23 included both opportunities and threats.

2.1 Opportunities

2.1.1. New spectrum for ice cloud imaging near 243 GHz (AI.14)

Ice clouds include very fine particles, that can be imaged only at very high frequencies [1]. The Ice Cloud Imager (ICI) is a radiometer that will be dedicated to performing measurements of ice clouds. Two of the channels of ICI [2] aimed at operating near 243 GHz, where there was no allocation to spaceborne radiometers. On this Agenda Item (AI), WRC-23 agreed to create two new bands dedicated to passive remote sensing: 239.2-242.2 GHz and 244.2-247.2 GHz, which correspond to the frequencies and bandwidths planned for ICI. The creation of these two new frequency bands will provide protection from interference to any future radiometer that will operate there.

2.1.2. New spectrum for polar ice sheet sounding near 45 MHz (AI.12)

Building on the experience of sensors aimed at exploring below the surface of planetary bodies, there are candidate satellite missions that would make it possible to observe below Earth's ice sheets for the first time. These types of instruments need to operate at very low (for remote sensing) frequencies. Within Europe, the STRATUS mission [3] aims at operating a radar in the 40-50 MHz band. However, there was no frequency band allocated for active sensors in those frequencies. WRC-23 agenda item 1.12 aimed at creating a new allocation for missions like STRATUS. WRC-23 agreed to create the new allocation, but added that the new allocation could be used only under certain conditions, which limit radar operations to the polar regions and limit the power flux density that the radar emissions can generate at the surface of the Earth. Even with these limitations, it is expected that potential new sensors in the 40-50 MHz band would be able to operate correctly, and therefore this WRC-23 decision enables a new type of science retrieval over polar ice sheets.

2.1.3. Protection for radiometers in the 36-37 GHz band (AI 9.1 topic d)

WRC-19 had defined a regulatory framework for uplinks and downlinks of commercial satellite constellations, including in the 37.5-38 GHz band. However, it was highlighted that the new regulatory framework did not include the necessary restrictions to protect radiometers operating in the 36-37 GHz band. Under Agenda Item 9.1 topic d, WRC-23 agreed to limit the EIRP

density from commercial constellations into the 36-37 GHz band, in order to protect the radiometers in that band from interference.

2.1.4. New inter-satellite links near 18 GHz (AI 1.17)

Communication links between satellites may be useful for future EO missions to coordinate operations of satellites and to improve the downlink performance of science data. Under agenda item 1.17, WRC-23 agreed to create regulatory conditions to allow new inter-satellite links which could be used by various spectrum users, including scientific satellites.

2.2. Threats

On the other hand, several AIs of WRC-23 represented threats for the remote sensing community. These included:

- Potential interference near 2 GHz to the ground stations used by scientific satellites (AIs 1.4 and 1.18);
- Potential interference to radiometers in various bands:
  - near 7 GHz (AI 1.2)
  - 10.65 GHz (AI 1.2)
  - 18.7 GHz (AIs 1.16 and 1.17)
  - 22.3 GHz (AI 1.10);
- Potential interference to SARs near 10 GHz (AI 1.2);
- Potential interference into several bands, used both for science measurements and data links (AI 9.1 topic c).

After numerous discussions held in the 4-year long preparatory process, for most of these threats, the WRC-23 agreed on solutions that provide adequate protection to EO sensors and to the ground stations used by EO missions. The WRC decision that does not sufficiently protect sensors was on AI 1.2, related to future 5G networks in the 6.425-7.125 GHz band.

2.2.1. 5G networks in the 6.425-7.125 GHz band

Under AI 1.2, WRC-23 agreed to identify the 6.425-7.125 GHz band for future mobile networks. For remote sensing, this band corresponds (for most sea conditions) to the peak sensitivity to changes in the sea surface temperature [4], and in fact it has been used by radiometers since the 1970s. However, radiometers operating near 7 GHz have no regulatory protection. Therefore, protection of radiometers was not taken into account by WRC. 5G networks in the 6.425-7.125 GHz band are expected to cause RFI to spaceborne radiometers. However, it should be noted that this band was not identified for 5G for all the countries mentioned in AI 1.2, and that 5G will need to coexist with incumbent spectrum users on the ground (Wi-Fi and ground stations used by commercial satellites), and that it will need to protect uplinks of commercial satellites. These elements are expected to, indirectly, also reduce somewhat the impact of RFI from 5G into radiometers.

3. Start of preparation for WRC-27

WRC-23 has also defined the agenda for WRC-27 [5]. This agenda includes again several potential threats and some opportunities for remote sensing. Probably the main threat for the upcoming WRC will be again related to mobile networks, since the new targeted bands includes frequencies that are used by most scientific satellites to downlink their measurements to their ground stations. The opportunities for remote sensing include potential new spectrum for radiometers in C-band and potential additional protection for radiometers in certain bands above 86 GHz, as well as potential spectrum for space weather sensors.

4. Conclusion and discussion

The decisions taken at WRCs have clear consequences on the operations and on the RFI experienced by remote sensing missions. However, the scientific community is only marginally involved in the discussions on WRC topics. More awareness and more involvement of scientists in those discussions would be beneficial for the science community at large. \

One ongoing initiative to improve coordination between scientists and frequency managers, is the creation, by the European Space Agency, of a new group called ESSEO (European Scientists on Spectrum for Earth Observation). ESSEO, which is chaired by ECMWF, will aim at describing in detail the connections between WRC topics and the current and foreseen remote sensing applications.

5. References

[1] S. A. Buehler, C. Jimenez, K. F. Evans, P. Eriksson, B. Rydberg, A. J. Heymsfield, C. J. Stubenrauch, U. Lohmann, C. Emde, V. O. John, T. R. Sreerekha, C. P. Davis, "A concept for a satellite mission to measure cloud ice water path, ice particle size, and cloud altitude," *Quarterly Journal of the Royal Meteorological Society*, Vol. 133, 2007.

[2] V. Kangas, S. D'Addio, U. Klein, M. Loiselet, G. Mason, J.C. Orlhac, R. Gonzalez, M. Bergada, M. Brandt and B. Thomas, "Ice cloud imager instrument for MetOp Second Generation," In *2014 13th Specialist Meeting on Microwave Radiometry and Remote Sensing of the Environment (MicroRad)* (pp. 228-231). IEEE. March 2014.

[3] L. Bruzzone, F. Bovolo, L. Carrer, E. Donini and S. Thakur, S., "STRATUS: A new mission concept for monitoring the subsurface of polar and arid regions," In *2021 IEEE International Geoscience and Remote Sensing Symposium IGARSS* (pp. 661-664). IEEE. July 2021.

[4] D.M. Le Vine and E. Dinnat, "The multifrequency future for remote sensing of sea surface salinity from space," *Remote Sensing*, *12*(9), p.1381, 2020.

[5] International Telecommunication Union, "Resolution COM6/23 - Agenda for the 2027 world radiocommunication conference", in the *Provisional Final Acts of the World Radiocommunication Conference 2023* (https://www.itu.int/dms_pub/itu-r/opb/act/R-ACT-WRC.15-2023-PDF-E.pdf).

ESSEO – A new group to help interactions between the EO science community and the frequency regulatory world

Stephen English[1], Yan Soldo* [2], Giulia Panegrossi[3], Jesse Andries[4], Alessandro Battaglia[5], Philippe Chambon[6], Markus Dreis[7], Patrick Eriksson[8], Bruno Espinosa[9], Karsten Fennig[10], Chawn Harlow[11], Kenneth Holmlund[12], Flávio Jorge[13], Yann Kerr[14], Andrea Monti-Guarnieri[15], Catherine Prigent[16], Josep Roselló[2] and Melody Sandells[17]

[1] ECMWF, Reading, United Kingdom, stephen.english@ecmwf.int
[2] ESA/ESTEC, Noordwijk, The Netherlands, yan.soldo@esa.int
[3] CNR, Rome, Italy, giulia.panegrossi@artov.isac.cnr.it
[4] WMO, Geneva, Switzerland, jandries@wmo.int
[5] Politecnico di Torino, Torino, Italy, alessandro_battaglia@polito.it
[6] Météo-France, Toulouse, France, philippe.chambon@meteo.fr
[7] EUMETSAT, Darmstadt, Germany, markus.dreis@eumetsat.int
[8] Chalmers University, Gothenburg, Sweden, patrick.eriksson@chalmers.se
[9] ESA/ESOC, Darmstadt, Germany, bruno.espinosa@esa.int
[10] DWD, Offenbach am Main, Germany, karsten.fennig@dwd.de
[11] UK Met Office, Exeter, United Kingdom, chawn.harlow@metoffice.gov.uk
[12] Independent, work4ken@gmail.com
[13] Akkodis for ESA/ESTEC, Noordwijk, The Netherlands, flavio.jorge@ext.esa.int
[14] CESBIO, Toulouse, France, yann.kerr@cesbio.cnes.fr
[15] Politecnico di Milano, Milano, Italy, andrea.montiguarnieri@polimi.it
[16] CNRS, Paris, France catherine.prigent@obspm.fr
[17] Northumbria University, Newcastle upon Tyne, United Kingdom, melody.sandells@northumbria.ac.uk

PoS(RFI2024)070

This paper aims to introduce a recently formed group relevant for frequency management and for the Earth Observation (EO) science community.
The group is called ESSEO (European Scientists on Spectrum for Earth Observation) and was formed in early 2023. It was formed as an ESA (European Space Agency) initiative, and it is chaired by the ECMWF (European Centre for Medium-range Weather Forecast). Several European and international organizations are represented in the group, including universities, meteorological, climate and research centers.

A major goal of this new group is to narrow the gap between EO science community and the frequency regulatory world. EO scientists rely heavily on a "clean" electromagnetic spectrum. Yet, EO scientists are not always aware of the discussions taking place in frequency regulatory fora that may have a direct impact on the availability of RFI-free data. At the same time, frequency managers do need to be kept up to date with changes in the background in priorities, driven by evolving science maturity in applications.

Since the major frequency regulatory activity is the preparation for the World Radiocommunication Conference (WRC), the work of ESSEO has started there. In 2023, when the final agenda for the WRC-27 was not available yet, the group worked on the preliminary agenda for WRC-27 as well as some additional topics that had been discussed within ITU. This work resulted in a first publication by ESSEO titled "Views on Potential Topics for the WRC-27 Agenda".
Since early 2024, the group has been building on this work, this time addressing the final agenda for WRC-27. The goal is that a new document will be published before the end of the year.
The document will also spell out the connections between each WRC-27 agenda item, and the United Nations' Sustainable Development Goals (SDGs).
Further plans for the group include a document with detailed scientific background about the links between science applications and frequency bands, which would complement the 2024 publication.

In doing this work, ESSEO helps frequency managers in Europe (mostly in ESA and EUMETSAT) by providing a solid scientific background for the frequency regulatory topics, and by providing additional information on the sensitivity/importance of the different frequency bands.
In addition, the group provides informed views on the presence of RFI (Radio Frequency Interference) in various bands as well as on their impact on scientific applications, and it could be useful in reflecting cases of RFI documented in the scientific literature within ITU and other similar fora, when appropriate to do so.

ESSEO has started to interact with other relevant groups, such as the Committee on Radio Frequencies (CORF) in the US, the WMO Expert Teams on Radio Frequency Coordination and on Space Systems and Utilization (ET-RFC and ET-SSU) and in Europe with the ACEO (Advisory Committee on Earth Observation) and the ESSC (European Space Sciences Committee).

The presentation will introduce the group, its goals, the work already performed and discuss possible future plans.

Earth Observation Data Links: Regulatory Challenges and Opportunities

Flávio Jorge *[(1)], Yan Soldo [(2)], Steven George [(3)] and Josep Rosello [(2)]
[(1)] Akkodis for European Space Agency, Noordwijk, The Netherlands, flavio.jorge@ext.esa.int
[(2)] European Space Agency, Noordwijk, The Netherlands, yan.soldo@esa.int, josep.rosello@esa.int
[(3)] Starion for European Space Agency, Noordwijk, The Netherlands, steven.george@ext.esa.int

Spaceborne Earth observation (EO) missions play a vital role in monitoring the Earth system, enabling applications ranging from sub-surface to atmosphere.

Some of its more scientific applications include, for example, the detection of sub-surface water reservoirs, the measurement of soil moisture, ocean temperature and salinity, ice thickness and wind speed, the characterization of atmospheric temperature, pressure and humidity, as well as of the different hydrometeors, essential in climate and weather operational services.

The range of EO enabled applications expand beyond the scientific applications and touch many governance areas including, for example, the infrastructure, including heritage, monitoring and conservation, territorial defense, safety and security, territorial planning and ordering, economic growth monitoring, commercial trading, transport and mobility efficiency, pollution control and population health and wellbeing assessments.

From the regulatory standpoint, spaceborne EO missions are designated as radiocommunication *space stations*. They collect data measured by instruments they carry onboard, and the effective and efficient reception of these data on ground, by the so-called *payload data transmissions* (PDT), is critical to enable the abovementioned applications.

These EO data links are, typically, operated in the framework of the radiocommunication service designated by *Earth exploration-satellite service* (EESS), defined in the International Telecommunication Union (ITU) Radio Regulations (RR) as "a radiocommunication service between *earth stations* and one or more *space stations*, which may include links between *space stations*, in which information relating to the characteristics of the Earth and its natural phenomena, including data relating to the state of the environment, is obtained from *active sensors* or *passive sensors* on Earth *satellites (...)*".

As the radio regulatory framework evolves, a number of challenges and opportunities arise. The effective continuous delivery of EO data as a service requires that stakeholders take the opportunities and mitigate the challenges.

The agenda for the World Radiocommunication Conference (WRC) 2027 and the preliminary agenda for WRC 2031 include several items that pose challenges to the current and future operations of EO data links, as well as open exciting opportunities for future EO missions. The WRC-27/31 agendas will be reviewed and the relevant agenda items will be assessed from the EO data links standpoint.

Future EO missions have increasing spectrum requirements for transmitting down to the ground the scientific data collected on-board by payload instrumentation (passive and active). Innovative spectral-efficient microwave space communication technologies (e.g. frequency-reuse schemes by means of polarization diversity) are key in maximizing the use of existing spectrum resources and in meeting future EO mission spectrum requirements.

RFI 2024

Building a global map of low frequency radio interference from orbit with DORA

Yifan Zhao(1), Daniel C. Jacobs(1), Titu Samson(1), Judd Bowman(1), and Marc-Olivier R. Lalonde(1)
(1) Arizona State University, Tempe, USA, amyzhao@asu.edu

1 Introduction

The existence of radio frequency interference (RFI), particularly human-made RFI such as FM radio, presents a challenge to existing 21-cm experiments that aim to make the first measurements of hydrogen during the Dark Ages, Cosmic Dawn, and Epoch of Reionization. Current 21-cm experiments aim to avoid RFI by building instruments in remote locations, far from human interference. However, usage patterns change with time, leading to exploration for new sites and mitigation strategies. A global survey of usage could help identify quiet regions. Meanwhile, space-based experiments have been proposed as alternative radio quiet locations. We evaluate the feasibility of a space-based 21-cm experiment by evaluating the presence of RFI in different space environments, including low-Earth orbits and high altitude balloons. We do this in two ways: with simulations of the RFI environment using FM radio databases, and with direct measurement with a radio spectrometer aboard the DORA cubesat deployed in September 2024. Studying the presence of RFI from low-Earth orbit will allow for global spectrum monitoring, which can help us plan for future 21-cm missions accordingly. In addition, DORA will raise the technology readiness level (TRL) of key technologies needed for a space-based 21-cm experiment.

2 Background

One of the last unexplored epochs spans the time between the surface of last scattering, known as the Cosmic Microwave Background (CMB), and Cosmic Dawn (CD), when the first stars formed and reionized the universe during the Epoch of Reionization (EoR). We refer to this period as the Dark Ages. The only direct probe of the Dark Ages is neutral hydrogen and its radiation from its spin-flip transition, which radiates at a wavelength of 21-cm. The redshifted 21-cm line of neutral hydrogen gas should be visible today as a spectral distortion in the cosmic microwave background at frequencies less than 200 MHz, matching redshifts 25 to 6. The Dark Ages, Cosmic Dawn, and EoR epochs can be studied using the redshifted 21-cm signal.

However, the difficulty of observing the 21-cm line from the early universe stems from its weak radiation signature and the existence of sky-noise and bright foreground radiation, which dominates the measurement. As a result, instruments that measure in this bandpass need to be highly precise. Current instruments that measure in this wavelength, such as the Owens Valley Radio Observatory Long Wavelength Array (OVRO-LWA) in California, the Low-Frequency Array (LOFAR) in the Netherlands, and the Experiment to Detect the Global Epoch of Reionization Signature (EDGES) [2] in Australia are all terrestrial-based instruments.

Terrestrial factors greatly influence the sensitivity of these instruments. Modeling instrument variation has shown that key systematics depend heavily on the beam of the antenna, and the beam is affected by factors such as the composition of the ground plane, the shape of the ground plane, and even the shape of the horizon [1]. Soil, vegetation, and atmospheric humidity also play an important role [3]. Other terrestrial factors include diffraction in the ionosphere, which changes the effective beam pattern on the sky and absorbs incoming radio waves, and, importantly, interference by radio signals such as the FM band which is visible most everywhere on Earth.

To mitigate the effects of human-made RFI, most 21-cm experiments are conducted in remote areas, where human activity is limited. Low-Earth orbit, or high-altitude balloon experiments, could possibly be an option for a low-RFI environment. However, studies of the RFI environment for such experiments are needed. In addition, measuring the global 21-cm signal with an airborne instrument has not been attempted before, and requires significant development to miniaturize the calibration and data recording hardware.

PoS(RFI2024)070

3 RFI simulations of possible orbits and balloon tracks

To study the RFI environment in a near-space environment, population density maps, shipping routes, and FM radio databases were surveyed, and simulations of the RFI environment for a hypothetical space-based 21-cm experiment in low-Earth orbit or on a high pressure balloon were made. We compared the results of our simulations with RFI-flagged data from EDGES, and Fig. 1 shows the results of these initial simulations. Over the same time period, a space-based 21-cm experiment on a high pressure balloon flying at a roughly steady latitude of -47° flagged a much lower percentage of RFI than EDGES did. The constant change in the RFI environment for an orbiting space-based 21-cm experiment allows for a lower averaged percentage of data lost to RFI.

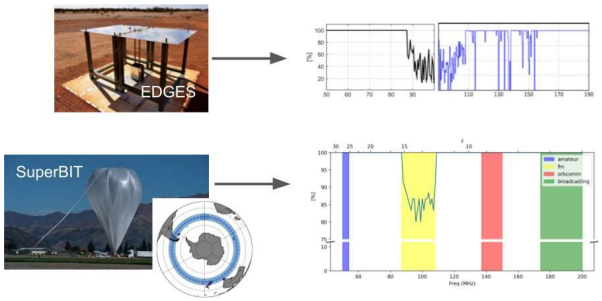

Figure 1. (top) Percentage of data flagged due to RFI on EDGES, a terrestrial global 21-cm experiment [2]. (bottom) Simulated percentage of data that would be flagged due to RFI on a hypothetical high-pressure balloon experiment.

4 DORA Cubesat Spectrometer

DORA is a student-run cubesat program with a payload modeled after a miniaturized version of EDGES, sent to low-Earth orbit for RFI monitoring of a space-like environment suitable for a 21-cm experiment. In this section, I will introduce the specifications of the "EDGES in Space" payload on the DORA cubesat. DORA has been delivered to NASA in May 2024, is slated to launch in August 2024, and deploy from the ISS in September 2024.

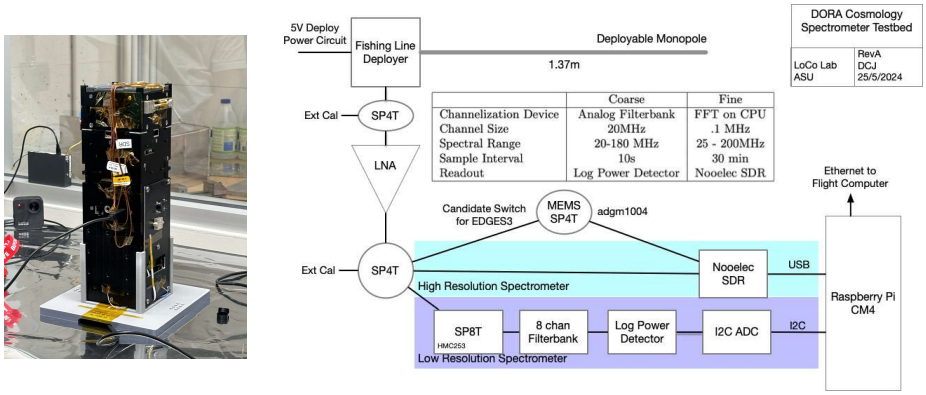

Figure 2. Block diagram of the DORA RF payload.

References

[1] N. Bassett, D. Rapetti, K. Tauscher, B. D. Nhan, D. D. Bordenave, J. J. Hibbard, and J. O. Burns, "Lost horizon: Quantifying the effect of local topography on global 21 cm cosmology data analysis," *ApJ*, **923**, 1, 2021, pp. 33.

[2] J. D. Bowman, A. E. E. Rogers, R. A. Monsalve, T. J. Mozdzen, and N. Mahesh, "An absorption profile centred at 78 megahertz in the sky-averaged spectrum," *Nature*, **555**, 2018, pp. 67-70.

[3] R. F. Bradley, K. Tauscher, D. Rapetti, and J. O. Burns, "A ground plane artifact that induces an absorption profile in averaged spectra from global 21 cm measurements, with possible application to EDGES," *ApJ*, **874**, 153, 2019.

Collaboration with Cellular Networks for RFI Cancellation at Radio Telescope

Shuvam Chakraborty[1], Gregory Hellbourg[2], Dola Saha[1], Aveek Dutta[1]
[1] Department of Electrical and Computer Engineering, University at Albany, SUNY, NY, USA
[2] Department of Radio Astronomy, California Institute of Technology, CA, USA

The increasing demand for electromagnetic spectrum to support next-generation (xG) communication networks generates unwanted radio frequency interference (RFI) in protected bands used for radio astronomy. Traditionally, RFI mitigation is performed solely at the radio telescope without collaboration with the interfering sources. This study introduces a novel method for signal characterization and subsequent cancellation by leveraging eigenspaces derived from both telescope and transmitter signals. Unlike conventional time-frequency domain analyses, which are limited by fixed characterizations (e.g., complex exponential in Fourier methods) and cannot adapt to changing statistics of the RFI observed in communication systems, our approach provides a more adaptive solution. Using real-world astronomical signals and practical simulated LTE signals (both downlink and uplink) as RFI sources, we evaluate our method's effectiveness under various propagation conditions based on preset benchmarks and standards. Our analysis demonstrates that we can remove 89.04% of the RFI from cellular networks, significantly reducing excision at the telescope and improving data throughput by making previously corrupted time-frequency bins usable.

1. Introduction

Radio astronomy has significantly advanced our understanding of the universe through observations across the electromagnetic spectrum. Despite this, only a small fraction (1-2%) of the spectrum below 50 GHz is allocated for scientific use, where most commercial radio communication occurs. Expanding the observable spectrum is essential due to the red-shifting of spectral lines caused by the expanding universe and the need for broad bandwidth radio continuum observations to increase the signal-to-noise ratio of weak radio sources. To avoid RFI from human activities, radio telescopes are typically situated in remote areas. However, with the increasing demand for spectrum by xG networks, the challenge of mitigating RFI in these protected bands has become more critical.

This paper proposes a collaborative approach with cellular networks for RFI cancellation at radio telescopes. By utilizing eigenspaces derived from both the telescope and transmitter signals, our method adapts to the changing statistical properties of RFI, providing a more effective mitigation strategy compared to conventional time-frequency domain analyses.

2. Methodology

Our approach involves signal decomposition and reconstruction using singular spectrum analysis (SSA) based on the Karhunen-Loève transform (KLT, Figure 2). The LTE signal at the base station (BS) and the composite signal at the telescope are decomposed to obtain eigenfunctions. In our SSA-based implementation of KLT, the window length (e.g. digital samples window length) is empirically estimated to be L = 500, satisfying the necessary condition L > M, where M ~ 300 is the dominant eigenspace dimensionality. RFI cancellation and reconstruction are performed under various wireless channel scenarios, with reconstruction quality averaged over 100 simulations to smooth out any outlier behavior.

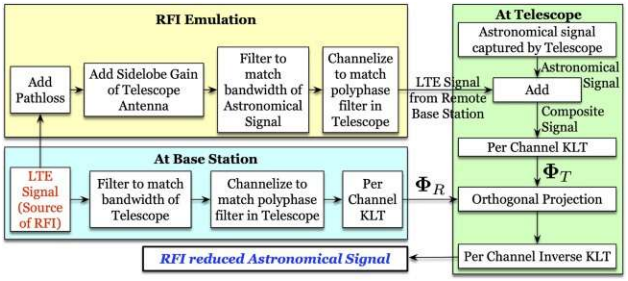

Figure 1 Block diagram of the RFI collaborative cancellation concept between the antenna tower and the radio telescope.

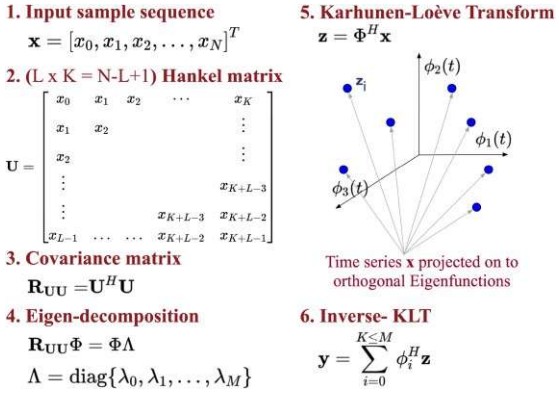

Figure 2 Geometry of KLT-based signal characterization.

3. Results

Experimental results using a downlink signal as RFI propagated through an AWGN channel establish a baseline for the proposed RFI cancellation method. Parameter space exploration investigates the effects of interference-to-noise ratio (INR) at the telescope, frame occupancy in LTE RFI, and time synchronization error between the RFI source and the telescope. Results indicate that our method achieves a reconstructed quality factor (RQF) of $4.13e^{-4}$ for the rectified astronomical signal at an estimated INR of 5 dB at the telescope.

Further analysis shows that RQF decreases with increasing INR, as higher RFI power leads to better characterization and improved reconstruction quality. The effect of time synchronization error between the BS and telescope is also investigated, showing a maximum RQF of $4.6e^{-4}$ at a 320 ns delay.

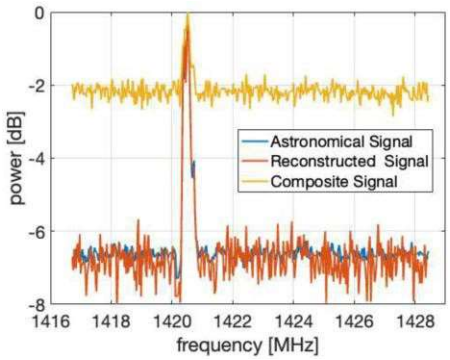

Figure 3 Comparison between uncorrupted astronomical signal (galactic HI spectral line) in blue, RFI-corrupted signal involving a cellular downlink signal (in yellow), and reconstructed signal in red after applying the proposed approach.

4. Conclusion

Our collaborative method with cellular networks for RFI cancellation significantly improves the quality of astronomical observations by removing 89.04% of RFI from cellular networks. This approach reduces the need for excision at the telescope and enhances data throughput by making previously unusable time-frequency bins available for scientific analysis. Future work will focus on further refining the method and exploring its application to other communication systems.

Watermarking of OFDM for Pseudonymetry

Meles G. Weldegebriel[(1)], Gregory Hellbourg[(2)], Ning Zhang[(1)], Neal Patwari[(1)]
[(1)] Washington University in St Louis, USA
[(2)] California Institute of Technology, USA

This abstract presents new results for pseudonymetry, a closed-loop feedback mechanism where active transmissions are watermarked with a pseudonym that, if it interferes with a protected passive radio receiver, can be demodulated and used to force the transmitter off the band. We focus on amplitude-based watermarking of orthogonal frequency division multiplexing (OFDM) packets. Our findings quantify the ability of a passive receiver to decode the watermark at very low signal-to-noise ratio (SNR) and assess the impact on the intended communication link. Using a testbed of software-defined radios, we demonstrate that the experimental implementation of pseudonymetry closely matches the theoretical analysis. Our results highlight a fundamental trade-off in the design of pseudonymetry for OFDM and provide a practical pseudonym receiver design.

1. Introduction

The radio spectrum is a finite and crucial resource used for wireless communications, radio navigation, radio astronomy, and Earth sensing services. Sharing spectrum between users is essential to meet growing demand in all these areas. However, radio frequency interference (RFI) often dominates spectrum policy debates, leading to overly conservative propagation models that protect primary users but limit reuse in areas where secondary users would unlikely interfere. For instance, the FCC allocation of the 6-7 GHz band for indoor Wi-Fi 7 faced opposition from incumbent microwave tower operators, citing potential interference and difficulties in identifying and removing specific interfering devices.

Despite large geographic radio quiet zones (RQZ) and regulatory interference protection rules, passive receivers like radio telescopes increasingly suffer from interference from multiple sources. Coexistence between passive and active radio services typically involves RFI detection and cancellation, interference thresholds and propagation models, or manual/nascent technologies cooperation between users. Pseudonymetry, an interference remediation cooperative protocol, extends these approaches by enabling the passive receiver to identify the interference source and submit its pseudonym to a database, ensuring that the transmitter changes band.

2. System Model

Pseudonymetry involves passive receivers (primary users) and pseudonymetry transmitters (secondary users) using OFDM modulation for data communication. The system includes a database for storing interference reports with decoded pseudonyms and timestamps. Each pseudonymetry transmitter watermarks its transmitted signal with a low-rate pseudonym that can be decoded by the passive receiver even when the received power is below the OFDM packet demodulation threshold. When interference occurs, the passive receiver uploads an interference report to the database, and pseudonymetry transmitters must periodically check the database and move off the channel if interference is reported.

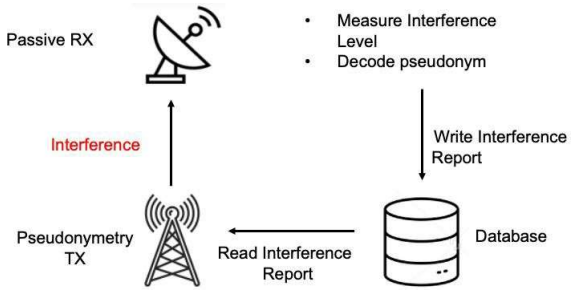

Figure 1 Pseudonymetry architecture with cooperation between the pseudonymetry transmitter and the passive receiver through a database.

3. Pseudonym Generation and Watermarking of OFDM

We analyze the pulse amplitude modulation (PAM) watermarking scheme, where the watermarked transmit signal is given by:

$$s_p(t) = [1 + q(t)] \sum_{n=0,k=0}^{N-1,K-1} \sqrt{E_b a_{n,k} \phi_{d,k}(t - nT_d)}$$

where T_d is the data symbol period, $\phi_{d,k}(t)$ is the orthonormal waveform for the data symbols, $a_{n,k}$ is the amplitude of the waveform during the d-symbol period, and $q(t)$ is the amplitude watermark signal.

The watermark signal $q(t)$ is designed to be demodulated at very low SNR, balancing the trade-off between watermark detection and the impact on data signal demodulation. Pseudonym bit decisions are made by comparing a short-term average received power to a threshold.

A heuristic approach estimates the pseudonym receiver threshold by computing the average power for each p-symbol and setting the threshold to the average of the middle 70% of the Z-values, disregarding the smallest and largest 15% of samples. This method simplifies the receiver design and closely approximates the optimal threshold.

4. Performance Analysis

We derive theoretical formulas for the probability of pseudonym bit error at the passive receiver and the probability of data bit error at the intended OFDM receiver. The average probability of error is a function of the modulation index, the number of data samples per pseudonym symbol, and the energy per bit. Analytical results show that pseudonym bit detection is possible even at low energy per bit Eb/N0 values, while watermarking causes a small impact on the intended wireless system's data demodulation performance.

5. Experiments

Experiments conducted on the Platform for Open Wireless Data-driven Experimental Research (POWDER) validate the analysis. We use a testbed with software-defined radios (SDRs) to demonstrate low power pseudonym detection and compare the heuristic threshold estimation with the Expectation Maximization (EM) algorithm and an ideal threshold. Results show that the heuristic approach yields the best error performance.

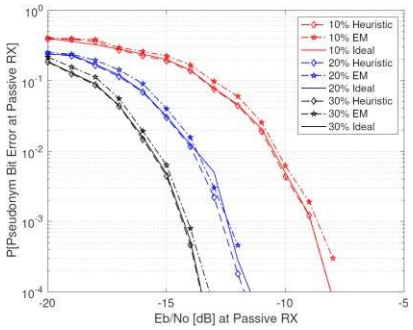

Figure 2 Probability of p-bit error vs. Eb/N0 for the heuristic, EM, and ideal threshold estimation techniques.

6. Conclusion

Pseudonymetry is a cooperative spectrum sharing protocol enabling passive receivers and active wireless transmitters to coexist by using RF signal watermarking and a database feedback loop to stop offending transmissions. Our study of OFDM signal watermarking demonstrates that watermark detection is possible at low Eb/N0 values, with minimal impact on OFDM data demodulation. The practical pseudonym receiver implementation closely matches the theoretical performance, advancing pseudonymetry system design for OFDM signals. Future work will explore further aspects of the pseudonymetry system, including cost implications, integration with other sharing architectures, and security and privacy implications.

Assessing and Mitigating RFI for the DSA-2000 : Comprehensive Analysis and Flagging Strategies

Gregory Hellbourg
Department of Radio Astronomy, California Institute of Technology, USA

The Deep Synoptic Array (DSA-2000) is a future survey radio telescope that will operate in the 0.7-2 GHz range, a frequency band heavily allocated to active services. This abstract provides a comprehensive list of radio frequency interference (RFI) in the DSA-2000 band, describes the protocol to establish this list, and outlines the RFI mitigation strategies planned for the telescope. Additionally, this paper addresses the problem of efficient and fast data flagging for the DSA-2000, which is crucial due to its stringent requirements for real-time processing, sensitivity, and data quality.

1. Introduction

The DSA-2000, designed at the California Institute of Technology, is a planned survey radio telescope comprising 2000×5 -meter dish antennas distributed over a 15×19 km elliptic area. It is optimized for radio surveys in terms of sensitivity and survey speed, operating in the 0.7-2 GHz range. The telescope will achieve high sensitivity through a large collecting area and custom-made non-cryo-cooled low-noise receivers, resulting in a system temperature of 25 K and a system-equivalent flux density (SEFD) of 2.5 Jy. Survey speed is maximized by a wide field of view of 10.6 deg² and a near real-time imaging pipeline, referred to as a "radio camera."

The DSA-2000 will face significant challenges from RFI due to its operating frequency range, which is nearly fully allocated to active services. The Radio Astronomy Service (RAS) benefits from limited protections in approximately 3% of the DSA-2000 frequency range through co-primary allocations enforced by the National Telecommunications and Information Administration (NTIA). However, the remainder of the telescope frequency range is allocated to active services, including terrestrial, airborne, and space-borne systems, which can cause interference.

2. RFI Levels and Survey

RFI impacts radio telescopes in various ways, classified into different levels based on their severity. Spectrum surveys have been conducted at multiple DSA-2000 candidate sites to understand the RFI environment better. These surveys capture spectrum data over the 0.5-2.5 GHz range using calibrated passive quasi-omnidirectional antennas connected to real-time spectrum analyzers. The data collected are analyzed to identify active RF services that could interfere with the DSA-2000, providing a comprehensive list of current and potential future sources of RFI.

The state of Nevada, with its low population density, low terrestrial radio infrastructure density, and topography featuring natural radio frequency shielding, has been selected as the main candidate for hosting the DSA-2000 observatory. Despite this, the telescope must still contend with terrestrial, airborne and space-borne services. Examples include terrestrial transmitters such as cellular communications and point-to-point microwave links, aeronautical services (ADS-B), and satellites services such as GNSS, satellite communications (Iridium, Inmarsat, Ligado), and NOAA satellites downlinks.

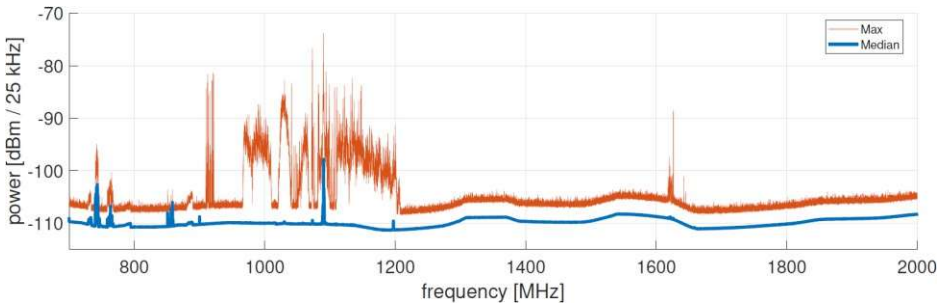

Figure 1 Median and maximum spectra observed with a donut-shaped quasi-omni antenna from the DSA-2000 candidate site.

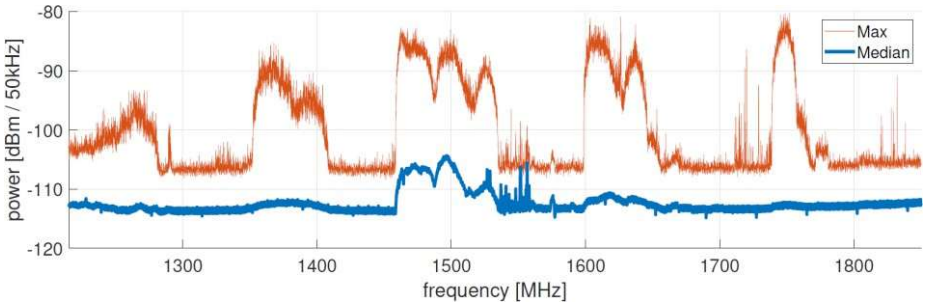

Figure 2 Median and maximum spectra observed with a DSA-2000 prototype feed oriented towards the sky.

3. RFI Mitigation Strategies

The DSA-2000 will implement a multi-stage RFI mitigation strategy based on the present and future RFI surveys and the real-time requirements of the telescope. These strategies include tunable notch filters in the analog signal chain to attenuate specific bands, auto-correlation flaggers to identify misbehaving antennas, time-domain flaggers to blank high-power time samples affected by wideband RFI, visibility-domain flaggers to excise statistical outliers before the imaging process, and image quality control flaggers to remove single-frequency channel images based on their noise properties.

4. Data Flagging in Real-Time Processing

Efficient on-the-fly data flagging is crucial for the DSA-2000 due to its real-time processing requirements. The data flagging strategy for the DSA-2000 involves both the F-engine and X-engine levels. The F-engine, responsible for data digitization, channelization, quantization, and packetization, deploys flaggers that detect data corruption by comparing the instantaneous auto-correlation spectrum with a reference spectrum measured in a controlled environment. Deviations from the standard spectrum indicate potential data corruption due to analog electronics failures or strong RFI.

At the X-engine level, more sensitive data quality assessments are required. The X-engine flaggers use spectral kurtosis to detect non-Gaussianity in the data, which indicates the presence of RFI. The spectral kurtosis is calculated for local clusters of visibilities, and clusters exceeding a specified threshold are flagged as erroneous and set to zero. This approach helps mitigate the impact of RFI on the final data products by ensuring that corrupted data are identified and discarded before further processing.

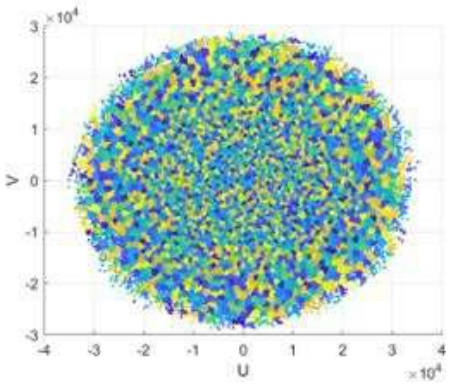

Figure 3 Clusters of visibilities at Dec = 88 degrees in the UV-domain for the DSA-2000 configuration.

5. Conclusion

The DSA-2000 faces significant challenges from RFI due to its operating frequency range. This paper provides a comprehensive assessment of the RFI environment for the DSA-2000 and outlines the planned mitigation strategies. The implementation of multi-stage RFI mitigation techniques and efficient real-time data flagging strategies will enable the DSA-2000 to achieve its scientific objectives while minimizing the impact of RFI. Future work will focus on evaluating the performance of these approaches with real and simulated telescope data to ensure their effectiveness and optimize the detection and false alarm rates.

RFI Sources and Different Mitigation Techniques Adopted at uGMRT

S. Sureshkumar*(1), Pravin Raybole(1), Ankur(1), Sanjeet Rai(1) and Vilas Bhalerao(1)
(1) GMRT Observatory, NCRA-TIFR, Pune, India, skumar@gmrt.ncra.tifr.res.in

Abstract

The Giant Meter Wave Radio Telescope (GMRT) array is spread over 14 km radial distance with 30 antennas of 45-meter diameter covering 100 MHz – 1500 MHz frequency band[1,2]. The telescope is located away from cities and free from industries with thin population in and around the array. Over two decades with increase in human settlement, advancement in communication, transport, industries, electrical power lines and modern equipment for better living standards have increased the radio frequency interference (RFI) to the GMRT array telescope. Figure 1.0 shows the RFI ambience recorded over a decade at the upgraded GMRT array. Ever-increasing interference affecting the RFI ambience around the GMRT and affect the sensitivity of the telescope by increasing the receiver temperature with interference in addition to the loss of usable RF spectrum.

Protecting the RFI ambience in and around GMRT is a challenge with a seamless frequency coverage using wideband feed and receiver systems operating at lower frequency band. This paper presents the selective RFI mitigation methods adopted for various internal and external sources of interference to the telescope, giving the types of interferences with statistics over decades and different solutions adopted to each source of RFI to protect uGMRT from the ever-increasing RFI for continued quality of observation. The paper presents the various solutions adopted to sustain with interferences like mobile signals[3], satellite interference[4], aircraft signals, wireless signals and TV transmission.

In addition, the effect of strong interference on the receiver dynamic range and performance degradation is studied and the modifications to the receiver system is presented here with a narrow band low noise amplifier to reduce out of band interference, switchable notch filters down the receiver chain which can be turned ON and OFF when needed, variable attenuator to bring the receiver to linear operation in the presence of strong interference. Finally, the paper presents some of the other challenges in protecting the RFI ambience around the uGMRT array with 5G transmission, Railway line, increasing industries, power line with government regulatory authorities.

Keywords—Radio frequency interference, Radio astronomy, Radio Telescope, RFI Mitigation

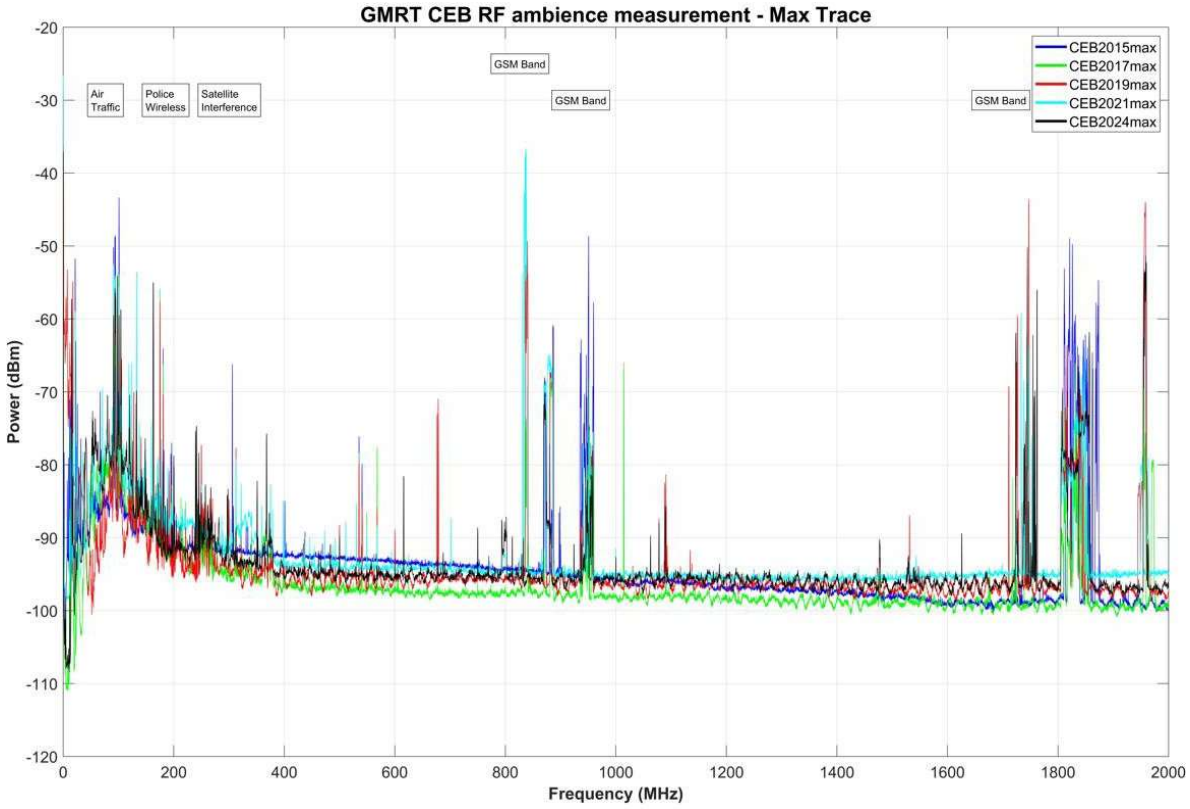

Figure 1. RFI ambience at uGMRT from the year 2015 to 2024.

References

[1] Swarup, G., Ananthkrishnan, S., Kapahi, V.K., Rao, A.P., Subrahamanya, C.R., and Kulkarni, V.K. (1991) "The Giant Metrewave Radio Telescope" Current Science, vol. 60, pages 90-105

[2] Yashwant Gupta et.al. "The upgraded GMRT: Opening new windows on the radio universe", Current Science, vol. 113, no.4, 25 August 2017.

[3] Pravin Ashok Raybole, S. Sureshkumar "RFI2010- Proceeding of Science - External sources of RFI at the GMRT: Method for control and co—existence with commercial users", 29-31 March 2010 Groningen, Netherlands.

[4] Pravin Ashok Raybole, S. Sureshkumar, Santaji Katore and Sanjeet Rai, "Real time prediction, detection and co-existing with satellite interference at GMRT", RFI2016, Socorro, New Mexico.

RFI 2024

Strategy for WiFi interference detection in weather radar applications

Andy Moreno Rodriguez(1)(3), Jorge Cogo(2) and Juan Pablo Pascual(1)(3)
(1) Instituto Balseiro, UNCUYO-CNEA, Av. Bustillo 9500, San Carlos de Bariloche, Argentina
(2) Universidad Nacional de Río Negro, Anagasti 1463, San Carlos de Bariloche, Argentina
(3) Consejo Nacional de Investigaciones Científicas y Técnicas (CONICET)

1 Introduction

In 2003 the International Telecommunication Union (ITU) decided to assign the frequency bands 5.150-5.350 and 5.470-5.725 GHz to wireless access systems, including Wireless/Radio Local Area Networks (WLAN/RLAN), as long as they do not cause interference to existing systems that operate in these bands, such as C-band weather radars. The idea was that they coexist with weather radars, requiring wireless access systems to use a dynamic frequency selection function (DFS) to check for the presence of radar signals before transmitting on a given channel. However, even today interference caused by WLAN/LAN networks to C-band weather radars is one of the limiting factors of their performance [1]. Figure 1(a) shows the reflectivity plan position indicator (PPI) of the measurements collected by the RMA1 Argentinian C-band weather radar, located in Córdoba city. The data were recorded on September 7, 2018, under clear air conditions. The PPI corresponds to a complete sweep of the horizontal polarization (HH), at 0.5 degrees elevation. In the image the segments of lines oriented radially of low to medium reflectivity values correspond to received signals of telecommunication links devices. In general, they are WiFi signals, i.e. signals of wireless local area networking devices based on the IEEE802.11 standard [2]. A challenge of the signal processing stage consist in identify the WiFi interference in order to reduce its effect over the weather radar products. There are techniques that identify the WiFi signals based on polarization properties [3] and others that identify them by image processing methods [4]. It is also possible to detect the interference using the deterministic waveform of the WiFi preamble at the matched filter output [5]. In this work, we tackle the problem of identify the WiFi interference in the weather radar from the periodic components of its signal structure.

2 WiFi detection algorithm

The IEEE standards 802.11a,ac,ax describe the physical layer specifications for WiFi systems that use orthogonal frequency division multiplexing (OFDM) in the 5 GHz band [2]. The data packets of the different clauses contain a preamble compatible with standard 802.11a operating in a 20 MHz channel bandwidth in the 5 GHz band. This preamble consists of a sequence of ten short symbols followed by a sequence of two long symbols. Each short symbol has a duration of 0.8 μs which results in a periodicity of this time interval. The long symbols have a length of 3.2 μs with a cyclic prefix of 1.6 μs, which gives a total preamble duration of 16 μs. Even when the C band weather radar systems operate in the same carrier frequencies range, the WiFi signal is completely distorted by the radar front-end and matched filter, because the system bandwidth and sample frequency are different to the required for the interference signal. However, the periodic structures of the preamble remain after matched filter output. This can be observed in Figure 1(b), where it is showed the in-phase component of a WiFi interference at this radar matched filter output. The signal corresponds to one pulse of the dataset described in the previous section, where there are only two WiFi signal packets plus noise.

In digital communication systems the periodic structures of the training sequences are used to symbol timing detection and to measure the carrier frequency offset [6]. One simple method is the delay and correlate algorithm, which searches for repetition in the received signal using a correlator and a maximum searcher. Let $y[m]$ be the received discrete-time baseband signal, then the auto-correlation, $r[k]$, of the received signal is given by

$$r[k] = \sum_{m=0}^{M-1} y^*[m+k]y[m+k+L], \tag{1}$$

where M is the repetition interval length and L is the separation between two adjacent intervals.

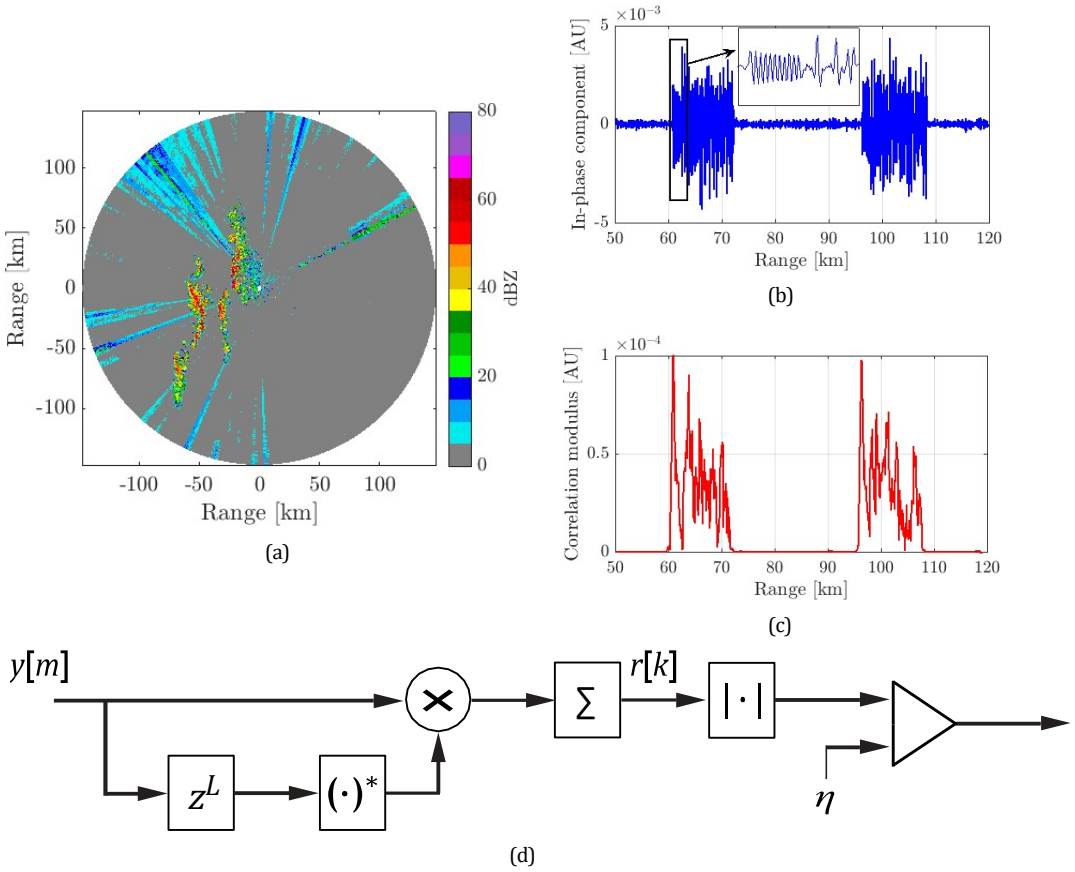

Figure 1. (a) PPI of reflectivity. (b) WiFi signal in weather data recorded. (c) Modulus of the weather data recorded auto-correlation. (d) Block diagram of the detection algorithm.

In this work, we present an algorithm to detect the WiFi signal over the data acquired for weather radars, based on the ideas used in digital communication systems. The detection strategy consists in an hypothesis test that employs the modulus of the auto-correlation $r[k]$ as the decision statistic, which is compared with a threshold, η. Figure 1(c) shows $|r[k]|$ for the same signal of the Figure 1(b), where M and L have been set with the number of samples corresponding to the half of the length of the short symbols training sequence. The result shows that $|r[k]|$ has a maximum peak at the beggining of each WiFi signal packet. Figure 1(d) shows the block diagram of the detection algorithm, where $y[m]$ represents the baseband radar received signal. The work includes the derivation of the test, that allows to determine the threshold value, the performance evaluation and the validation using real weather data.

References

[1] E. Saltikoff, J.Y. Cho, P. Tristant, A. Huuskonen, L. Allmon, R. Cook, E. Becker and P. Joe, "The Threat to Weather Radars by Wireless Technology," *Bull. Amer. Meteor. Soc.*, **97**, 7, August 2016, pp. 1159–1167, doi:10.1175/BAMS-D-15-00048.1.

[2] IEEE Standard 802.11, "Wireless LAN Medium Access Control (MAC) and Physical Layer (PHY) Specifications," 2016.

[3] R. Keränen, L. Rojas and P. Nyberg, "Progress in Mitigation of WLAN Interference at Weather Radar," in *Proc. 36th Radar Meteorol.*, **P15.336**, Colorado, USA, 2013.

[4] M. Peura, "Computer vision methods for anomaly removal," *Conf. on Radar Meteorology, ERAD*, pp. 312–317, Delft, Netherlands, 2002.

[5] O. Barba Leal, F. Rinalde, J. Cogo and J.P. Pascual, "WLAN Signal Detection in Weather Radar Data," in *Proc. XIX Workshop on Information Processing and Control (RPIC)*, San Juan, Argentina, 2021.

[6] Morelli and M., Mengali, U., "Carrier-frequency estimation for transmissions over selective channels," *IEEE Commun. Lett.*, **48**, 9, September 2000, pp. 1580–1589, doi: 10.1109/26.870025.

High-dynamic Range Radio Astronomy Systems, Interference Mitigation strategies, and a Test Setup for Experimenting Dynamic Spectrum Sharing

D. Anish Roshi*(1,2), E. Armas(2), C. Westcott(1,2), W. Dellinger(2), N. Patel(2), M. Burrett(3), W. Liu(4), D. Werthimer(4) and R. A. Rodríguez-Solís(5)
(1)Florida Space Institute, Orlando, USA, anish.damodaran@ucf.edu
(2)University of Central Florida, Orlando, USA
(3)Brigham Young University, Provo, USA
(4)University of California, Berkeley, USA
(5)University of Puerto Rico, Mayaguez, Puerto Rico, USA

1. Introduction

The radio spectrum is used by both 'active' services which radiate electromagnetic energy, and 'passive' services which receive radiation emitted from natural sources. Active services include cellular telephony and wireless internet; passive services include radio astronomy observations and remote sensing. So far, distinct frequency bands have been allocated for the different services. It has now been realized that this classic model of spectrum allocation cannot accommodate the demand for next-generation communication technology. One proposal to meet this mounting demand is for services to share spectrum dynamically. New and advanced technological solutions are required before dynamic spectral sharing can be implemented [1].

Our current research activities are centered around developing technology for dynamic spectrum-sharing to be used in radio astronomy applications. The areas we focus on are the development of (1) high-dynamic-range receiver systems, (2) radio frequency interference (RFI) mitigation techniques, and (3) an experimental setup for real-time implementation and testing of mitigation algorithms. A development setup is being built at the Experimental Astronomy Lab (EAL), University of Central Florida, to facilitate this research. We provide a description of the development setup in this paper.

2. Initial Development Setup

Our initial development setup consists of a 4-channel voltage recording system. Such a system will allow us to experiment with developing high-dynamic range receivers [see 2] and also make it possible for us to obtain data for off-line development of RFI mitigation techniques in the voltage and correlation domains. It would also be a prototype of the backend for the experimental setup that we would like to establish in the future. A simplified block diagram of the system is shown in Fig. 1 (top left). The system consists of an analog part, RFSoC 4x2 based digitizers, a 100 GbE link to transport the digitized voltages to a data acquisition computer and a Graphic processor unit (GPU) to accelerate signal processing. We implemented the analog circuitry using commercial components to have a high dynamic range (> 40 dB). This dynamic range is adequate to interface the system to the Deployable Low-band Ionospheric and Transient Experiment (DLITE) facility at Malabar, Florida, for initial testing and experimentation.

The RFSoC 4x2 board provides access to four 14-bit analog to digital converters (ADCs) in the AMD XCZU48DR Field Programmable Gate Array (FPGA). We have two modes of operation implemented in the FPGA firmware. In the first mode, the four analog inputs are sampled at 61.4 MHz, which provides a maximum operating baseband bandwidth of ~30 MHz. The digitized data from the four channels are transported to the acquisition computer through a 100 GbE link. The data rate to the acquisition computer is 3.7 Gbps. We record the data to 4 solid state disks (SSDs) attached to a PCIe SSD expansion card. The 4 TB capacity of the SSDs allows us to record data up to 2 hours from the 4 channel. In the second mode, the four analog inputs are sampled at 245.76 MHz, which provides a maximum operating baseband bandwidth of ~122 MHz. We plan to pass the data through the GPU in this mode for real-time implementation and testing of RFI mitigation algorithms. Currently, the digitized data taken with the second mode is recorded to the SSDs in a non-contiguous fashion for testing. Results from lab tests of the system are shown in Fig. 1 (right).

We are in the process of connecting the system to the DLITE-Malabar station. Two channels will be connected to the telescope, and the other two will be connected to a dual polarization reference antenna. These data sets will be used to

develop and test RFI mitigation strategies and techniques. We envision that our current efforts will lead to the creation of an experimental setup capable of acquiring data from a telescope and multiple reference antennas. This setup will help develop and test the real-time implementation of RFI mitigation techniques for radio astronomy.

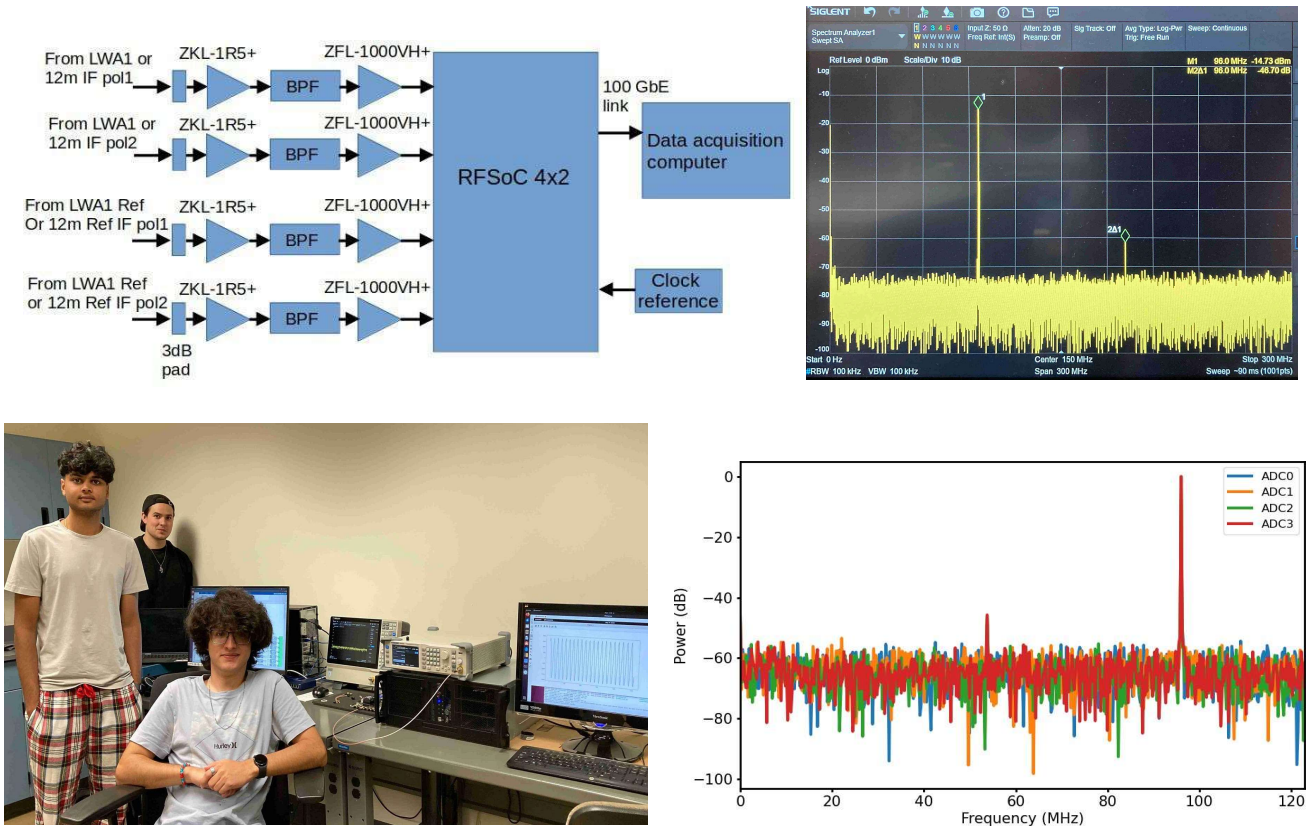

Figure 1. (top-left) A block diagram of the development setup built at the Experimental Astronomy Lab, UCF. **(bottom-left):** Undergraduate students working at the EAL. From left to right: N. Patel, W. Dellinger and E. Armas. **(Right):** The measured spectrum of a 96 MHz sine wave input to the system is shown in the bottom. For comparison the spectrum of the input signal measured using a spectrum analyzer is shown on the top. The level of the second harmonic relative to the fundamental is similar in both cases. The sampling frequency used was 245.76 MHz and so the second harmonic appears at the aliased frequency in the measured spectrum.

[1] M. Zheleva, C. R. Anderson, M. Aksoy, J. T. Johnson, H. Affinnih, C. G. DePree, "Radio Dynamic Zones: Motivations, Challenges, and Opportunities to Catalyze Spectrum Coexistence", IEEE Communications Magazine, **61**, 6, February 203, pp. 156 - 162, doi: https://doi.org/10.1109/MCOM.005.2200389

[2] D. A. Roshi, "Noise Figure Analysis of a 0 - 2.5 GHz directly digitized radio astronomy receiver system", https://carseuprm.org/resources/publication-rscs/

RFI 2024

Identification of RFI in the search of transient radio pulses from magnetars

S. B. Araujo Furlan*(1) (2), G. Gancio(3), G.E. Romero(3), E. Zubieta(3)(4),S. del Palacio(3)(5), F. García(3)(4)
(1) Instituto de Astronomía Teórica y Experimental, CONICET-UNC, Laprida 854, X5000BGR – Córdoba, Argentina, contact e-mail: susana.araujo@unc.edu.ar
(2) Facultad de Matemática, Astronomía, Física y Computación, UNC. Av. Medina Allende s/n , Ciudad Universitaria, CP:X5000HUA - Córdoba, Argentina.
(3) Instituto Argentino de Radioastronomía (CCT La Plata, CONICET; CICPBA; UNLP), C.C.5, (1894) Villa Elisa, Buenos Aires, Argentina
(4) Facultad de Ciencias Astronómicas y Geofísicas, Universidad Nacional de La Plata, Paseo del Bosque, B1900FWA La Plata, Argentina
(5) Department of Space, Earth and Environment, Chalmers University of Technology, SE-412 96 Gothenburg, Sweden

PoS(RFI2024)070

1 Abstract

The study of transient cosmic radio signals in astronomy has become extremely attractive in the last two decades, with discoveries such as Fast Radio Bursts (FRBs) and the presence of transient radio pulses in sources such as magnetars [1,2]. One of the major challenges in this field is to determine whether detected pulses are from an astronomical source or from terrestrial radio frequency interference (RFI). In the search for single pulses from both known astronomical sources, such as magnetars, and unknown sources, a dispersion measure (DM) search for single pulses is one of the main methods to detect them [3]. When the DM of the source is known, it is common practice to dedisperse the observation file only at the source's DM to search for single pulses, or to record the data using coherent dedispersion, which produces a file that is dedipersed at the specified value. When searching over a range of DM values, one would expect RFI to appear at low DM values. Only in cases where the RFI is intense could it be seen at higher values of DM, as shown in Figure 1.

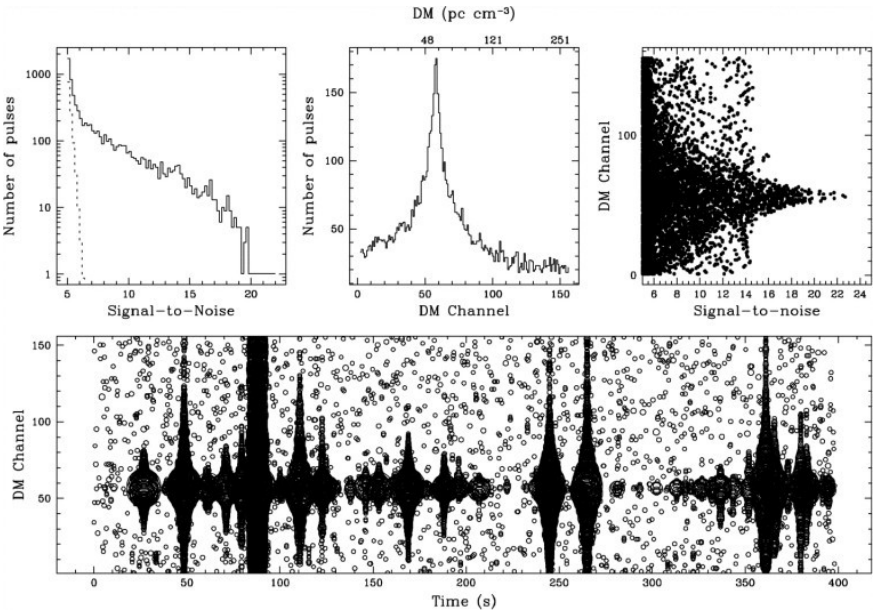

Figure 1. Figure taken from Cordes & McLaughlin work [3]. It shows a single-pulse search for the Crab pulsar. The pulsar has a DM of 56.8 pc cm^{-3}. The lower plot shows all pulses detected in each time series that were dedispersed at a different DM value. The size of the circle is linearly proportional to the S/N of the pulse. Pulses from the Crab are detected around the DM channel of 60. At 90 sec we see a column that crosses all DM channels, corresponding to a strong RFI.

We conducted a 10-day monitoring campaign of the radio-loud magnetar J1622-4950 from March 3, 2023 to March 12, 2023. We performed a single pulse search using the *PulsaR Exploration and Search TOolkit* (PRESTO) [4] software. We observed with the *Instituto Argentino de Radioastronomía* (IAR) radio telescopes "Carlos Varsavsky" (A1) and "Esteban Bajaja" (A2). Each antenna used a ROACH board in the receiver. For both antennas, the acquisition configuration was two circular polarizations with a center frequency of 1400 MHz and a total bandwidth of 400 MHz, with 512 frequency channels. Both antennas had a sampling time of 82 μs. This report focuses on the observations made with A2 because they were cleaner in terms of RFI.

While searching for pulsed radio emission from the magnetar, we found a periodic RFI with a period of about 10 seconds, consisting of a group of narrow pulses. The intriguing feature of this interference was that, after appearing and disappearing at low DM values, it reappeared at at least two specific higher DM values. We observed this feature on at least two of the ten days of observation. This behavior suggests that the interference was reconstructed at these DM values. At higher DM values, the RFI appears slightly shifted in time compared to the time series at DM=0. The general shape changes a little, but still consists of a group of narrow pulses. The presence of this RFI encourages us to be even more cautious when looking for transient emission in a limited DM range, as simply analyzing a limited range could lead to misinterpretation. It also emphasizes the importance of algorithms to distinguish between astronomical signals and RFI.

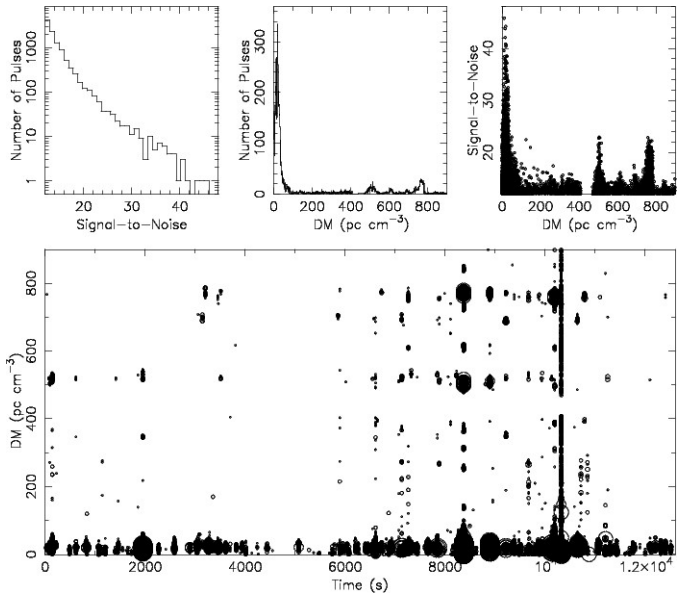

Figure 2. Single pulse search on March 6, 2023 for magnetar J1622-4950. The search was performed in a DM range of 0 ≤ DM ≤ 900. We can see that there is a lot of RFI at low DMs, and at DM ~ 520 and DM ~ 780 some RFI reappears with a higher SN than in the previous DM values. This can also be seen in the upper middle and right panels. The upper middle panel shows a histogram of the number of pulses vs. DM, and the right panel shows the distribution of SN vs. DM.

We have not identified the source of this periodic disturbance. It is present in observations made to date, although the previously reconstructed behavior is not replicated in every observation.

References

[1] Lorimer, D. R., Bailes, M., McLaughlin, M. A., Narkevic, D. J., and Crawford, F., "A Bright Millisecond Radio Burst of Extragalactic Origin", *Science*, vol. 318, no. 5851, p. 777, 2007. doi:10.1126/science.1147532.

[2] Camilo, F., "Transient pulsed radio emission from a magnetar", *Nature*, vol. 442, no. 7105, pp. 892–895, 2006. doi:10.1038/nature04986.

[3] Cordes, J. M. and McLaughlin, M. A., "Searches for Fast Radio Transients", *The Astrophysical Journal*, vol. 596, no. 2, IOP, pp. 1142–1154, 2003. doi:10.1086/378231.

[4] Ransom, S., "PRESTO: PulsaR Exploration and Search TOolkit", *Astrophysics Source Code Library*, 2011. ascl:1107.017.

RFI 2024

CLASSIFICATION AND CHARACTERIZATION OF RFI EVENTS FOR PASSIVE EARTH OBSERVATION BANDS

Adrian Perez-Portero[1,2,*], Jorge Querol[1,3], and Adriano Camps[1,2,4]

[1]CommSensLab – UPC, Universitat Politècnica de Catalunya – BarcelonaTech
[2]Institute of Space Studies of Catalonia (IEEC) – CTE-UPC
[3]University of Luxembourg, SnT, SigCom group, 29 Avenue JFK L-1855 Luxembourg
[4]ASPIRE Visiting International Professor, UAE University, CoE, POBox 15551 Al-Ain, UAE
[*]Correspondence: adrian.perez.portero@upc.edu

PoS(RFI2024)070

1 Introduction

Passive microwave remote sensing is widely used for numerous Earth Observation applications. Nowadays, it plays a crucial role in monitoring Earth's climate by measuring sea surface temperature, atmospheric water vapor, sea ice extent, and soil moisture, among many other variables. The widespread adoption of Global Navigation Satellite System (GNSS) signals is increasingly evident, driven by the expanding number of services relying on them for positioning, timing, and, more recently, Earth Observation applications such as GNSS-Radio Occultations (GNSS-RO) and GNSS-Reflectometry (GNSS-R). Both of these systems work with very faint signals, the latter even below the noise floor of commercial receivers, and are easily disturbed by Radio-Frequency Interference (RFI) [1].

Efforts to detect, locate, and record RFI signals are imperative for the comprehensive characterization of interference events and the formulation of effective mitigation strategies. A preliminary system demonstrating these capabilities was detailed in [2], featuring a GNSS L1/E1 band detection and location system with 2 MHz bandwidth. An enhanced iteration with a broader 100 MHz bandwidth was presented in [3]. In this work, the focus is placed on refining the detection algorithms for unidentified RFI signals in GNSS or passive microwave remote sensing bands, pinpointing the geographical origins of RFI sources, and employing Machine Learning techniques for the classification of interference events. In some cases, positional information allows for null-steering or shielding to mitigate RFI effects, whereas depending on the signal type, pulse blanking or signal excision are preferable. Deep learning, particularly neural networks [4], has shown success in RF signal classification. Convolutional Neural Networks (CNNs) can capture spatial patterns in spectrogram data, while recurrent neural networks (RNNs) can capture temporal dependencies in time-series signals.

2 Signal capture

Signal capture is performed using an evolved version of the L-RARO RFI Detection system [2], named RFI Detection, Location, and Classification (RFI-DLC) [3]. In the following subsections, both the hardware and processing algorithms to generate the datasets are presented.

RFI-DLC is based on multiple Software-Defined Radios working in parallel as 6 different RF chains. The antenna of each RF chain conforming a Uniform Circular Array has a ~60º beamwidth at -3 dB in the horizontal and vertical planes. By looking to the center from which a particular RFI arrives more strongly, these elements allow for the determination of the AOA with 60º of resolution in azimuth. Further improvements can be obtained by comparing the intensities of the RFIs as weighted by the antenna patterns of the array elements. The best Angle of Arrival (AoA) accuracy could be achieved by comparing the phase of the signals collected in consecutive elements, but this would require synchronous local oscillators (LOs) among the receivers, which was out of the scope for this project. The SDR used is based on the commercial Analog Devices 9363 Agile transceiver, coupled with a Xilinx Zynq Z7010 FPGA for signal processing. The receiving frequency can be tuned within the range defined by the GNSS monitoring requirement (L1/E1 ± 50 MHz), and it supports a sustained processing bandwidth of 4 MHz. Each SDR device samples the corresponding antenna signal at least at 4 MSps with a scanning strategy, looping through the 100 MHz band of interest, and performing RFI detection techniques.

Using signal processing together with a certain number of predefined RFI types, certain parameters are estimated on a best effort basis (Fig. 1).

- **Kurtosis (Normality Test) RFI detection** [5]: A statistical fourth-order derived moment able to determine if the received signal (GNSS plus thermal noise) contains any RFI signal. Temporal and Spectral Kurtosis are computed for robustness against blind spots.
- **Spectrogram-based RFI detection and characterization** [6]: Detect time and frequency anomalies in the GNSS signal and spectrum.
- **Parameter extraction** [7]: Extracting parameters from received signals through digital signal processing. The parameters that can be currently estimated are RFI Type (CW, Narrowband, Wideband, Chirp, and Pulsed), Center Frequency, Bandwidth, Power, Pulse Repetition Frequency, Duty Cycle, and Angle of Arrival.

3 Machine learning classification

Several factors contribute to the complexity of classifying RFI signals. RFI signals can come from a wide range of sources, both intentional and unintentional. These sources may emit signals with varying characteristics, making it challenging to develop a one-size-fits-all classification approach. The radio frequency environment is extremely dynamic, with changes in interference patterns occurring over time. New sources of interference may emerge, and existing ones may change their characteristics. This dynamic nature requires adaptive and real-time classification techniques, as only the Karhunen–Loève Transform (KLT) is absolutely agnostic to the RFI type [8]. RFI signals can exhibit complex and non-linear characteristics, often overlapping with legitimate signals. To address these challenges, machine learning and signal processing techniques are often employed for RFI signal classification [9]. These approaches leverage features extracted from the signal data (presented in the previous sections) to train models that can differentiate between interference and legitimate signals.

Convolutional Neural Networks (CNNs) are well-suited for processing grid-structured data, making them effective for RF signal classification tasks involving spectrogram data [10]. They can automatically learn hierarchical features and patterns from the input signals. Recurrent Neural Networks (RNNs) are designed for handling sequential data and are suitable for RF signals that exhibit temporal dependencies [11]. Long Short-Term Memory (LSTM) networks and Gated Recurrent Units (GRUs) are popular RNN architectures that can capture long-range dependencies in time-series signals. Autoencoders can be used for unsupervised feature learning [12]. By training an autoencoder on RF signal data, the network can learn a compact representation of the input signals. The encoded features can then be used for classification tasks. Due to the readily available labelled RFI data obtained from the classification algorithm shown in Fig. 1, an initial training of the network can be performed. Both CNN and RNNs can be used as classifiers for this task, which will approximate the performance of the original classification algorithm. Further improvements will be obtained through the use of transfer learning and autoencoders. Transfer learning involves pre-training a neural network on a large dataset and then fine-tuning it. Through the use of autoencoders and similar unsupervised networks, new training data can be captured and used for the classification that the algorithm could not deal with, such as overlapping RFI.

4 Conclusion

Employing machine learning for Radio-Frequency Interference (RFI) classification can provide a way of identifying and managing unwanted signals that arrive in unknown clusters and configurations. By building on top of proven signal processing algorithms for the initial training, and using unsupervised learning to refine the algorithm, we can adapt to unknown signals. These adaptive algorithms enhance accuracy, providing an efficient and dynamic approach to distinguish interference from genuine signals. Results of the training process will be presented in the conference.

5 Acknowledgements

Research funded by project “GENESIS: GNSS Environmental and Societal Missions—Subproject UPC”, Grant PID2021-126436OB-C21, sponsored by MCIN/AEI/10.13039/501100011033/ and EU ERDF “A way to do Europe”, and grant for recruitment of early stage research staff of Agència Gestió d’Ajuts Universitaris i de Recerca (AGAUR) Generalitat de Catalunya, Spain (FISDUR2020/105).

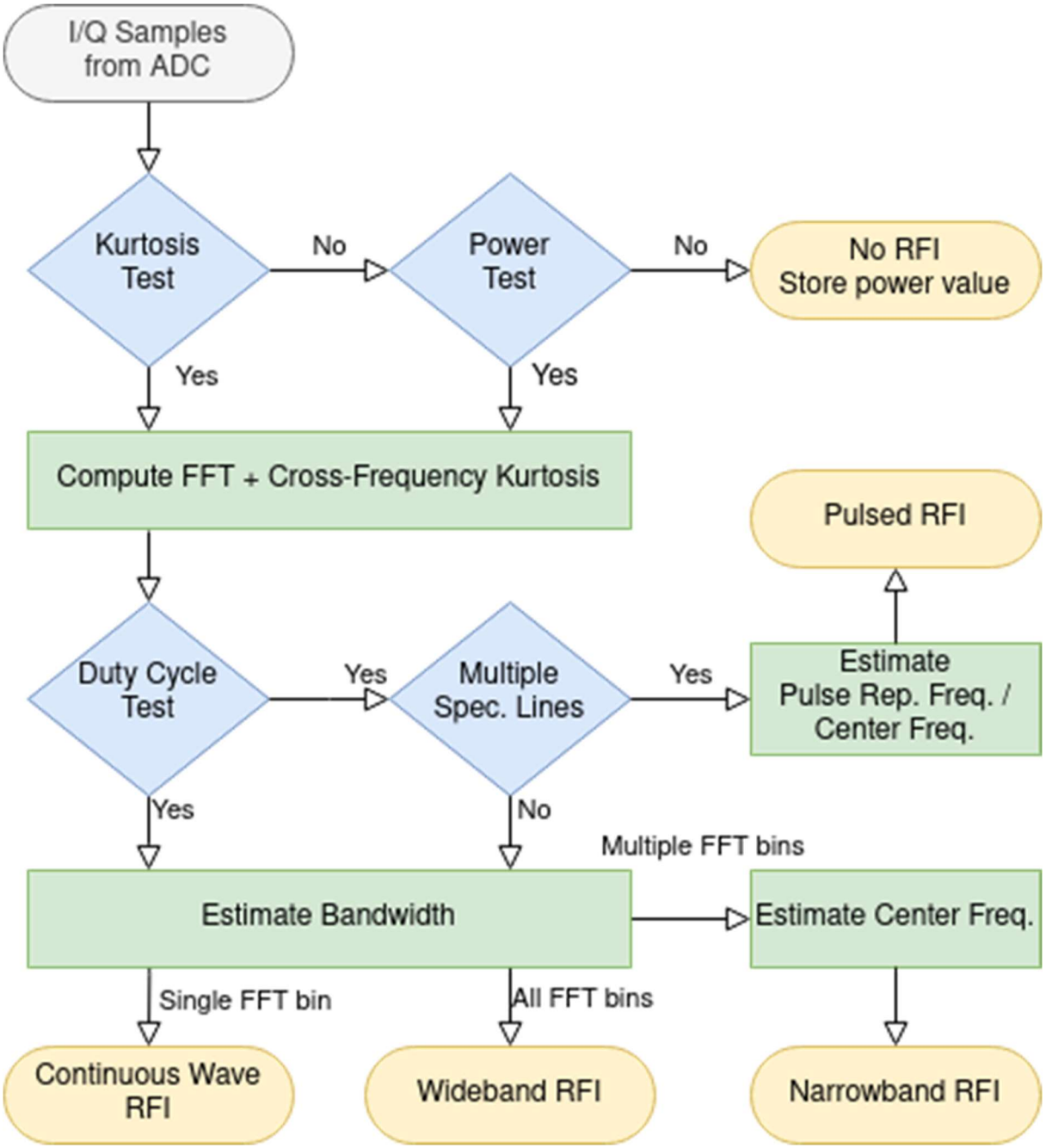

Figure 1. Signal processing algorithm for a priori classification of detected signals and parameter extraction.

(a) Instantaneous and noise floor power estimation of the incoming signal, showing how RFI does not perturb the noise floor estimation.

(b) Time and Frequency Kurtosis estimation in real-time, under the influence of a Pulsed RFI with a 50% duty cycle that goes undetected due to the blind spot of the Time Kurtosis, but is properly detected in the Frequency Kurtosis.

Figure 2. Real-time parameter estimation of Instantaneous Power, Noise floor, Frequency Kurtosis, and Time Kurtosis, under the effects of a time-limited Continous Wave RFI in Fig. 2a, and a Pulsed RFI in Fig. 2b.

References

[1] R. Oliva and E. Daganzo, "SMOS Radio Frequency Interference Scenario: Status and Actions Taken to Improve the RFI Environment in the 1400–1427 MHz Passive Band," *IEEE Transactions on Geoscience and Remote Sensing*, vol. 50, pp. 1427–1439, May 2012.

[2] J. Querol, R. Onrubia, D. Pascual, H. Park, and A. Camps, "A Radio-Frequency Interference detector for GNSS navigation and GNSS-reflectometry applications," in *International Geoscience and Remote Sensing Symposium (IGARSS)*, vol. 2017-July, IEEE, July 2017.

[3] A. Perez-Portero, J. Querol, and A. Camps, "Real-Time Direction Of Arrival Estimation And Characterization Of RFI Signals In GNSS Bands," in *IEEE International Geoscience and Remote Sensing Symposium*, 2023.

[4] S. Scholl, "RF signal classification with synthetic training data and its real-world performance," 2022.

[5] R. D. De Roo, S. Misra, and C. S. Ruf, "Sensitivity of the Kurtosis Statistic as a Detector of Pulsed Sinusoidal RFI," *IEEE Transactions on Geoscience and Remote Sensing*, vol. 45, pp. 1938–1946, July 2007.

[6] J. M. Tarongi and A. Camps, "Radio frequency interference detection and mitigation algorithms based on spectrogram analysis," *Algorithms*, vol. 4, no. 4, pp. 239–261, 2011.

[7] D. Welch, "Spectrum analyzer measurements," tech. rep., TekTronix, 1969.

[8] R. Díez-García, A. Camps, and H. Park, "RFI mitigation in microwave radiometry using the Karhunen–Loève transform," *IEEE Transactions on Geoscience and Remote Sensing*, vol. 61, pp. 1–13, 2023.

[9] P. N. Mohammed and J. R. Piepmeier, "Microwave radiometer RFI detection using deep learning," *IEEE Journal of Selected Topics in Applied Earth Observations and Remote Sensing*, vol. 14, pp. 6398–6405, 2021.

[10] T. Erpek, T. J. O'Shea, Y. E. Sagduyu, Y. Shi, and T. C. Clancy, "Deep learning for wireless communications," 2020.

[11] N. M. Foumani, L. Miller, C. W. Tan, G. I. Webb, G. Forestier, and M. Salehi, "Deep learning for time series classification and extrinsic regression: A current survey," 2023.

[12] S. Subray, S. Tschimben, and K. Gifford, "Towards enhancing spectrum sensing: Signal classification using autoencoders," *IEEE Access*, vol. 9, pp. 82288–82299, 2021.

PoS(RFI2024)070

Meeting the RFI requirement at uGMRT with a 400KVA Solar Inverter System

Pravin Ashok Raybole [(1)], S Sureshkumar [(1)], B S Patil [(1),] A K Nandi [(1),] Ankur [(1)], Sanjeet Rai [(1)]
[(1)] GMRT, NCRA-TIFR Pune, India, pravin@gmrt.ncra.tifr.res.in

1. Abstract

To satisfy the rising electricity demand and reduce carbon emissions at the same time, the Government of India has established a program to use renewable energy as an alternative source for energy requirements. The GMRT[1,2] proposes to install a solar power plant in the observatory premises for captive usage to comply with the policy requirements for High Tension (HT) consumers. GMRT plans to install ~ 400 KVA solar inverter systems to power 90% of the power required for the central electronics building at the array center. It is understood that all the DC and solar inverter systems are exempted from FCC Section 15, Class B regulations; therefore the commercially available solar inverters tend to produce strong broadband radio frequency interference. The broadband noise consists of high amplitude transient harmonic voltage spikes, ripples with discrete lines in the multiples of switching frequency which go all the way up to a few GHz. The power converters that uses Wide Band Gap (WBG) insulated-gate bipolar transistors (IGBT), Silicon Carbide (SiC) metal-oxide-semiconductor-field-effect transistors (MOSFETs) work at high frequencies and the microcontrollers are the primary sources of interference in the solar inverter systems. The second potential source of interference from solar inverter systems is through Conducted Emissions (CE) towards Solar panel and Radiated Emissions (RE) from off the panel. On the one hand, GMRT is a very sensitive low-frequency radio telescope, one has to be very careful and curb any self-generated RFI. On the other hand, the requirement to respect the norms for manufacturer warranty to remain valid, prevent us from designing a RFI mitigation solution requiring modifications to the hardware. To simultaneously meet these conflicting requirements, we have implemented a generic shielding solution [3,4,5]. The first level of shielding is provided to the inverter as shown in figure 1. The second level of shielding is provided by equipping the shielded inverter inside the marine grade container provided with suitable HVAC system, power cables, waveguides and power line filters. The RFI measurement results for a 27KVA solar inverter system taken as a case study is shown in figure 2 and figure 3 giving around 80 dB RF isolation. The communication with Inverter is established through fiber-based Ethernet connectivity for remote monitoring. The in-house developed shielded enclosure for the 400KVA solar power plant is cost-effective and suitable for outdoor installation with a RF isolation greater than 80 dB. As additional effort to lessen our carbon footprint and reduce power consumption, this paper also presents EMC performance of RFI-free LED lighting with motion sensor developed in-house for deployment at the central facility of the observatory.

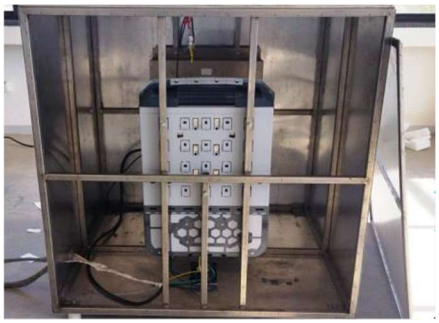

Figure 1.0 Prototype solar inverter with shielded enclosure.

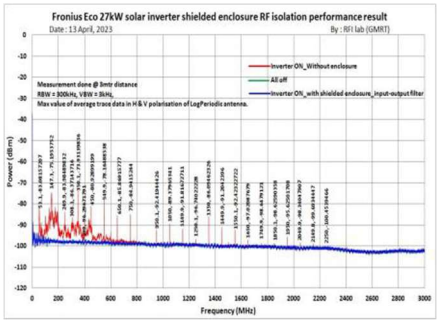

Figure 2.0 Shows the shielding effectiveness of the shielded enclosure.

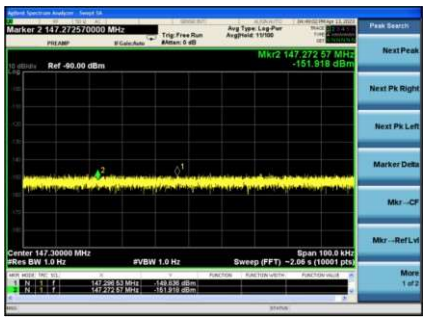

Figure 3.0 Shows clean spectrum at 147.3 MHz with shielded enclosure.

Keywords—Radio frequency interference, Solar power, RF shielding, Radio Astronomy.

References

[1] Swarup, G., Ananthkrishnan, S., Kapahi, V.K., Rao, A.P., Subrahamanya, C.R., and Kulkarni, V.K. (1991) “The Giant Metrewave Radio Telescope” Current Science, vol. 60, pages 90-105

[2] Yashwant Gupta et.al. “The upgraded GMRT: Opening new windows on the radio universe”, Current Science, vol. 113, no.4, 25 August 2017.

[3] Pravin Ashok Raybole, S. Sureshkumar, Sanjeet Rai, Ankur, “Laboratory building in a Faraday’s cage and Radio Frequency Interference monitoring, characterization and mitigation for the upgraded GMRT”, 32 nd URSI GASS, Montreal, 19-26 August 2017

[4] RF Pravin Ashok Raybole, S. Sureshkumar, Sanjeet Rai, Ankur, Shrikant Bhujbal, Lalit Chaudhary, “Shielded enclosure for radio telescope receiver electronics. IEEE MTT-S International Microwave and RF Conference (IMARC), Mumbai, 13-15 Dec 2019

[5] Architectural electromagnetic shielding handbook- Leland H. Hemming.

RFI monitoring at ALMA

Giorgio Siringo*(1), Sean Dougherty(1)
(1) Joint ALMA Observatory, Alonso de Córdova 3107, Vitacura , Santiago, Chile

An overview of the JAO spectrum management office plans for monitoring RFI at the ALMA site.

1 Introduction

The ALMA operational spectrum spans 35 - 950 GHz, divided in 10 non-contiguous frequency bands. Atmospheric water vapor attenuates emissions strongly within a large fraction of this frequency range. Also, the ALMA site is far enough from urban areas and is shielded from most ground-based emissions through distance. Hence, the risk of RFI is highest from sources in the proximity of the ALMA site [1].

2 RFI at ALMA

RFI has been identified from some of the ALMA systems. Other observatories on the Altiplano are also potential sources of emission with sufficient power to produce RFI at ALMA. To minimize this risk, operations between the observatories are coordinated by the JAO spectrum management office in collaboration with the members from the other observatories.

Emissions from telecommunication satellites operating over Chile pose an additional risk of RFI from the sky, for which ALMA does not have any protection. At this moment, SpaceX Starlink and Amazon Kuiper satellite constellations have been granted permission by SubTel, the regulatory authority for spectrum management in Chile, to operate seven and one gateway stations respectively in Chile. The nearest gateway station to ALMA is 540 km south-west of the ALMA site. We consider this distance sufficient to safeguard the ALMA systems from potential RFI due to the downlink signals to the gateway station.

3 Monitoring plan

It is in that context that the JAO spectrum management office has started a plan for RFI monitoring at the ALMA site, with multiple goals. The first step is to create a database of RFI. Such a database will be created using the ALMA receivers and antennas, thus reaching a sensitivity level comparable to ALMA single-dish science observations. Secondly, such knowledge of RFI levels, frequencies and possibly coordinates, will be used to develop mitigation strategies such as data excision and coordinated observing plans. Moreover, this knowledge will also serve as a baseline to monitor impact and evolution of the RFI at the site in the coming years.

References

[1] G. Siringo, S. Dougherty, "ALMA Spectrum and Radio Frequency Interference," *White Paper*, ALMA RFI Memo 152, July 2023

Experiences from Coordination with Satellite Constellations to Protect Radio Astronomy

Frank K. Schinzel*[1,2], Ashley B. Vanderley [1], Christopher De Pree[2] , Bang Nhan[2] , and Jonathan Williams[1]

[1] U.S. National Science Foundation, Alexandria, VA, U.S.A., fschinze@nsf.gov
[2] National Radio Astronomy Observatory, Charlottesville, VA, U.S.A.

Driven by technological advances and economics, an era of large satellite constellations has begun. This has led to a dramatic increase in the number of satellites in low Earth orbit (LEO) and with that an increase of transmissions into even the most remote areas on Earth and which are directly impacting radio and optical astronomical facilities. With the first launch of satellites by SpaceX for the Starlink satellite internet constellation in 2019, the National Science Foundation and SpaceX established a coordination agreement to ensure that this new satellite constellation meets international radio astronomy protection standards and to mitigate the impact on ground-based radio astronomy facilities. This agreement was amended in 2023 to include considerations for optical astronomy. Since then, additional coordination agreements have been established or are in the process of finalizing to include other emerging constellations, such as Amazon Kuiper or Eutelsat OneWeb. This presentation will include a broad overview of the content of these coordination agreements and provide a summary of recent experiments and measures for co-existence of radio astronomy facilities in an environment of growing satellite constellations in non-GSO orbits.

1. Satellite Coordination Agreements

The first coordination agreement between SpaceX and NSF set the stage and provided an example for close collaboration between the astronomical community and operators of large satellite constellations in planning, deployment, and during operation of fleets consisting of hundreds to tens of thousands of satellites. These agreements attempt to benefit the astronomical community and reduce the impact of these constellations on astronomical observations. We will be providing an overview and summary of the current state of coordination agreements, the benefits and challenges they provide for both parties involved, and how they could serve as an example for the global industry.

2. Coordinated Testing with the Starlink Satellite Constellation

Facilitated by NSF's coordination agreement, the National Radio Astronomy Observatory (NRAO) and Green Bank Observatory (GBO) in 2019 started working directly with SpaceX to jointly analyze and minimize the potential impacts from the Starlink system. We will provide a summary of coordinated testing that has been performed at the Green Bank Telescope (GBT) in the U.S. National Radio Quiet Zone and at the Karl G. Jansky Very Large Array (VLA) in New Mexico. These experiments include the deployment of Starlink User Terminals near the GBT and VLA, testing of frequency shifting and boresight avoidance, and testing in anticipation of Starlink providing supplemental coverage from space directly to mobile phones.

3. Operational Data Sharing (ODS) Framework

Coordinated testing with Starlink has led to the development of a sharing framework of current telescope status with satellite constellation operators. This operational data sharing (ODS) database allows satellite service providers to query telescope status through a representational state transfer (REST) API. Satellite constellations can use the observational metadata to adjust their transmission properties in real-time to avoid sensitive radio astronomy facilities. We will be presenting an overview of the ODS implementation and results from coordinated tests with VLA, the GBT, and the SpaceX Starlink team. The ODS framework is planned to be fully deployed and in production at the VLA by fall 2024.

Observations and simulations on the impact of satellite constellations on SKA Band 5 with the Onsala Twin Telescope

Authors: Hao Qiu (SKAO); Gary Hovey (Chalmers); Federico Di Vruno (SKAO)

The 10.6 GHz -10.7 GHz frequency range is an allocated band for Radio Astronomy. Recent satellite constellations aim to provide broadband internet such as OneWeb and Starlink are known to operate between the 10.7-15 GHz frequency bands. This also presents a challenging environment for the operation of sensitive wideband receivers on radio telescopes such as the Band 5b for the upcoming SKA-mid telescope as adjacent frequency channels may be polluted.

Recent spectrum management compatibility studies have limited the use between 10.7-10.95 GHz to protect the allocated Radio Astronomy frequencies.
We present observation results of OneWeb satellites with the Onsala Twin Telescope at 10.7-12.7 GHz to follow up on the practical implementation of the new regulations and impact to observation data.

Using real-time observation data of satellite emission properties, we present a software package to model the effect of satellite active emission for observation planning at telescope sites across the world. We demonstrate using real-time satellite coordinates, how the SKAO will be able to deploy this as an observation planning tool to actively avoid high contamination from known satellite RFI sources.

PoS(RFI2024)070

RFI 2024

New RFI Threats for Future Microwave Sounders: Development of new RFI Detection Strategies for 5G signals

Alexandra Bringer [(1)], Edward Kim [(1)]
[(1)] NASA Goddard Space Flight Center
Greenbelt, Maryland

1. Introduction

For the past 15 years, the National Weather Service (NWS) has been using microwave sounder measurements operationally from the Joint Polar Satellite System (JPSS) Program [1] satellites to produce weather forecasting worldwide. The weather forecasts are assimilating 3D atmospheric temperature and water vapor profiles from the microwave **Advanced Technology Microwave Sounder (ATMS)** from S-NPP, NOAA-20 and NOAA-21 and will also include data from two more ATMS units scheduled to be launched in 2027 and ~2032. ATMS was designed in the 1990's when Radio Frequency Interference (RFI) in was not an issue at sounding frequencies (20-200 GHz). Therefore, their design did not include RFI detection capabilities. However, given recent frequency allocations for communication applications at frequencies close to sounding frequencies, RFI is a new threat that needs to be assessed for ATMS and for future microwave sounders.

Figure 1 presents the zenith opacity as function of frequency [2]. The vertical black lines on this graph illustrates the location in frequency of the ATMS window and sounding channels. The color boxes highlight the frequency ranges where potential RFI threats are located. On this figure, three potential RFI sources have been identified. The first one is the 5G FR2 band (red box) which covers frequencies close to the first two ATMS channels (23 and 31 GHz). The second one concerns ATMS channels 3 and 4 (50 GHz) potentially impacted by Space X Earth to Space transmissions (blue box) in the recently-approved 47.2-50.2 GHz and 50.4-51.4 GHz ranges. The third potential source of RFI is located towards the higher frequencies and could impact ATMS channel 16 due to the use of the 81-86 GHz by Space X to downlink data (green box). Given those potential RFI threats, the next generation of microwave sounders need to include RFI detection capabilities to limit the impact of undetected RFI as this could lead to incorrect weather forecasts.

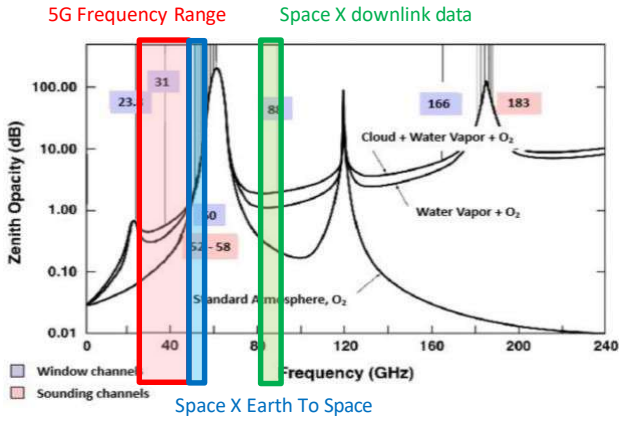

Figure 1: RFI Threats to ATMS window and sounding channels

In that context, the Near Earth Observing Network (**NEON**) program [3] which is the follow on to the JPSS program aims to design and launch **12** new microwave Sounders for Microwave-Based Applications (**SMBA**). Among the new features, the design of SMBA instruments will include **RFI detection capability**. For this conference, the study focuses on simulating the future microwave sounder measurements in presence of 5G RFI signals and on the development of new RFI detection strategies.

2. Initial Results and next steps

The initial step of this study consisted in understanding the nature of 5G signals. Figure 2 presents an example of the simulation of 5G signal in the FR2 Frequency Band () in the uplink configuration. The spectrum of this simulated 5G signal is illustrated in the left plot and demonstrates the broadband characteristics of 5G signals. It can also be noted that 5G signals exhibit

significant sidebands that might impact microwave sounders channels if 5G base stations and users are emitting in frequency bands adjacent to the sounding frequency channels.
The histogram on the right of Figure 2 shows the distribution of the time samples of the 5G signal and highlights the Gaussian shape of the distribution. This indicates that individual 5G signals will tend to act like broadband RFI and present similar characteristics to the uncontaminated white noise that is measured by a radiometer. This means that the contribution of a 5G signal and the underlying targeted scene is going to be more complicated to distinguish from one another. Additionnaly, telecommunication signals and therefore 5 signals are expected to be low power radiating upwards to Space creating insidious RFI which is a major concern as undetected RFI could bias weather forecasts.

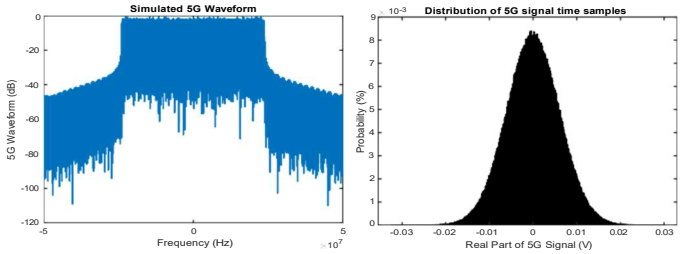

Figure 2: Example of 5G signal waveform (left) and their distribution in the time domain (right)

The goal of this work is to determine the best detection approach to detect RFI with 5G signal characteristics, i.e broadband signals with a low Signal to Noise Ratio (SNR). RFI detection algorithms have been implemented for NASA's Soil Moisture Active/Passive (SMAP) mission. However, in this case, the SMAP radiometer operates at L-Band and the RFI encountered at those frequencies were observed to be mostly narrowband, high power, pulsed RFI sources. Figure 3 presents an example of the probability of detection of 4 of the SMAP RFI detection algorithms [4] as a function of SNR for a narrowband RFI source (left) and for a broadband RFI source (right). It can be observed that the current algorithms work well to detect RFI when the SNR is moderate or large and when the source is narrowband but they fail in the case of low SNR broadband RFI sources (as highlighted by the red box). This indicates that these detectors will unlikely be successful for the detection of 5G signals and new approaches are needed. The next step of this study is to implement and test new RFI detection approaches that will be able

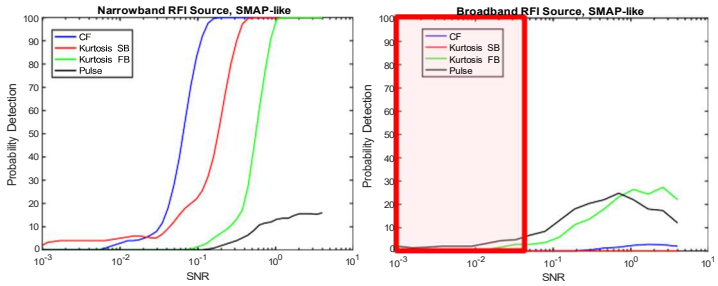

Figure 3: Probability of Detection of RFI detectors for a narrowband source RFI (left) and broadband RFI source (right) in a SMAP-like configuration

to detect low SNR, broadband signals. Traditional signal processing methods (cyclostationarity for instance) are being explored, and their performance will be assessed and reported at the time of the conference.
It is also important to consider the problem from the perspective of the victim (the radiometer onboard a satellite) and the simulation should generate an aggregation of thousands of 5G signals reaching the instrument which would represent the contribution of thousands of users observed within the radiometer footprint. The detection methods developed in the first step would also be tested on aggregated 5G signals and their performance will be assessed for different parameters (SNR, Frequency impacted, probability of detection, false alarm rates…).
This work is an important part of a simulation tool that is currently being developed for the NEON program. This tool aims to simulate realistic 5G networks over a targeted area on Earth and to produce the aggregated 5G signals that will then be received by the instrument. The status of the simulation tool will also be reported in the presentation.

4. References

[1] Goldberg, Mitchell. "The joint polar satellite system overview." In *IGARSS 2018-2018 IEEE International Geoscience and Remote Sensing Symposium*, pp. 1581-1584. IEEE, 2018.
[2] Lyu, C.H., Kim, E.J., Mccormick, L.M., Leslie, R.V. and Osaretin, I.A., 2021. JPSS-1 ATMS postlaunch active geolocation analysis. *IEEE Transactions on Geoscience and Remote Sensing*, *59*(11), pp.9462-9471.
[3] Kim, E.J., 2021, July. Next-Generation Leo Microwave Sounders: Options and Tradeoffs. In *2021 IEEE International Geoscience and Remote Sensing Symposium IGARSS* (pp. 1504-1506). IEEE.
[4] Piepmeier, J.R., Johnson, J.T., Mohammed, P.N., Bradley, D., Ruf, C., Aksoy, M., Garcia, R., Hudson, D., Miles, L. and Wong, M., 2013. Radio-frequency interference mitigation for the soil moisture active passive microwave radiometer. *IEEE Transactions on Geoscience and Remote Sensing*, *52*(1), pp.761-775.

Monitoring correction of RFI on SAOCOM Synthetic Aperture Radar data

Juan Pablo Cuesta Gonzalez[1], Hugo Videla [2]
[1] CONAE, Buenos Aires, Argentina, jpcuesta@conae.gov.ar
[2] CONAE, Córdoba, Argentina, jpcuesta@conae.gov.ar

Radio frequency interference (RFI) is a well-known problem in low-frequency radar remote sensing. In synthetic aperture radar (SAR) image processing, RFI can severely degrade image quality, distort polarimetric signatures, and increase SAR phase noise levels. To address this, a set of algorithms have been implemented in the SAOCOM data processing chain, which reliably detect and mitigate RFI in SAR observations. Furthermore, data on RFI detection from all SAOCOM acquisitions is stored in the SAR Engineering and Calibration Facility databases. This information is used to map RFI presence globally and over different time periods, providing valuable input for SAR system operations.

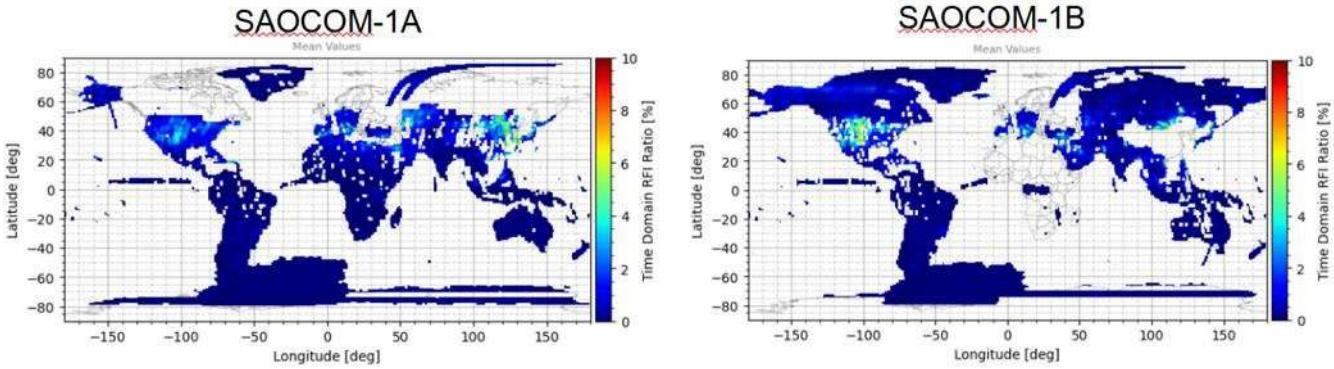

Figure 1. RFI monitoring maps example, derived from time domain interference detection algorithms over SAOCOM satellites data during the first semester of 2023

PoS(RFI2024)070

RLAN interference in weather radars: initiatives for their mitigation by the Argentina Meteorological Service

Martin Rugna*[(1)], Luciano Vidal [(1)], Aldana Arruti [(1)], Daichi Kitahara[(2)], Juan Ruiz[(3)], Ramon de Elía[(1)] and Tomoo Ushio[(2)]
[(1)] Servicio Meteorológico Nacional, Buenos Aires, Argentina, mrugna@smn.gob.ar
[(2)] Osaka University, Osaka, Japan
[(3)] Centro de Investigaciones del Mar y de la Atmósfera, Buenos Aires, Argentina

1. Introduction

Radio local area networks (RLAN), such as those generated by conventional routers can interfere weather radar signals, what represents a significant challenge, both in the context of real-time analysis of imagery at a forecast office and in the context of quantitative applications such as precipitation estimation [1, 2]. Interference is expected when the transmitting wireless device operates in a frequency close to that of the radars. These signals, when received by the radar and processed as genuine, backscattered echoes appear mostly as radial lines on radar images and, as a result, contaminate the data for all applications.

Since 2011, there has been an increasing interference of radar data in Argentina by RLAN signals within the protected portion of the spectrum on C-band (5600 to 5650 MHz as indicated by the National Radiocommunication Administration) [3]. This interference has been particularly severe since late 2012. As observed in [1], in 2015 data of almost half of the radar coverage was contaminated, with reflectivity values close to the ones generated by heavy rain and hailstones (>55 dBZ). As a national project for radarization of the country became a reality [4], the necessity for accounting for the causes and location of the sources became apparent. The majority of these recently installed radars were situated near urban areas due to infrastructure reasons and vulnerable to interference from these surrounding areas.

While some radial line interferences originating from the Sun can be useful for assessing the antenna pointing and the condition of the processing chain [5, 6], these are seen at higher antenna elevations and at precise times of the day. Many efforts are made to eliminate all kinds of interference, partly in spectrum vigilance [7] and in postprocessing via quality control techniques [8]. This abstract shows the efforts led by the Argentina National Meteorological Service (SMN for its name in spanish) and the way towards a collaborative endeavor to obtain the best possible radar data in increasingly adverse situations.

2. Postprocessing methods, wireless devices monitoring and results

Starting in 2017 and knowing that the interferences are of mostly constant power, we implemented a simple filter that consisted in reconverting the reflectivity data back to received power and applying a threshold for all the data. This had the advantage of retaining high reflectivity values at long distances, although the relatively lower values of larger storm borders and weak but growing storms may fall below the threshold. This method also has the advantage of having low computation time, and hence capable of being integrated to the operational imagery that is available to the public.

This method was then refined in the operational quality control of [8] which also addresses other non-interference issues on radar data (e.g. attenuation correction), resulting in a higher run time. The RLAN interference removal technique employs a radial-by-radial method that utilizes a similar power filtering approach but applies an iterative method known as RANSAC that tries to remove outliers when fitting a linear model. By classifying storm echoes as outliers, data points within the fitted model, extended by 7 dBZ, are removed. Figure 1 illustrates the effectiveness of this method on a single radial.

Building on previous experience with contaminated radar data, in [9] we created a static mask of non-meteorological echoes. This involved discriminating between rain and no-rain radar volumes and then generating a pixel-by-pixel reflectivity average for two years of data. Applying a threshold to the frequency of reflectivity values, the resulting mask effectively identifies ground clutter near the radar and RLAN interference at medium to long ranges. This mask is integrated into the quality control process defined in [8], using a quality index of the overall data based on the methodology described in [2]. When interference is detected within precipitation echoes, interpolation is used to reconstruct the interfered data.

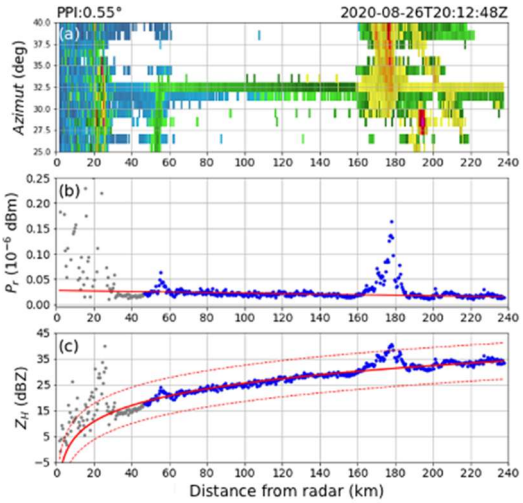

Figure 1. Reflectivity data for the lowest PPI of an operational volumetric scan. On panel (a) a RLAN interference appears as a complete line of reflectivity data centered in 32,5° of azimuth. (b) Converted reflectivity data from the selected radial in (a) to received power; the interference is observed to have a constant power and is adjusted through a linear fit in red. (c) Power data and linear fit converted back to reflectivity with the dashed red lines indicating a 7 dBZ threshold.

More recently, we tested the ability of wireless devices to change or ban specific transmitting channels using a Dynamic Frequency Selection (DFS) system [7]. Using the configurations outlined by US Federal Communications Commission (FCC) and the European Telecommunications Standards Institute (ETSI) we planned a short experiment in one of the most severely affected radars, which also covers Argentina's largest urban area. On a cloud free day, we used the radar in receive-only mode to snapshot the interference field, then transmitted a series of pulses that should trigger the DFS in the wireless devices and check with receive-only data if a change was noted. This experiment proved that while some devices appeared to acknowledge the presence of a weather radar, most of them didn't, and eventually the ones that disappeared throughout the experiment appeared back in the data.

The SMN is now testing advanced processing techniques based on the manipulation of level 1 data. These techniques have been developed and implemented by the radar manufacturer, INVAP S.E. The initial version of this processing system is implemented in all radars manufactured by the company, enabling the SMN to distribute cleaner images to the public.

[1] E. Saltikoff, J. Y. N. Cho, P. Tristant, A. Huuskonen, L. Allmon, R. Cook, E. Becker, and P. Joe, "The threat to weather radars by wireless technology," *Bulletin of the American Meteorological Society*, vol. 97, no. 7, pp. 1159–1167, Jul. 2016.
[2] A. Jurczyk, J. Szturc, I. Otop, K. Ośródka, and P. Struzik, "Quality-Based Combination of Multi-Source Precipitation Data," *Remote Sensing*, vol. 12, no. 11, p. 1709, May 2020, doi: https://doi.org/10.3390/rs12111709.
[3] Ente Nacional de Comunicaciones (ENACOM), *Cuadro de Atribución de Bandas de Frecuencias de la República Argentina (CABFRA)*, https://www.enacom.gob.ar/cuadro-de-atribucion-de-bandas-de-frecuencias-de-la-republica-argentina-cabfra-_p1588 May 2024.
[4] A. Rodríguez et al., "SiNaRaMe: El Primer Sistema Integrado de Radares Hidro-Meteorológicos de Latinoamérica," *Revista de la Facultad de Ciencias Exactas, Físicas y Naturales*, vol. 4, no. 1, pp. 41–41, Mar. 2017. Available: https://revistas.unc.edu.ar/index.php/FCEFyN/article/view/14614
[5] M. Rugna, L. Vidal, and R. de Elía, "Verificación de la orientación de la antena de los radares meteorológicos de INTA utilizando la radiación solar," *El Abrigo*, Mar. 2017. Available: https://repositorio.smn.gob.ar/handle/20.500.12160/382
[6] I. Holleman, A. Huuskonen, M. Kurri, and H. Beekhuis, "Operational Monitoring of Weather Radar Receiving Chain Using the Sun," *Journal of Atmospheric and Oceanic Technology*, vol. 27, no. 1, pp. 159–166, Jan. 2010, doi: https://doi.org/10.1175/2009jtecha1213.1.
[7] D. Kitahara et al., "Experiments on WLAN Interference Reduction by Dynamic Frequency Selection in C-Band Weather Radars," *AMS - 40th Conference on Radar Meteorology*, Aug. 23, 2023. https://ams.confex.com/ams/40RADAR/meetingapp.cgi/Paper/426025.
[8] A. Arruti, P. Maldonado, M. Rugna, M. Sacco, J. J. Ruiz, and L. Vidal, "Sistema de Control de Calidad de Datos de Radar en el Servicio Meteorológico Nacional. Parte I: Descripción del algoritmo," *El Abrigo*, Mar. 2021. Available: https://repositorio.smn.gob.ar/handle/20.500.12160/1537
[9] D. Giménez, L. Vidal, M. Rugna, R. de Elía, and L. Giordano, "Climatología de ecos no meteorológicos de la red de radares SINARAME," *El Abrigo*, Sep. 2021. Available: https://repositorio.smn.gob.ar/handle/20 500.12160/1685

Approaches and Methodologies for the Detection, Characterizing, and Mitigation of Passive Sensor Data Corrupting Emissions (DMiPS)

Beau Backus[(1)], TBS* [(1)], and TBS[(2)]
[(1)] NOAA/NESDIS, Silver Spring, USA, beau.backus@noaa.gov
[(2)] TBS

1. Introduction

The National Oceanic and Atmospheric Administration (NOAA) National Environmental Satellite Data and Information Services (NESDIS) is interested in exploring methodologies, services, tools, and capabilities that can be applied towards detecting, identifying, characterizing, and mitigating anthropogenic radio frequency (RF) emissions within or adjacent to the RF bands used for passive sensing by Earth exploration satellites.

2. Overview

Domestic USA and International radio regulations contain frequency ranges, passive bands, where no radio frequency transmissions are allowed. [1] However, it's possible that excessive anthropogenic energy may be present within those bands regardless. Adjacent services often have regulatory limits regarding the energy level of out-of-band emissions that are allowed from those services that may contaminate nearby passive bands. As current and future telecommunication services, satellite and broadband-aviation uplinks in millimeter wave bands are increasingly implemented there are similarly increasing interference risks to passive sensors, to include the operational microwave sensors used by environmental space sensing systems. This interference may degrade the data used by Numerical Weather Prediction (NWP) Models and other applications, with resulting accuracy degradation. [2]

NESDIS is seeking to formulate a comprehensive long-term solution to interference as communication and passive instrument technologies evolve. Naturally occurring emissions are generally very weak compared to anthropogenic emissions originating from other radio services and it is essential that anthropogenic emissions are identified and kept from adversely contaminating collected Earth observation data.

3. Objectives

The goal of NOAA/NESDIS is to develop efficient, repeatable, and effective methods to identify anthropogenic sources of interference of passive microwave remote sensing, so contaminated data can be accurately flagged and removed. Through this study, NOAA is looking to reduce the risk to current NOAA and partner space systems, and implement the lessons learned from studies and current operations to design more robust future systems.

It can be assumed that the level of RFI is gradually increasing over time with the aggregation of single low level interfering signals up to a point when RFI becomes obvious. Thus, RFI can be expected to move from undetectable levels, then to levels of "insidious" data corruption, and then to levels of blatant data contamination, such that the data can only be discarded. (See figure 1.) Insidious data corruption means there could be RFI (data corruption) induced into the measurements unnoticed for a significant period as the measurements are erroneously taken as correct measurements without any interference component.

Therefore, monitoring of the development of mass market RF intensive applications is a factor for consideration in the characterization process. This also requires building up monitoring records on measurements of already operational instruments

to have reference data which can be later consulted and compared once the deployment of these RF intensive applications increases. This allows for long term RFI trend observations.

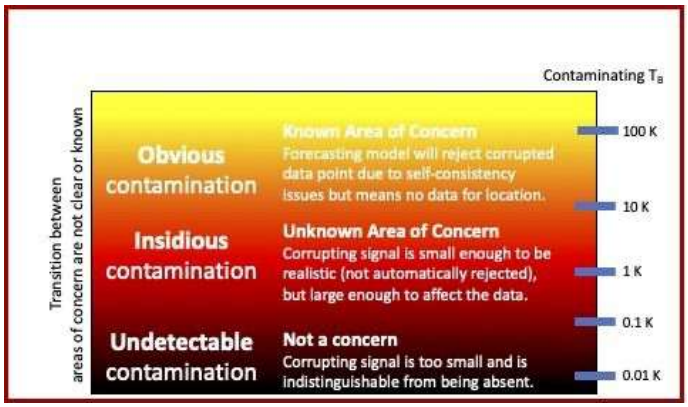

Figure 1. Three levels of data contamination to be addressed.

An important aspect is in the identification of the breadth and diversity of the passive band data that may be contaminated by adjacent band, high density, users. The sources of data that NOAA handles include a variety of other administrative meteorological sources that are sharing data, commercial organizations that are providing contracted environmental data, and other non-NOAA US agencies. Use of mapping and flagging processes will be most optimally utilized by establishing and maintaining global standards for mapping, flagging and related data processing.

As part of this endeavor, NOAA/NESDIS is funding joint partnerships with other organizations, versed or interested in the development of processes and architectures for the effective and comprehensive characterizations and mitigations of passive band sensor data corrupting emissions globally. Under the Joint Venture (JV) program, NOAA/NESDIS will leverage current and developing technologies and, jointly with other partners, achieve the objectives of this project.

[1] ITU Radio Regulations; Articles 1, Edition of 2020, RR5-152 pp 100, footnote 5.340.

[2] Stephen English. "The value of passive bands used by microwave instruments in Numerical Weather Prediction" Slide 1 (nationalacademies.org) © ECMWF, October 23, 2020

The phantom menace: Direct-to-cell service and radio astronomy

Federico Di Vruno[1,2]
[1] SKA Observatory, Macclesfield, United Kingdom, Federico.divruno@skao.int
[2] IAU Centre for the Protection of the Dark and Quiet Skies from Satellite Constellation Interference, Paris, France

1. Introduction

The advent of direct-to-cell (D2C) technology, which enables communication from Low Earth Orbit (LEO) satellites directly to ordinary cellphones, promises to revolutionize global connectivity, especially in underserved and remote areas. Several companies such as Linx, AST and Science, and Starlink are seeking to establish this as a service. However, this technological breakthrough poses significant challenges to radio astronomy. This abstract explores the regulatory and technical aspects of the impact of D2C technology on radio astronomy.

2. Technology

D2C is proposed as a means to augment the reach of ordinary cellphone networks where the terrestrial infrastructure does not reach. By using satellites in LEO, operators are hoping to reach more underserved areas in the world without the need to have special ground terminals. There are challenges for this technology as ordinary cellphones are intended to communicate with base stations on the ground at relatively close proximity, LEO satellites will be in the best cases further than 350km away. Therefore satellites will have to transmit as much more powerful signal towards the ground and be much more sensitive to pickup the uplink of cellphones.

2. Regulatory aspects

From a regulatory perspective, the use of certain frequency bands for this type of application is becoming a contentious issue. There are proposals to re-use IMT (the terminology used by the International Telecommunication Union for cellphone services), registered under the provision RR 4.4 of the ITU. This provision is a tool for national administrations that allows to use a frequency band not assigned to a certain service (in this case satellite transmissions) on the basis of “non-interference and no protection”. This use of the provision RR 4.4 can allow administrations to use some frequencies while they keep working on the Agenda Item 1.13 for the World Radiocommunication Conference 2027 of the ITU-R where other bands might be assigned for this application.

3. Effects on Radio Astronomy

Radio telescopes rely on protected frequency bands to observe celestial phenomena without terrestrial interference in addition to wider observations done in an opportunistic basis. What normally enables the wider observations of radio astronomy is the national protections of radio telescopes that sometimes can even go to the establishment of Radio Quiet Zones. The proliferation of D2C technology will effectively move IMT base stations from the ground to the sky, drastically changing the situation for radio astronomy. This work will review the technology, explore some of the regulatory challenges and asses the potential impact to radio astronomy as well as some possible mitigations.

RFI 2024

An Evaluation of a New Method of Calculating RFI with Kurtosis

Sylvia Llosa*(1), Arvind Aradhya(1), and Kevin Gifford(1)
(1) University of Colorado Boulder, Boulder, United States, sylvia.llosa@colorado.edu

1 Abstract

This paper presents a novel method for calculating spectral kurtosis called Frequency Separated Spectral Kurtosis (FSSK) that eliminates the need for Fast Fourier Transform (FFT) by leveraging Software Defined Radio (SDR) technology to directly separate and analyze frequency components. Traditional methods involve converting In-phase and Quadrature (IQ) data using FFT before computing kurtosis, a process that can be computationally intensive and time-consuming. Our approach, however, performs kurtosis analysis on already parsed frequency data, significantly enhancing efficiency.

The primary advantage of this method is the ability to identify Radio Frequency Interference (RFI) in real time, which is critical for applications requiring immediate RFI detection and mitigation. This experiment captures data from radio frequency (RF) sensors deployed at a radio astronomy site. This evaluation aims to detail the implementation of the new method, compare its performance against traditional techniques, and explore its broader implications for real-time spectral analysis.

2 Introduction

Radio Frequency Interference (RFI) is a significant, worsening problem in an increasingly digital world. Detecting RFI in real time, as quickly and as computationally efficiently as possible, is therefore of utmost importance. Real-time detection enables prompt mitigation measures, safeguarding sensitive radio astronomy observations and communication systems from disruptions caused by unwanted radio signals. Spectral kurtosis, as a method capable of identifying and characterizing RFI signatures in the frequency domain, plays a pivotal role in these efforts. By leveraging advanced signal processing techniques such as spectral kurtosis, this work aims to enhance the resilience of radio systems against the growing challenges posed by RFI.

In the most idealized scenario, such as at an RA facility, where the signal environment is exceptionally quiet, it is hypothesized that the results of spectral kurtosis measurements will exhibit minimal variation across different methods of calculation. This is predicated on the absence of any distinct frequency-specific content, which would otherwise cause certain frequency channels to exhibit disproportionately high kurtosis values. Additionally, in such a noise-dominated environment, all frequency channels are expected to approximate Gaussian distributions, thereby minimizing the impact of the specific method used to compute kurtosis. Consequently, in these conditions, the spectral kurtosis should yield consistent results, irrespective of the computational approach employed.

Spectral kurtosis was developed in the 1980s for detection of Non-Gaussian signals in sonar systems by Dwyer [1]. However it is a known effective method for detecting RFI in other environments [2]. Multiple papers showed that SK offers advantages over Power Spectral Density calculations in certain applications as "it indicates at each frequency bin, if the signal contains nonstationary, stationary harmonic or mixing process" [4]. Smith et al. evaluates the effectiveness of spectral kurtosis (SK) as a statistical method for detecting and mitigating radio frequency interference (RFI) against realistic simulated RFI signals of various modulation types, data rates, duty cycles, and carrier frequencies [3]. This process provides a multi-resolution analysis, capturing both low-frequency and high-frequency details.

The spectral kurtosis equation is as follows:

$$K_z(m) = \frac{\kappa_4\{X^t(m), X^t(m), X^t(m), X^t(m)\}}{[\kappa_2\{X^t(m), X^t(m)\}]^2}. \quad (1)$$

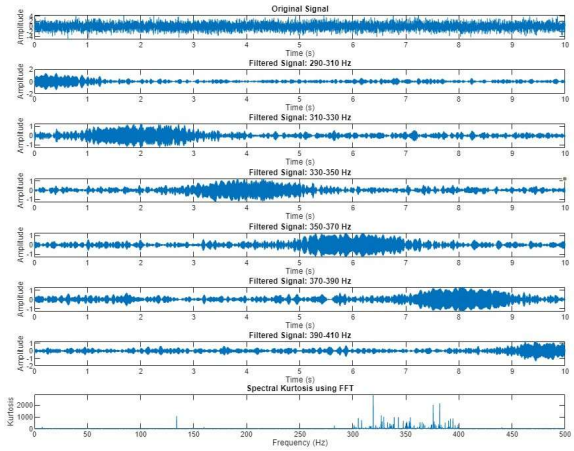

Figure 1. Predicted Spectral Kurtosis from Simulated Data

The equivalence between separating frequencies with a Software Defined Radio (SDR) and subsequently calculating kurtosis versus performing a Fast Fourier Transform (FFT) followed by spectral kurtosis calculation hinges on their handling of the signal's frequency-domain representation. Figure 1 shows the equivalence in simulated data. When an FFT is applied to a time-domain signal, it decomposes the signal into its constituent frequency components, each characterized by amplitude and phase information. Spectral kurtosis, in turn, quantifies the peakedness or flatness of the spectral distribution at each frequency component. Similarly, using an SDR to first separate frequencies achieves a comparable result by directly accessing the amplitude information at these separated frequencies without the intermediate step of FFT computation. Therefore, performing kurtosis on these separated frequency components from the SDR approach is mathematically equivalent to calculating spectral kurtosis after an FFT.

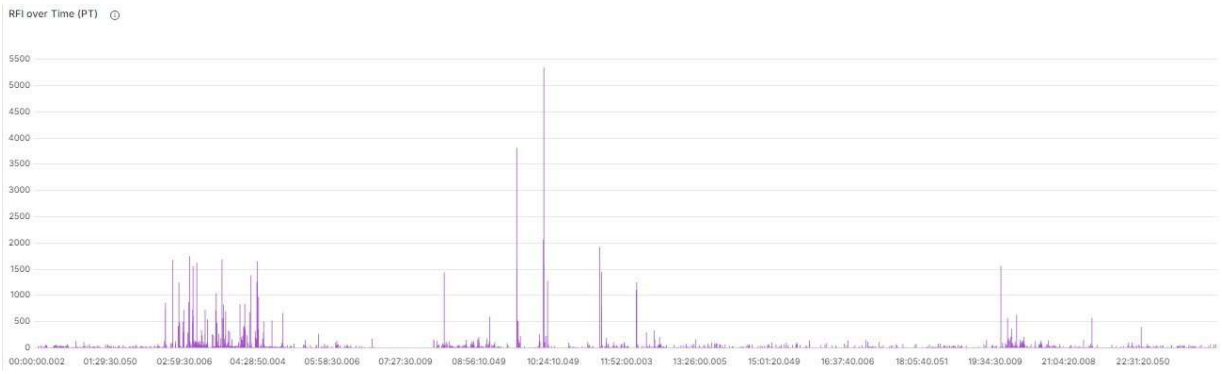

Figure 2. Real-Time Kurtosis Gathered from RF Sensors Deployed at an RA Site at 915 MHz over a 26 MHz Bandwidth During an RFI Event

References

[1] R. Dwyer. "Detection of non-Gaussian signals by frequency domain Kurtosis estimation". In: *ICASSP '83. IEEE International Conference on Acoustics, Speech, and Signal Processing*. Vol. 8. 1983, pp. 607–610. DOI: 10.1109/ICASSP.1983.1172264.

[2] Emmanuel Morales Butler et al. "Detecting RFI in Radio Astronomy Data from the 12-m Arecibo Telescope Using the Generalized Spectral Kurtosis Estimator". In: *American Astronomical Society Meeting Abstracts*. Vol. 244. American Astronomical Society Meeting Abstracts. June 2024, 210.02, p. 210.02.

[3] Evan Smith, Ryan S Lynch, and DJ Pisano. "Simulating spectral kurtosis mitigation against realistic radio frequency interference signals". In: *The Astronomical Journal* 164.4 (2022), p. 123.

[4] Valeriu Vrabie, Pierre Granjon, and Christine Serviere. "Spectral kurtosis: from definition to application". In: (Jan. 2003).

EXPERIMENTAL RESULTS OF A K-BAND RFI DETECTION PAYLOAD FOR POCKETQUBES

G. Gracia-Sola (1), S. Podaru(1), R. Almirall-Jou (1) and A. Camps(1)(2)(3)
(1) CommsSens Lab, UPC, Dept. of Signal Theory and Communications, BarcelonaTech, 08034 Barcelona
(2) Institut d'Estudis Espacials de Catalunya IEEC/CTE-UPC, 08034 Barcelona.
(3) SPIRE Visiting International Professor, United Arab Emirates University, CoE, PO Box 15551, Al Ain, UAE

1 Introduction

During the past years, there has been an increase in the number of wireless devices. The recent authorization of adjacent bands for the new 26 GHz 5G communications band, specifically spanning from 24.25 GHz to 25.25 GHz, has raised concerns regarding possible radio-frequency interference (RFI) from these emissions. These interference pose a risk to the water vapor measurements in the 23.8 GHz band, potentially compromising the effectiveness of passive Earth Observation readings, and having a negatively impact on numerical weather forecasts [1].

In 2022, the Frequency Allocations in Remote Sensing (FARS) Technical Committee from the IEEE Geoscience and Remote Sensing Society (GRSS) tasked the development of a RFI monitoring payload to detect the possible RFI in the 23.8 to 24.8 GHz band [2]. This payload, presented in Fig. 1 has been designed to fit in the PocketQube pico-satellite being developed as part of the "IEEE GRSS Open PocketQube Kit" educational project, a 1P PocketQube of 50x50x50 mm^3, average low power consumption of less than 250 mW, allowing low altitude constellation deployments for low cost, and low revisit times [3]. This manuscript presents initial experimental results from a series of drone test flights conducted to evaluate the K-band RFI detection payload for a PoquetQube. The study includes a comparison between the expected and actual performance of the payload.

2 RFI Detection Payload

The K-band RFI detection payload consists of a RF super-heterodyne receiver front-end (Fig. 1b) that down-converts and amplifies the measured band between 23.8 and 24.8 GHz, to a fixed intermediate frequency of 869 MHz and provides a voltage output proportional to the RF input power in dBm using a Received Signal Strength Indicator (RSSI) (Fig. 2) [4]. The output from the RSSI is measured by the PoquetQube's On-Board Computer ADC, and processed on-board to flag bins with possible interference. A 2x2 linear patch antenna obtains the RFI for the payload.

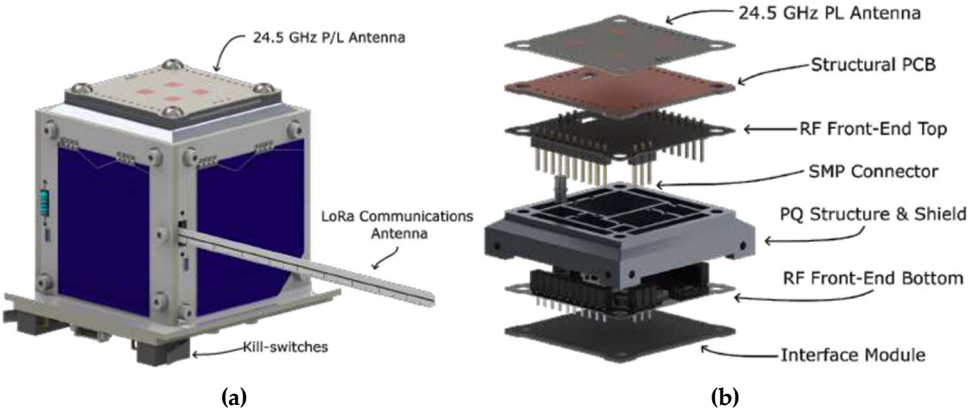

Figure 1. a) PoCat-3 with the b) K-band RFI detection payload installed on top showing the 2x2 patch antenna array at K-band.

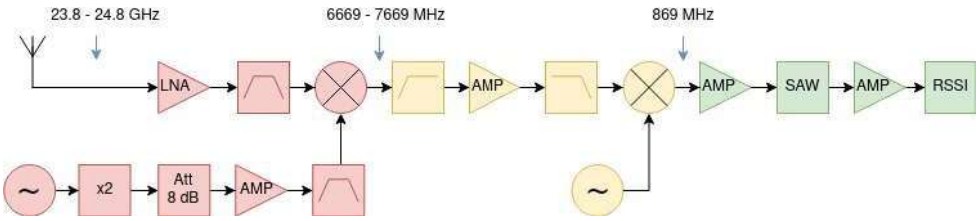

Figure 2. Functional block diagram of the RFI-5G payload. Each frequency stage is color coded in red, yellow and green.

The payload scans the complete 1 GHz band in 10 MHz frequency bins, and obtains 1000 samples in each frequency bin. Due to the PocketQube limitations in size, power and processing capabilities, the RFI monitoring payload implements components off-the-shelf (COTS) and runs a simplified set of detection algorithms. The statistics of each bin (i.e. mean, standard deviation, skewness and kurtosis) are computed for the detected signal power in dBm. Statistical, time and frequency detection algorithms are used to flag the frequency bins with presence of RFI [5] [6].

3 Drone Campaign

The drone campaigns consist of pre-planned flights at varying altitudes over an agricultural field in Vilafranca del Penedés (Catalonia, Spain), creating heatmaps with the detection and positioning of the RFI emitters. Several RFI emitters were strategically positioned in three different patterns and configurations: either forming a 3x5 matrix at similar distances of around 10 m, forming a diagonal with clusters of three RFI emitters per point, or grouping all the emitters to perform vertical ascends and descends. During each of the tests, the location and position of the RFI emitters is recorded, as well as the orientation of the payload antenna in relation to the RFI emitters. The RFI emitters are made of different off-the-shelve radar modules, used for close-proximity detection. These radars operate at frequencies around 24 GHz with frequency modulated continuous-wave (FMCW) and at different power levels and frequencies. This allows to detect RFI at different frequencies.

4 Results

The drone flight campaigns were performed successfully. When placing the RFI emitters in a 3x5 mesh configuration and flying at a height of around 10 m (3) the footprint of the antenna is around 5 m. From the detection heatmap (Fig. 3a) it can be seen how there is an increased number of RFI detection from the payload around the location of the RFI emitters, and outside the range of the emitters the amount of detection decreases. The statistical measurements retrieved by the payload (Fig. 3b), i.e., the mean, standard deviation, skewness and kurtosis, also show peaks which correspond to the moment at which the payload was being flown over the emitters.

On the other hand, when the RFI emitters were placed in a diagonal pattern and the drone was flown at 20 m height (Fig. 4), the antenna footprint is around 12 m. In this case, the flight path of the drone causes the payload to obtain more than one measurement over the same emitter, and, moreover, there are positions within the drone track in which the payload is measuring more than one emitter at the same time. For this reason, the detection heatmap (Fig. 4a) shows a large increase of RFI detection in the area. Despite that, it can be seen how the detections happen around the diagonal of the RFI emitters, and outside the diagonal the amount of detections decreases. The statistical measurements (Fig. 4b) also show how the amount of peak values have decreased when compared to the 3x5 configuration, ensuring that the payload is only seeing the RFI emitters in the diagonal. The increased peak value is due to the higher presence of RFI for a same measurement point.

5 Conclusions

Sample data acquired from the test campaigns indicate that the payload possesses the ability to identify RFI within the frequency range of 23.8 to 24.48 GHz. The RFI-5G payload was able to detect the RFI emitters placed within the field using the detection algorithms and processing the measured data. The mean is useful to detect strong and continuous RFI, whereas the standard deviation and kurtosis show how they can detect variable RFI with smaller average power than when using only the mean, that is, at higher altitudes. Despite the individual RFI emitters having low transmitted power, the combined emissions generate an overall power density sufficient for the payload to detect them at different heights. This article aims to demonstrate the RFI-5G payload capabilities and

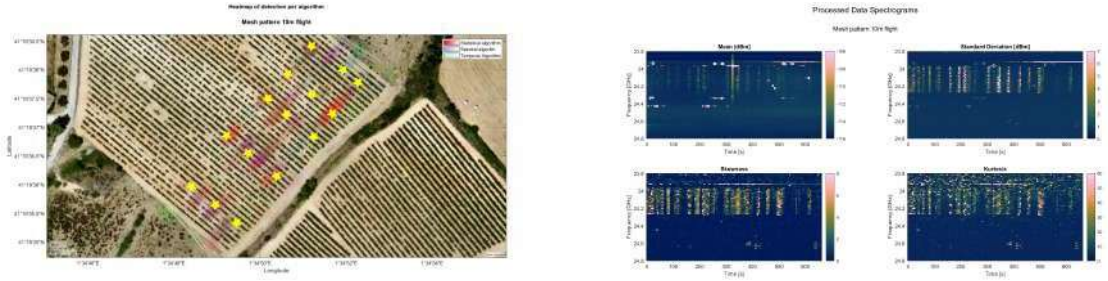

(a) (b)

Figure 3. a) Detection heatmap for the 10 m flight over the RFI emitters in a 3x5 mesh configuration, yellow stars represent the location of the emitters, and b) Statistical measurements, i.e., mean, standard deviation, skewness and kurtosis.

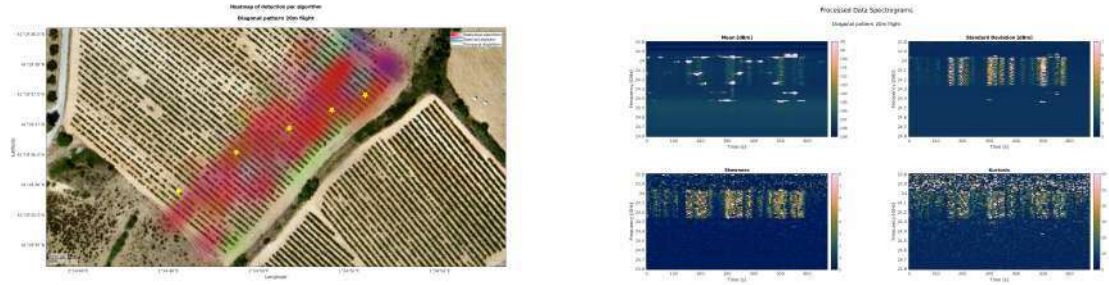

(a) (b)

Figure 4. a) Detection heatmap for the 20 m flight over the RFI emitters in a 3x5 mesh configuration, yellow stars represent the location of the emitters, and b) Statistical measurements, i.e., mean, standard deviation, skewness and kurtosis.

highlight the potential challenges that combined radio-frequency emissions near the 23.8 GHz water vapor band could present. A continuation of this work will be to obtain real field measurements around 5G tower stations to measure the presence of real RFI. PoCat-3 has been selected as part of the ESA "Fly Your Satellite! 4" program.

6 Acknowledgments

This work was sponsored by the Frequency Allocations in Remote Sensing (FARS) Technical Committee of the IEEE Geoscience and Remote Sensing Society (GRSS). This project was also sposored in part by the project "GENESIS: GNSS Environmental and Societal Missions – Subproject UPC", Grant PID2021-126436OB-C21 funded by the Ministerio de Ciencia e Investigación (MCIN)/Agencia Estatal de Investigación (AEI)/10.13039/501100011033 and EU FEDER “Una manera de hacer Europa”.

References

[1] L. Shultz, K. Seitter and J. Bunting, “REPLY COMMENTS OF THE AMERICAN GEOPHYSICAL UNION, AMERICAN METEOROLOGICAL SOCIETY AND NATIONAL WEATHER ASSOCIATION” *American Metheorological Society*, July 2021, online: https://www.ametsoc.org/index.cfm/ams/about-ams/ams-position-letters/ams-agu-and-nwa-comments-to-fcc-on-protecting-the-24-ghz-spectrum-band/.

[2] G. Gracia-Sola, S. Podaru, A. Alcantara, A. Garcilla-Morilla, L. Contreras-Benito, A. Perea, and A. Camps, "Design, Implementation and Testing of a 24 GHz 5G Band RFI Detection Payload for a Pocketqube", *IGARSS 2023 - 2023 IEEE International Geoscience and Remote Sensing Symposium*, 2023, pp. 693–696, doi: 10.1109/IGARSS52108.2023.10281480.

[3] S. Podaru, G. Gracia-Sola and A. Camps, "The IEEE Geoscience and Remote Sensing Society “Open PocketQube Kit”: An affordable open source approach to Earth observation missions [Education in Remote Sensing]", *IEEE Geoscience and Remote Sensing Magazine*, 2023, pp 163–170, doi: 10.1109/mgrs.2023.3321479.

[4] Linear Technology, "LT5537 Wide Dynamic RangeRF/IF Log Detector", *Analog Devices*, September 2023, online: https://www.analog.com/media/en/technical-documentation/data-sheets/5537fa.pdf.

[5] J. Querol, A. Perez and A. Camps, "A Review of RFI Mitigation Techniques in Microwave Radiometry", *Remote Sensing*, 2019, doi: 10.3390/rs11243042.

[6] J.M. Tarongi and A. Camps, "Normality Analysis for RFI Detection in Microwave Radiometry", *Remote Sensing*, 2010, pp 191–210, doi: 10.3390/rs2010191.

RFI Detection Considerations for Future Operational Radiometers

Edward Kim*(1)
(1) NASA Goddard Space Flight Center, Greenbelt, USA, ed.kim@nasa.gov

1. Introduction

The familiar weather forecasts that society depends on rely on operational microwave radiometers (particularly microwave sounders) to provide unique all-weather, global input observations at daily or near-daily intervals [1]. A long list of additional weather and climate products also rely on these operational radiometer observations. Improvements in both sensor capability as well as forecast model capability have resulted in steadily-improving forecasts. Today's forecasts can predict weather 7 days in advance with the same skill that a decade or two ago used to only achieve a 3-day forecast. This beneficial situation has built up since the first operational microwave radiometers in the 1980s. A recent study [2] indicates that forecast improvements will not saturate with the addition of more microwave sounder observations. And, New Space companies—with the advent of cubesats—are proposing several new cubesat and smallsat sounders.

However, several significant changes related to radio frequency interference (RFI) are occurring that are worth considering. This paper will attempt to consider them from the viewpoint of future operational radiometers—focusing on microwave sounders.

2. Changes in Progress

Operational sounder programs have long lifetimes—decades vs. the much-shorter lifetimes of research satellite missions or cubesats. For example, the Advanced Technology Microwave Sounder (ATMS)—part of the current international operational backbone constellation under the Joint Polar Satellite System (JPSS) [3]—ATMS was designed in the 1990s when RFI at sounder freqs (20-200 GHz) was not a threat in anyone's mind. Mobile phones primarily used frequencies <1 GHz then [4], and were just transitioning from brick-sized units to something that actually fit in your hand. Just as importantly, on-board computational technology was not very capable or mature. As a result, the requirements for ATMS (constructed in the first part of the 1990s) did not consider RFI. Eumetsat's next-generation sounder, the MicroWave Sounder (MWS), designed "only" a decade ago, when the RFI threat was much less than it is today, also includes no explicit capabilities for RFI detection. And, when it begins launching, MWS will be a primary part of the operational sounder backbone for decades.

Now, wireless communications is everywhere—even in orbit, and uses spectrum up to W-band (Table 1), with monthly announcements of future system designs using higher and higher bands and bandwidths. Interestingly, at the same time, forecast models are becoming more sensitive to bias in their microwave inputs (~0.1K and decreasing)---the primary users of sounder observations are becoming more sensitive to RFI!

Table 1. Spectrum already allocated or being considered for use near sounding bands.

- 23.8 GHz: 24.25 GHz to 27.5 GHz, 5G communications [5]
- ~50 GHz: 47.2 – 50.2 GHz and 50.4 – 51.4 GHz, SpaceX Starlink [6]
- 88.2 GHz: 81.0-86.0 GHz, SpaceX Starlink [7]

These are examples of programmatic opportunities not happening often enough to adapt to changes. Redesigning and re-building ATMS or MWS is not realistic. ATMS units will continue to be part of the operational constellation until 2040. NOAA's new Near Earth Orbit Network (NEON) program, the successor to JPSS, will be operational from the early 2030s to 2050. One lesson to be learned is that you *will* be stuck with your sensor capabilities for decades. Can you imagine attending the RFI conference in 2050 and wondering why your predecessors didn't do more to address RFI when they had the chance in the 2020s?

One cure, being considered for NEON's next-gen sounder, the Sounder for Microwave Brightness Applications (SMBA), is to explicitly require RFI detection capability [8]. On-board computation technology has advanced to the point where detection

(and possibly mitigation) algorithms can be run on-board a satellite. NASA's Soil Moisture Active Passive (SMAP) mission did so with two 24 MHz wide channels [9], and processing power has grown enough to now be able to handle sounder bandwidths.

Flexibility will be a powerful ally since the nature of RFI will change. When you also add the capability to re-program on-orbit, you have a powerful and flexible tool to address RFI. Without these capabilities, it will be difficult to mee the observational needs of operational weather forecasts.

Radiometer performance metrics that are purely science-based have an unstated assumption that no RFI is present. This is not realistic. The fundamental purpose of a sensor requirement is to ensure that a capability is available in the sensor. If you ignore a key threat, your requirement cannot do what it is supposed to do. RFI detection (and mitigation) should be considered in your sensor requirements from the beginning. This is already true for new sensors being considered today, and will remain true for future sensor specification efforts as well.

Even ranking the utility of a band needs to consider this unstated assumption. For example, the 118 GHz temperature sounding band is often considered less useful than the 50 GHz temperature sounding band. However, the 50 GHz region is under increasing threat from RFI [6], so an assessment of the utility of the 118 GHz band in the timeframe of future satellite programs must consider RFI in order to be valid.

These are some of the RFI-related considerations faced today by operational programs contemplating new radiometers. The changes and the associated reactions are significant, with immediate impacts to sensor specifications, but also to how satellite data that may be contaminated with RFI is used. The presentation will go into further detail concerning options and consequences, as well as discussing additional examples.

[1] S. Kalluri, Editor. NOAA technical report NESDIS 155. *Satellite Microwave Sounding Measurements in Weather Prediction: A Report of The Virtual NOAA Workshop on Microwave Sounders*. DOI 10.25923/WKGD-PW75

[2] Duncan, D.I., Bormann, N. & Hólm, E.V., 2021: On the addition of microwave sounders and numerical weather prediction skill. Q J R Meteorol Soc, 1– 16. Available from: https://doi.org/10.1002/qj.4149

[3] Goldberg, Mitchell. "The joint polar satellite system overview." In *IGARSS 2018-2018 IEEE International Geoscience and Remote Sensing Symposium*, pp. 1581-1584. IEEE, 2018.

[4] https://en.wikipedia.org/wiki/Motorola_MicroTAC

[5] J. Houts and E. Kim, *The Spectrum Outlook for Earth Remote Sensing Post WRC-19,* IEEE IGARSS 2020. Accessed from: https://ntrs.nasa.gov/api/citations/20205003647/downloads/IGARSS2020_RFI_v6.pdf

[6] Federal Communication Commission Report No. SAT-01768 " Satellite Licensing Division and Satellite Programs and Policy Division Information Actions Taken", DA-23-997, October 2023: https://docs.fcc.gov/public/attachments/DA-23-997A1.pdf

[7] Federal Communication Commission, "Order and Authorization", DA-24-222, March 2024: https://docs.fcc.gov/public/attachments/DA-24-222A1.pdf

[8] Request for Information – Near Earth Orbit Network Program's Sounder for Microwave-Based Applications Instrument. https://sam.gov/opp/3d4324812287484599b83672eb06ee98/view

[9] P. N. Mohammed, M. Aksoy, J. R. Piepmeier, J. T. Johnson and A. Bringer, "SMAP L-Band Microwave Radiometer: RFI Mitigation Prelaunch Analysis and First Year On-Orbit Observations," in *IEEE Transactions on Geoscience and Remote Sensing*, vol. 54, no. 10, pp. 6035-6047, Oct. 2016, doi: 10.1109/TGRS.2016.2580459.

RFI 2024

Broadband Radio Emission Detected from Starlink Satellites Below 100 MHz

Xiang Zhang*(1), Philippe Zarka(2), Cedric Viou(3), and Alan Loh(4)
(1) Observatoire de Paris, Meudon, France, xiang.zhang@obspm.fr
(2) Observatoire de Paris, Meudon, France, philippe.zarka@obspm.fr
(3) Observatoire Radioastronomique de Nançay, Nançay, France, Cedric.Viou@obs-nancay.fr
(4) Observatoire de Paris, Meudon, France, alan.loh@obspm.fr

PoS(RFI2024)070

While satellite mega-constellations have significantly improved communication technologies, they have also raised concerns within the astronomical community regarding potential observational contamination. Satellites are recognized sources of radio frequency interference (RFI). Last year, unintended radio emissions from the Starlink constellation have been detected by LOFAR [1] and MWA [2]. These emissions include broadband radiation in the range of 110 to 188 MHz [1], as well as narrowband emissions with bandwidths less than 12 kHz [1,2].

To further assess the potential impact of Starlink on low-frequency radio astronomy, particularly in the search for exoplanets, we conducted a 40-hour observational campaign using NenuFAR in the 30-78 MHz range. We generated dynamic spectra from approximately 400 beams covering the field of view, before searching for radio bursts in these dynamic spectra. Upon detecting a burst, we created images limited to the time and frequency range of the burst and compared the burst locations with the predicted satellite paths derived from Two-Line Elements (TLEs).

During our observational campaign, multiple Starlink satellites were detected emitting broadband signals. An example is given in Figure 1, where two Starlink satellites passed through the beam, resulting in two bursts between 45-68 MHz within 10 minutes.

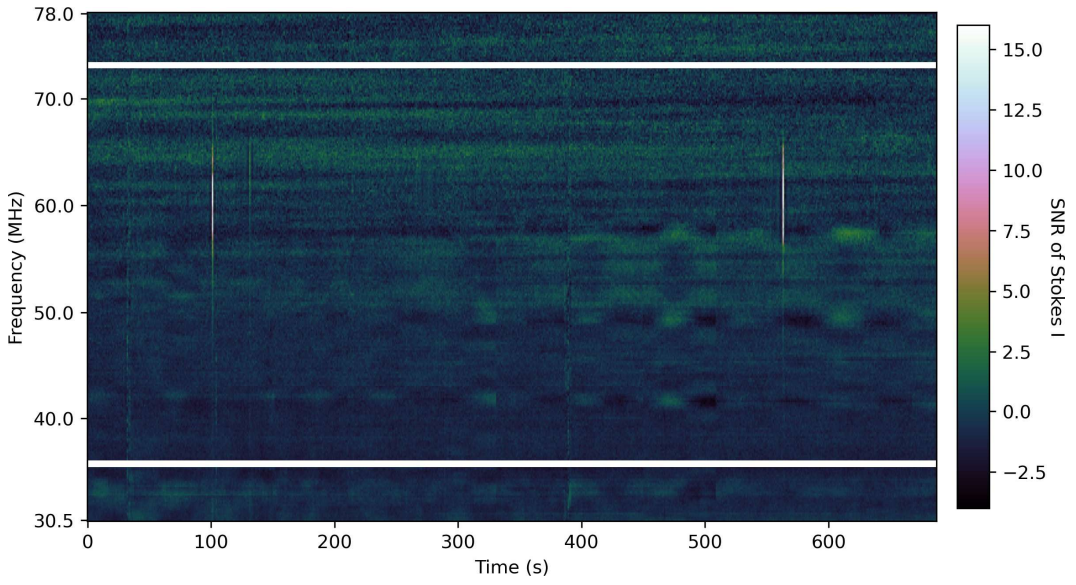

Figure 1. Stokes I dynamic spectrum from a NenuFAR beam, showing two bursts caused by two passing Starlink satellites. The beam direction is fixed at a specific [RA, DEC] in the sky.

The origin of this broadband emission remains under investigation. Hypotheses include the reflection of solar bursts, reflection of ground-based RFI, and intrinsic emissions from the satellites potentially due to mechanical issues. We've scheduled follow-up observations to further explore these possibilities.

References

[1] Di Vruno, F., B. Winkel, C. G. Bassa, G. I. G. Józsa, M. A. Brentjens, A. Jessner, and S. Garrington. "Unintended electromagnetic radiation from Starlink satellites detected with LOFAR between 110 and 188 MHz." Astronomy Astrophysics 676 (2023): A75.

[2] Grigg, D., Tingay, S. J., Sokolowski, M., Wayth, R. B., Indermuehle, B., Prabu, S. (2023). Detection of intended and unintended emissions from Starlink satellites in the SKA-Low frequency range, at the SKA-Low site, with an SKA-Low station analogue. Astronomy & Astrophysics, 678, L6.

Dark and Quiet Skies, the regulatory landscape

Federico Di Vruno[1,2]

[1] SKA Observatory, Macclesfield, United Kingdom, Federico.divruno@skao.int
[2] IAU Centre for the Protection of the Dark and Quiet Skies from Satellite Constellation Interference, Paris, France

The use of space has seen a steep increase in the last 5 years. The population of satellites in Low Earth Orbit (LEO) with the purpose of providing low latency internet connectivity, Earth observation services, and other applications has more than tripled since 2019. While this can bring better opportunities for unconnected communities, and provide more data for many vital applications such as disaster management, it can also bring many challenges. Reflection of sunlight on the satellite's surfaces can severely affect optical astronomy and it can sometimes be seen by the unaided eye, appearing as moving stars in the night sky. In the radio domain, the strong downlinks and the possibility of producing unintentional electromagnetic radiation (UEMR) from the onboard electronics can interfere with radio astronomy observations.
Advocates for the protection of the night sky and optical and radio astronomy have named this issue as the protection of the Dark and Quiet Skies.

The International Astronomical Union, together with other astronomical observatories has started two streams of action:

- The regulatory stream: where permanent observers of the UN Committee on the Peaceful Uses of Outer Space (COPUOS) have advocated for the establishment of guidelines for the protection of D&QS. And spectrum managers for radio astronomy have been working at the ITU-R to protect radio astronomy, especially against large satellite constellations in Radio Quiet Zones (RQZ).

- On a more practical approach, the International Astronomical Union has established, in collaboration with the SKA Observatory and the US National Optical-Infrared Laboratory (NOIRLab), the Centre for the Protection of the Dark and Quiet Skies from Satellite Constellation Interference (IAU CPS): the aim of the CPS is to bring together all stakeholders (in particular satellite industry) to find implementable mitigation measures that can minimize the impact on astronomy. The CPS has divided its work in four Hubs, namely: "Policy", "Industry and Technology", "Community Engagement" and "SatHub".

The regulatory stream has recently obtained two important achievements, the establishment of an agenda item about Dark and Quiet Skies at the Scientific and Technical Subcommittee of UN COPUOS and also an agenda item for the ITU-R World Radiocommunication Conference 2027 to study the effects of satellite constellations on radio astronomy and in particular in RQZ. This work will discuss the history and current status of the two agenda items, what does each one means and which can be the possible future steps in seeking regulation to protect the Dark and Quiet Skies.

Dark and Quiet Skies

Carolina Eugenia Catani [(1)], Josefina Peres [(1)]
[(1)] CONAE, Buenos Aires, Argentina, ccatani@conae.gov.ar
[(2)] CONAE, Buenos Aires, Argentina, jperes@conae.gov.ar

The astronomical activity in the Argentine Republic celebrates a history of more than 150 years, both amateur and professional. As a systemic research activity, it is considered that it began in 1871 when Domingo Faustino Sarmiento founded the Astronomical Observatory of Córdoba. The work "Córdoba Durchmungsterung", contains the catalog of positions and stellar brightness, a world reference of the southern skies, until today (Sisteró, 1994:167). From then on, Argentine astronomy advances in the construction of scientific knowledge, having an outstanding place at world level, holding privileged places in its territory for the activity.

On the other hand, space activity has been reborn with the incursion of private sector, allowing new (and more) actors to participate in this economic-social and industrial space world, democratizing access and influencing the decisions of the States in their public policies and regulations. Little by little, the States are no longer the only holders of knowledge and control of the sector, as was the case at the beginning of the space era, to make way for new investors and actors from the non-governmental sector (Catani, et al., 2022). This circumstance is beginning to be seen incipiently in Argentina as well.

Society benefits from greater technological progress and its applications, but in almost equal measure it has been seen that security, peace and sustainability of outer space activities are put at risk as a result of the increased congestion of space traffic and objects launched into space, which has also led to increased pollution by space debris, and an impact on radio frequencies, among others.

Although the scientific community, academia and nations have laid the foundations at the international level to provide solutions for the sustainability of space activities, a new problem has recently begun to be discussed in different communities and international forums (including COPUOS): the dark and quiet skies. Astronomers were the first to raise their hands, warning that this was a new problem that required attention. However, their approach goes beyond the question of astronomical observation *stricto sensu*.

The current counterpoint between the interests and needs of modernity in the development of cities or those of the satellite sector that propose to provide access and connectivity to vast regions of the Earth through mega constellations (to cite an example) with those of astronomy (Earth-Space / Space-Space) for the research and study of the universe for the benefit and interest of all Humanity1, also put in tension both economic and industrial interests, as well as ethical and political values and principles.

In the present intervention, we propose to introduce the current state of attention in the international agenda, taking in particular the case of COPUOS and what is expected in terms of regulations and recommendations resulting from the work of this commission. However, we will ask ourselves if it is really considered an international agenda item as it seems to be, or if there are still tensions regarding the homogeneous acceptance of its treatment.

[1] Principle I of the Declaration of Legal Principles Governing the Activities of States in the Exploration and Use of Outer Space, Approved by the General Assembly of the United Nations in its resolution 1962 (XVIII), of December 13, 1963 and later included in Article I of the Treaty on Principles Governing the Activities of States in the Exploration and Use of Outer Space, Including the Moon and Other Celestial Bodies (TEU) of 1967

International Implications of the U.S. National Spectrum Strategy: Perspectives from the Meteorological Community

Renée A. Leduc[(1)*], Beau Backus[(2)], Jordan Gerth[(3)] and V Chandrasekar[(4)]
[(1)] Narayan Strategy, Arlington, Virginia, U.S.A. renee@narayanstrategy.com
[(2)] Applied Physics Laboratory, Johns Hopkins University, Columbia, Maryland, U.S.A. Beau.Backus@jhuapl.edu
[(3)] Space Science and Engineering Center, University of Wisconsin-Madison, Madison, Wisconsin, U.S.A. Jordang@ssec.wisc.edu
[(4)] Department of Electrical and Computer Engineering, Colorado State University, Fort Collins, Colorado, U.S.A. Chandrasekaran.Venkatachalam@colostate.edu

The U.S. National Telecommunications and Information Administration (NTIA), the agency managing U.S. federal government use of spectrum, recently developed a National Spectrum Strategy (NSS) for the U.S. and a related Implementation Plan. In early 2023, the NTIA sought government and non-government inputs to the strategy with opportunities to provide written comments and oral presentations in response to their three established "pillars" of the strategy. One of those pillars was focused on developing a spectrum pipeline "to ensure U.S. leadership in spectrum-based technologies" to drive economic growth [1]. The American Meteorological Society, led by its Committee on Radio Frequency Allocations, provided both oral remarks in a public comment session and comprehensive written comments in this process.

AMS' input to the NSS provided a comprehensive overview of the specific areas of spectrum relied upon by meteorologists in support of developing and communicating weather forecasts to protect life and property, with a particular focus on the importance of passive spectrum. In addition, the major themes of the comments highlighted the societal importance of spectrum allocated to the U.S. federal government (especially for technology operated by the National Oceanic and Atmospheric Administration (NOAA) and the National Aeronautics and Space Administration (NASA)), noting how this federal allocation of spectrum is used extensively across the federal, public, private, non-profit, and academic sectors to support the life and safety needs of people across the nation and world. Spectrum use benefits multiple weather-sensitive segments of the economy, such as (but not limited to) aviation, land and sea transportation, energy exploration and production, agriculture, fishing, outdoor recreation, and professional sports [2].

In November 2023, prior to the World Radiocommunications Conference–2023 (WRC-23), the Executive Office of the President released a Presidential Memorandum on modernizing U.S. spectrum strategy and the NSS, including 2,700 megahertz of spectrum for potential repurposing [3]. NTIA collaborated with the Federal Communications Commission (FCC) and other U.S. federal agencies to prepare an NSS implementation plan, which was released in March 2024 and provides the roadmap for the completion of the spectrum pipeline studies [4].

The bands to be studied over two years include 3.1-3.45 GHz, 5.03-5.091 GHz, 7.125-8.4 GHz, 18.1-18.6 GHz, and 37.0-37.6 GHz bands, overlapping or adjacent to many existing meteorological applications:

- The 3.1-3.45 GHz band is above an allocation for active S-band NOAA weather/precipitation radars that are deployed throughout the U.S.
- The 7.125-8.4 GHz band includes earth-to-space and space-to-earth weather satellite data relays, and the 7.3 GHz passive band useful for soil moisture and sea surface temperature.
    - The ITU AI 1.19 intends to study the addition of a EESS (p) allocation at 8400-8500 MHz, which should be another factor in the 7.125-8.4 GHz band studies, would be a good opportunity to further develop the right language for adjacent band protections for EESS (p).
- The 18.1-18.6 GHz and 37.0-37.6 GHz bands are adjacent to useful EESS allocations due to their partial transparency to clouds, allowing for the passive sensing of oxygen and water vapor absorption through the atmospheric column. The EESS allocations are at 18.6-18.8 GHz and 36-37 GHz, respectively.

This paper, to be presented at RFI 2024 in Bariloche, Argentina, will highlight the meteorological relevance of the spectrum pipeline bands highlighted in the NSS and currently being studied. The paper will include policy and regulatory analysis on the U.S. domestic factors that will likely impact the studies, but also the international implications of these U.S. domestic decisions. These pipeline bands cover an array of critical meteorological observations from data relay from geostationary and polar satellites, to passive and active observations. The fundamental purpose of this paper will be to grow awareness and foster

dialogue within and between science communities to ensure we proactively understand the potential implications to Earth and space sciences of these U.S. decisions.

[1] U.S. Department of Commerce. Request for Comment: Development of a National Spectrum Strategy. U.S. Federal Register. 16 Mar 2023. 16244-16247.

[2] American Meteorological Society. Written Comments on the National Spectrum Strategy. 17 April 2023. https://www.ntia.gov/sites/default/files/publications/american_meteorological_society.pdf

[3] U.S. Secretary of Commerce. National Spectrum Strategy. 13 Nov 2023. https://www.ntia.gov/report/2023/national-spectrum-strategy-pdf.

[4] NTIA. National Spectrum Strategy Implementation Plan. 12 March 2024. https://www.ntia.gov/sites/default/files/publications/national-spectrum-strategy-implementation-plan.pdf

Evaluation of RFI Affecting Weather Radars in C-Band

Roberto Costantini* [(1)], and Federico Renolfi[(2)]
[(1)] INVAP S. E., San Carlos de Bariloche, Argentina, rcostant@invap.com.ar
[(2)] INVAP S. E., San Carlos de Bariloche, Argentina, frenolfi@invap.com.ar

One of the biggest problems suffered by C-band weather radars is the interference generated by WiFi equipment, with which they share the frequency band.

To evaluate the impact of RFI on weather radar products, we consider two statistical metrics:

a) A metric related to interference density. It measures the proportion of "clean" (non-interfered) pulses that are expected to be per burst in each radial. This metric gives an indication of the quality of the products once the interference filter is applied, given that even when the filter acts with the greatest efficiency the quality of the estimates will suffer a degradation depending on the number of "clean" pulses.

b) A metric related to the intensity of interference: the "Interference equivalent reflectivity" for each azimuth/distance cell. Roughly speaking, a weather phenomenon whose reflectivity is above this level will be only slightly affected by the RFI, while reflectivity below it could suffer degradations based on the first metric.

These two metrics depend exclusively on the interference scenario (not the radar or the interference filter) and allow:

- evaluate the severity with which a radar site is affected by RFI;
- monitor the medium and long-term temporal evolution of the interference scenario: installation of new RFI sources and increase in the traffic intensity of existing ones;
- optimize the RFI filter for a given scenario.

A data survey has been carried out using the operational radars of the SINARAME network of Argentinian meteorological radars affected by interference.

The methodology consists of collecting data with the radar programmed to operate in a standard mode but with transmission disabled. The azimuthal 360° are scanned at the elevation most affected by RFI, and the data are then processed offline to produce the maps of "clean pulses vs. azimuth" and "Interference equivalent reflectivity vs. azimuth-distance".

RFI 2024

Impacto de la RFI en los radares meteorológicos Banda C y las técnicas para su detección, predicción y mitigación

Luis A. Celaya(1),
(1) INVAP S.E, Buenos Aires, Argentina, lcelayaprieto@invap.com.ar

1 Introducción

Los radares meteorológicos son componentes esenciales para la comprensión y predicción del tiempo, no obstante, su funcionamiento se ve cada vez más comprometido por la interferencia de radiofrecuencia (RFI) proveniente de diversas fuentes. Esta interferencia puede degradar significativamente la calidad de los productos del radar, afectando la precisión de los datos y la confiabilidad de los pronósticos meteorológicos [1] [2] [3] [4] [5]. En este artículo, se presenta una revisión del impacto de la RFI en los radares meteorológicos de *Banda C*, explorando sus efectos perjudiciales y las técnicas actuales para su detección y predicción. Se discuten los desafíos asociados con la mitigación de la RFI y la necesidad de desarrollar soluciones innovadoras para garantizar el funcionamiento continuo y confiable de estos sistemas críticos. **Palabras clave:** Radar Meteorológico, *Banda C*, interferencia de radiofrecuencia, RFI, detección de RFI, predicción de RFI, mitigación de RFI, ecos fantasmas, pérdida de sensibilidad, degradación de la calidad de productos del radar, monitoreo del espectro, análisis de patrones, modelos de predicción.

2 Efectos de la RFI en los radares meteorológicos de Banda C:

Aparición de ecos fantasmas: Se generan ecos falsos en las imágenes del radar, dificultando la distinción entre precipitación real y señales de interferencia [1] [2] [3] [4] [5].
Pérdida de sensibilidad: Reduce la sensibilidad del radar, limitando la detección eventos meteorológicos [1].
Degradación de la calidad de los productos: Introduce ruido y distorsión en las imágenes del radar, dificultando su interpretación y análisis [1] [2] [6].

3 Algunos enfoques para la detección y predicción de RFI:

Monitoreo del espectro: Permite identificar las fuentes de interferencia y su ubicación. Los entes reguladores nacionales cuentan con sistemas y mecanismos para el monitoreo constante, por ejemplo, el *Sistema Nacional de Comprobación Técnica de Emisiones* (SNCTE) en Argentina, conformado por 6 centros de comprobación técnica, 20 estaciones remotas, y 24 unidades móviles [7].
Análisis de patrones: El análisis de los patrones de los ecos de radar puede revelar la presencia de RFI, ya que los ecos de interferencia suelen presentar características distintivas. Con base en esta información se pueden aplicar técnicas de filtrado y procesamiento digital de señales [1]. En [4], se presenta un algoritmo de detección de RFI que combina la medición de la desviación estándar normalizada de la potencia recibida (STD) y el índice de calidad de la señal (SQI) para identificar la presencia de interferencia RFI en señales de radar. Este algoritmo se implementa utilizando una configuración de hardware sencilla, denominada "RHunt" (abreviatura de RLAN Hunter), que consiste en un receptor WiFi comercial conectado a una Raspberry Pi. Este dispositivo se conecta permanentemente a la cadena de recepción del radar, permitiendo un monitoreo continuo de la presencia de RFI. Un valor elevado de STD indica un cambio abrupto en la potencia recibida, lo cual, en base a análisis de patrones, puede asociarse con la presencia de fuentes de interferencia externas. Sin embargo, el algoritmo no se limita a la medición de STD, sino que también considera el valor del SQI. La combinación de un STD alto y un SQI bajo se identifica como un indicador confiable de interferencia WiFi externa. Otros enfoques se basan en estudiar el efecto de la RFI sobre la velocidad Doppler [8]; sincronización y detección de tramas OFDM IEEE 802.11/802.11a para obtener la información de la subcapa MAC [9] [10]; identificación de señales bajo el estandar IEE 802.11a localizando el preámbulo de cada trama [11].
Modelos de predicción: Los modelos de predicción de RFI utilizan datos históricos y análisis de tendencias para estimar la probabilidad y la intensidad de la interferencia en el futuro, permitiendo una mejor preparación y gestión

de la información. En 2021, el *Servicio Meteorológico Nacional Argentino* (SMN) desarrolló un modelo de predicción de RFI, analizando dos años de datos de la red SINARAME (Sistema Nacional de Radares Meteorológicos Argentinos) [12]. Este análisis permitió caracterizar estadísticamente los sitios de radar, identificando patrones y tendencias de interferencia. Otros modelos, se centran en la cuantificación del efecto que tiene la RFI en la estimación de los productos meteorológicos [13].

Cancelación adaptativa: Consiste en identificar y cancelar señales de RFI específicas utilizando modelos matemáticos. La UIT-R S.734 [14] estudia diferentes ejemplos de cancelación adaptativa, los cuales se basan en el principio de generar una señal de "anti-interferencia" que sea idéntica a la señal de RFI, pero con fase invertida. Al sumar esta señal anti-interferencia a la señal recibida, ambas se cancelan mutuamente, eliminando así la interferencia y permitiendo que la señal deseada se recupere. Esta recomendación [14] revisa la aplicación de estos métodos de cancelación a nivel de *banda base*, *frecuencia intermedia* (FI) y con filtros adaptativos; específicamente aplicados al *Servicio Fijo por Satélite*. Al momento de la revisión, si bien se demostró una alta efectividad, las limitaciones en el desarrollo tecnológico sugerían cierta complejidad y altos costos. En la actualidad, el rápido avance de los microprocesadores, DSP, FPGA y GPU; permite la implementación de algoritmos complejos capaces de dotar a los sistemas de capacidades de adaptación y seguimiento del entorno [15]. En el caso particular de los Radares Meteorológicos, [5] implementó cuatro algoritmos de filtrado de clutter tanto para datos simulados como para datos reales de las regiones de Córdoba y Bariloche; concluyendo que los filtros adaptativos presentaban mejores estimaciones con menor sesgo y varianza, además de tener la capacidad de recuperar las muestras del fenómeno eliminadas.

Filtrado digital: Su objetivo es eliminar señales de RFI de banda estrecha o de banda ancha mediante filtros digitales utilizando para ello técnicas de procesamiento de imágenes. El Servicio Meteorológico Nacional en Argentina (SMN), ha venido trabajando junto a investigadores de universidades y en estrecha colaboración con INVAP S.E en el desarrollo de algoritmos para el filtrado de pixeles afectados por ecos de origen no meteorológicos [6]. Básicamente, consiste en la aplicación secuencial de filtros que permiten corregir y/o eliminar los píxeles de radar asociados a la variable reflectividad, respetando una relación de compromiso (datos de interés vs calidad) en los valores umbral de cada parámetros de los filtros, de tal manera que permita mantener datos de reflectividad que son de interés meteorológico y se descarten aquellos pixeles que se encuentre muy comprometidos debido a la interferencia [16]. Los filtros implementados fueron: Filtro de Interferencia electromagnética, Tope de eco, Coeficiente de correlación copolar, Ecos aislados, bloqueo topográfico, atenuación y reflectividad faltante [6][16]; cuyos detalles de su implementación operativa se discuten en [17], además se fueron aplicando optimizaciones, mejoras y nuevos filtros [18].

4 Desafíos y soluciones futuras:

La mitigación de la RFI en los radares meteorológicos de banda C sigue siendo un desafío complejo debido a la naturaleza dinámica y diversidad de las fuentes de interferencia. Se requieren soluciones innovadoras que combinen técnicas de detección y predicción avanzadas con algoritmos de procesamiento de señal robustos para garantizar el funcionamiento confiable de estos sistemas críticos. Organizaciones, agencias y entes reguladores a nivel global se encuentran evaluando los aspectos técnicos, desafíos y posibles soluciones para la coexistencia de radares meteorológicos con otras tecnologías. El *Centro Común de Investigación de la Comisión Europea* (EC DG JRC) ha iniciado un estudio exhaustivo sobre este tema, presentando conclusiones preliminares que evalúan cualitativamente las opciones potenciales para mitigar el problema de coexistencia [19]. Para determinar la viabilidad de las soluciones propuestas, se han establecido métricas clave que abarcan aspectos técnicos, organizativos y económicos: complejidad técnica, complejidad de la organización, costos de implementación, costos de despliegue, riesgo de ineficacia, riesgo potencial de que la opción propuesta genere otros problemas no planificados. Por su parte, desde *La Unión Internacional de Comunicaciones*(ITU) se han revisado diferentes aspectos técnicos y operacionales, además de los principales problemas de RFI; planteándose la determinación de criterios de protección con el establecimiento de valores umbrales mínimos admisibles y de referencia [20]. La evaluación meticulosa de las opciones disponibles, considerando las métricas clave establecidas, permitirá identificar las soluciones más adecuadas para garantizar el funcionamiento confiable de estos sistemas y asegurar un futuro libre de interferencias. Se están explorando nuevas técnicas de detección y predicción de RFI, así como algoritmos de procesamiento de señal más robustos, para mejorar la eficacia de las soluciones de mitigación [8]. La colaboración entre organizaciones y entes de diferentes países es fundamental para compartir conocimientos, experiencias y recursos en la búsqueda de soluciones efectivas a la problemática de la RFI. Es necesario actualizar las regulaciones y normas para garantizar la protección del espectro electromagnético y la coexistencia armoniosa de los radares meteorológicos con otras tecnologías. En conjunto, estos esfuerzos garantizarán que los radares meteorológicos de *banda C* continúen desempeñando un papel fundamental en la protección de la población, proporcionando información precisa y oportuna para la predicción meteorológica y la toma de decisiones críticas.

References

[1] *RECOMENDACIÓN UIT-R M.1638*, UIT-R. [Online]. Available: https://www.itu.int/dms_pubrec/itu-r/rec/m/R-REC-M.1638-0-200306-S!!PDF-S.pdf

[2] J. Yin, "Advanced techniques in clutter mitigation and calibration for weather radars," Ph.D. dissertation, Delft University of Technology, 2019.

[3] "Desafíos y necesidades de espectro radioeléctrico en argentina." [Online]. Available: https://www.argentina.gob.ar/sites/default/files/informe_consulta_publica_de_espectro_02.pdf

[4] S. Maximilian, F. Michael, M. David, H. Cornelius, and R. Benjamin, "Rf-interference detection and mitigation in the dwd c-band weather radar network." [Online]. Available: https://egusphere.copernicus.org/preprints/2022/egusphere-2022-692/egusphere-2022-692-manuscript-version2.pdf

[5] T. Javier, "Filtrado de clutter terrestre en aplicaciones de radar meteorológico." [Online]. Available: https://ricabib.cab.cnea.gov.ar/742/1/Trujillo.pdf

[6] A. Aldana, M. Paula, R. Martin, S. Maximiliano, R. Juan, and V. Luciano, "Sistema de control de calidad de datos de radar en el servicio meteorológico nacional - parte i: Descripción del algoritmo," Servicio Meteorológico Nacional Argentina, Tech. Rep. SMN 2021-86, Marzo 2021. [Online]. Available: https://www.researchgate.net/publication/352192392

[7] Control del espectro, sistema de control técnico de emisiones. [Online]. Available: https://www.enacom.gob.ar/control-del-espectro_p328

[8] D. Benoit, "Mitigación de interferencia wifi en radar meteorológico a partir su efecto sobre la velocidad doppler," Master's thesis, Instituto Balseiro, Universidad Nacional de Cuyo, Centro Nacional de Energía Atómica, 2023. [Online]. Available: https://ricabib.cab.cnea.gov.ar/1186/

[9] M. Daniel, "Demodulación y síntesis de señales ofdm, ieee 802.11," Diciembre 2021. [Online]. Available: https://ricabib.cab.cnea.gov.ar/1108/1/1Milan%C3%A9s_Chau.pdf

[10] D. Maia, "Sincronismo en sistemas de modulación multiportadora que emplean ofdm," Master's thesis, Instituto Balseiro, Universidad Nacional de Cuyo, Centro Nacional de Energía Atómica, 2023. [Online]. Available: https://ricabib.cab.cnea.gov.ar/1222/1/1Desamo.pdf

[11] B. L. Omelio, "Caracterización y detección de interferencia wlan/rlan en radares meteorológicos," Diciembre 2019. [Online]. Available: https://ricabib.cab.cnea.gov.ar/874/1/1Barba_Leal.pdf

[12] G. Diego, V. Luciano, R. Martin, d. E. Ramon, and G. Leando, "Climatología de ecos no meteorológicos de la red sinarame," Servicio Meteorológico Nacional Argentina, Tech. Rep. SMN 2021-103, Marzo 2021. [Online]. Available: https://www.researchgate.net/publication/355973572

[13] C. Laura, "Estudios del efecto de la interferencia wifi sobre los productos de radar meteorológico," Diciembre 2021. [Online]. Available: https://ricabib.cab.cnea.gov.ar/1109/

[14] *Utilización de canceladores de interferenciaen el servicio fijo por satélite*, UIT-R. [Online]. Available: https://www.itu.int/dms_pubrec/itu-r/rec/s/R-REC-S.734-0-199203-I!!MSW-S.doc

[15] M. José and S. Joan, *Filtros Adaptativos*. [Online]. Available: https://openaccess.uoc.edu/bitstream/10609/77806/1/Proceso%20avanzado_M%C3%B3dulo%203_Filtros%20adaptativos.pdf

[16] R. Juan, M. Paula, R. Martin, C. Paola, A. Aldana, V. Luciano, G. Yanina, and S. Paola, "Desarrollo de un sistema de control de calidad para datos de radar." [Online]. Available: http://hdl.handle.net/20.500.12160/930

[17] S. Maximiliano, A. Aldana, M. Paula, R. Martin, R. Juan, and V. Luciano, "Sistema de control de calidad de datos de radar en el servicio meteorológico nacional - parte ii: Implementación operativa," Servicio Meteorológico Nacional Argentina, Tech. Rep. SMN 2021-87, Marzo 2021. [Online]. Available: https://www.researchgate.net/publication/352192490

[18] R. Federico, C. Roberto, V. Daniel, and B. Victor, "The argentinian meteorological radar rf interference filter performance evaluation," CONGREMET, Ed. [Online]. Available: https://www.researchgate.net/publication/343509977

[19] *Presentation on preliminary findings of JRC study regarding interference from 5 GHz WAS/RLANs to meteorological radars - update*, RSCOM. [Online]. Available: https://circabc.europa.eu/sd/a/0855adf3-7846-48fd-bf3b-fbfea3802818/RSCOM20-50rev2%20JRC%20study%20interference%20radars%205%20GHz.pdf

[20] *Aspectos técnicos y operacionales de los radares meteorológicos en tierra*, UIT-R. [Online]. Available: https://www.itu.int/dms_pubrec/itu-r/rec/m/R-REC-M.1849-2-201901-I!!PDF-S.pdf

RFI 2024

RFI Evaluation of the SKA Mobile Radio System

Jason Fynn [1] and Riaan Wolhuter [2]
[1] SA Radio Astronomy Organisation, Cape Town, South Africa, jfynn@sarao.ac.za
[2] Stellenbosch University, Stellenbosch, South Africa, wolhuter@sun.ac.za

1 Introduction

The Square Kilometre Array (SKA) astronomical telescope project is a major international scientific effort with the biggest components in Australia and South Africa. The South African High Frequency component will consist of 199 radio telescopes operating in a Very Long Baseline Interferometry (VLBI) array. The combined observational capabilities should enable understanding of the cosmos to completely new levels. To date, 73 telescopes have been constructed. The project is situated in a remote part of central South Africa selected for the low-density population and low RFI levels. The eventual footprint of the project will be 200 x 200 km and the telescope positions (red circles) are as per Figure 1. The use of any device possibly emitting RFI is restricted by the Karoo Central Astronomical Advantage Area Act (KCAAA), to protect the radio spectrum in the area. The observational band of the array stretches from 300 MHz to 25.5 GHz and excludes, the use of most radio frequency (RF) based devices in the area. However, a project of this scale requires inter-personnel communication for emergencies, general site operations and contractors during the construction period. Therefore, a wide area Mobile Radio Communication System (MRS) enabling these functions is being implemented. It should clearly not present an RFI threat, and this paper covers the processes followed to ensure such compliance. The MRS will provide coverage via 5 repeaters, situated as per the yellow icons in Figure 1 and with typical coverage radius of 70 - 80 km.

Figure 1: SKA Telescope- and MRS Repeater positions in South Africa

2 Telescope RFI Risk Threshold levels

The threshold limits applicable in the KCAA area are known as the South African Radio Astronomy Services (SARAS) Protection Levels, [1] and [2]. The SARAS levels are a direct implementation of ITU recommendation 769.2 (ITU-R RA769.2) [3] and define an interference level applicable to the SKA site. The SARAS threshold as well as a –100 dBm saturation level and a 10 dBm damage threshold as defined in [2] are used to enforce a radio quiet zone (RQZ). Any system deployed within the RQZ must comply with the applicable thresholds with respect to intentionally or non-intentionally radiated emissions. The cryocooled telescope LNA's have a -185 dBm sensitivity level over the observation bandwidth, from which the SARAS level is derived. This was also the value utilised in our analysis.

3 The Mobile Radio System (MRS) - Repeater Equipment

The MRS coverage is intended to span the entire telescope extent and the operational frequency band was chosen as 40 MHz, to ensure that the carrier is below the SKA observation band (OB) and to prevent any carrier harmonic intruding into the OB. Furthermore, apart from harmonics, any item of electronic equipment deployed on site must be EMI certified and each repeater rack complete with power supply, duplexer and backhaul data switch, was characterised in an anechoic chamber. The results are depicted in **Error! Reference source not found.**.

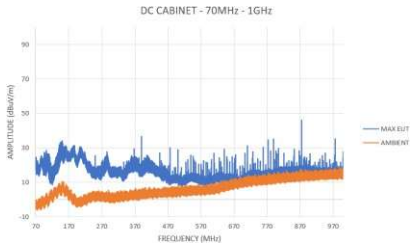

Figure 2: Repeater anechoic chamber EMI characteristic

The most potentially problematic repeater site is Jaskloof, due to its close proximity to some telescopes. Therefore, point to multipoint link (PTMP) calculations were carried out from Jaskloof to all telescopes, as shown in Figure 3.

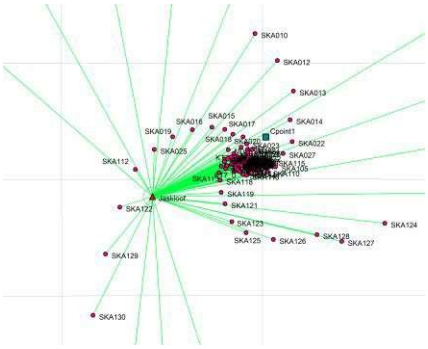

Figure 3: Jaskloof - Telescope PTMP EMI link calculations

4 Base Station Radios

A further possibility is possible EMI from the base station radios, as installed at different security check points around the site, of which one, CPoint1, is indicated on Figure 3. Similar PTMP link calculations as done for the Jaskloof Repeater, were carried out, ie. 269 in each case, using the Pathloss 5 calculation tool [4]. The condensed results from both these are presented in Table 1.

Table 1: Extract from RFI PTMP calculations

Site S1	Emission level (dBm)	Freq. (MHz)	Site S2	RSSL (dBm) S2	Free space loss (dB)	Diffraction loss	Net path loss (dB)	Path length (km)
Jaskloof	-50	870	SKA112	-165.34	108.94	9.65	115.34	7.66
Jaskloof	-50	870	SKA122	-186.66	109.54	30.36	136.66	8.2
Cpoint1	-60	600	SKA023	-171.34	101.7	12.93	111.34	4.825
Cpoint1	-60	600	SKA020	-172.87	102.69	13.46	112.87	5.409
Cpoint1	-60	600	SKA018	-174.27	105.95	11.59	114.27	7.866
Cpoint1	-60	600	SKA024	-174.36	102.58	15.05	114.36	5.34

5 Conclusion and Summary

The repeater EMI was measured at -50 dBm at 870 MHz, worst case, while the Base Station radios were similarly found to radiate -60 dBm at 600 Mhz. In the repeater case, the only two telescopes with RSSL above the sensitivity floor, were SKA112 & 122 respectively, both at close distance and consequent small path losses, as per Table 1. It was decided to shield the entire repeater in a 60 dB attenuating cabinet. A larger no. of telescopes is affected by the base station radio EMI, but not by much, ie. typically 5 – 14 dB over the -185 dBm limit. Complete shielding is not practical in this case and further measurements will be taken in an in situ installed situation. It is possible that the aluminium skin of the security hut wall material could well provide the additional attenuation required. The RFI receive levels were individually calculated for all telescopes and from all repeaters and base stations. The repeater at Limietkop was also found to present a threat to a single telescope, ie. SKA026 and had to be shielded. The equipment is manufactured commercially and the EMI is well within international specifications, but a telescope LNA at 10K is another matter and all risks have to be quantified and mitigated, if necessary.

6 References

[1] Government Gazette, "Regulations on Radio Astronomy Protection Levels in Astronomy Advantage Areas declared for the Purpose of Radio Astronomy," 2012.

[2] A. Otto, J. Jonas and F. Di Vruno, "Applying Telescope Protection Levels to Measurement Data," 2021.

[3] ITU Radiocommunication Assembly, "ITU-R RA.769-2 Protection criteria used for radio astronomical measurements," 2003.

[4] *Pathloss5*© Propagation planning software, **Contract Telecommunication Engineering Ltd.** Delta, British Columbia, Canada. www.pathloss.com

[5] R. Wolhuter, A. Otto, C. Van der Merwe, J. Fynn, J. Havenga, "A Band Comparison Investigation for RFI Emission Mitigation by a Mobile Radio Communications Network for the SKA Radio Astronomy Project" (RFI 2019, 23-26, Sept. 2019, Toulouse, France.

[6] R Wolhuter, J Fynn, "A Non-Interfering Radio Communication System for the SKA Astronomy Project" (Contel 2023, July 6-8, Graz, Austria).

[7] A. Otto, R. Wolhuter, J. Fynn, J. Havenga "Radio Frequency Interference from an Operational Communications Network in a Radio Astronomy Environment" (RFI 2019, 23-26 Sept. 2019, Toulouse, France).

RFI and SMAP: Results and Trends in Almost 10 years of L-band RFI Observations

Paolo de Matthaeis, Priscilla Mohammed, Alexandra Bringer and David Le Vine
NASA Goddard Space Flight Center, Greenbelt, MD, USA

The NASA Soil Moisture Active and Passive (SMAP) mission, launched at the beginning of 2015, is providing global measurements of brightness temperature for the estimation of soil moisture, freeze/thaw state and sea surface salinity. The SMAP radiometer operates within the protected Earth Exploration Satellite Service passive - EESSS (passive) frequency allocation at 1400-1427 MHz. However, unwanted signals, in the form of illegal in-band transmissions and out-of-band emissions from transmitters operating at frequencies adjacent to this allocated spectrum has been a source of radio-frequency interference (RFI) in this band. For this reason, the SMAP radiometer included what probably still is the most advanced signal processing system for the detection and filtering of RFI [1].

Since the beginning of the mission, the SMAP RFI Team has focused on improving the performance of the interference detection and filtering, documenting the occurrence of RFI, locating its source and reporting to the authorities. The lifetime of the SMAP radiometer is approaching 10 years, and the amount of data collected, along with the different characteristics of the interference signals, has allowed research on RFI trends. One example is provided in Figure 1, which shows the evolution of the global number of RFI sources observed by SMAP over the duration of the mission.

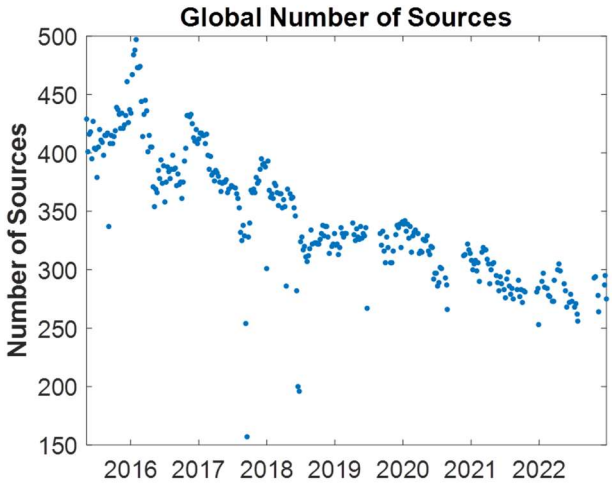

Figure 1. Evolution of the global number of RFI sources observed by the SMAP radiometer.

Analyses show a slow decreasing trend of the number of strong sources indicating an improvement in the RFI environment. The results also indicate seasonal variations which are particularly noticeable over China.

Results of the work of the SMAP RFI Team during these past years will be summarized and an update on trends originally reported in [2] will be presented.

References

[1] J.R. Piepmeier et al., “Radio-frequency interference mitigation for the Soil Moisture Active Passive microwave radiometer,” *EEE Transactions on Geoscience and Remote Sensing*, vol. 42, no. 1, pp. 761–775, Jan. 2014.

[2] A. Bringer *et al*., "Properties of the RFI Environment at 1400–1427 MHz as Observed by the Soil Moisture Active/Passive Mission Microwave Radiometer," in *IEEE Journal of Selected Topics in Applied Earth Observations and Remote Sensing*, vol. 14, pp. 7259-7267, June 2021.

Passive Remote Sensing of Sea Surface Temperature: Opportunities and Threats at the World Radiocommunication Conference 2027

Paolo de Matthaeis[1,2,3], Beau Backus[1,4], Raúl Díez-García[1,5] and Mingliang Tao[1,6]
[1] IEEE Geoscience and Remote Sensing Society
[2] NASA Goddard Space Flight Center, USA
[3] University of Maryland, Baltimore County, USA
[4] Johns Hopkins Applied Physics Lab, USA
[5] Telespazio UK Ltd., Luton, UK
[6] Northwestern Polytechnical University, Xi'an, China

1. Introduction

A World Radiocommunication Conference (WRC) is organized by the International Telecommunication Union (ITU) every four years to revise and update the Radio Regulations (RR), which determine the use of the radio frequency spectrum by radio services. The next World Radiocommunication Conference, WRC-27,will be held at the end of 2027 (WRC-27). The WRC-27 agenda contains several topics of relevance to microwave remote sensing, called Earth Exploration Satellite Service (EESS) in ITU terminology. This presentation will specifically address one of them.

2. Agenda Items relevant to passive remote sensing at C-band

At the World Radiocommunication Conference 2023 (WRC-23), frequency bands with the range 6425-7125 MHz were identified for use by the terrestrial component of International Mobile Telecommunications (IMT), with some small differences by ITU Region [1].

Microwave radiometers have been using these frequencies for many years, however they do so without an EESS allocation and they are only recognized by **RR Footnote 5.458**. Their measurements are essential for estimating global sea surface temperature (SST) and used in combination with other frequencies for other applications such as measuring soil moisture, temperature of the ocean surface and sea surface wind through clouds. 6425-7250 MHz is a unique frequency range for SST observations, since it corresponds to the peak sensitivity to this geophysical parameter.

IMT deployment following this WRC-23 decision is expected to greatly increase the level of interference received by these instruments. Recognizing the importance of these measurements, an agreement was reached at WRC-23 to establish **Agenda Item 1.19** for WRC-27 to seek new allocations in the 4200-4400 MHz and 8400-8500 MHz bands to complement the measurements with the range 6425-7125 MHz [2]. These agenda item falls under the responsibility of the Working Party (WP) 7C, which oversees all activities related to remote sensing systems within the Study Groups of the International Telecommunication Union – Radiocommunication Sector (ITU-R).

However, a threat to both potential new allocations and existing operations of microwave radiometers for SST observations comes from another WRC-27 agenda item. **Agenda Item 1.7** is encouraging development of technical conditions for the use of International Mobile Telecommunications (IMT) in the frequency bands 4400-4800 MHz, 7125-8400 MHz and 14.8-15.35 GHz. ITU-R WP 7C is a Contributing Group for this agenda item.

2. Discussion

Opportunities and threats to passive remote sensing measurements of SST by WRC-27 Agenda Item 1.19 and Agenda Item 1.7 will examined and discussed in this presentation. In particular, the focus will be on the impact, positive or negative, on the remote sensing community and on the challenges from the point of view of remote sensing scientists and engineers.

References

[1] Resolution 220 (WRC-23) in *ITU World Radiocommunication Conference 2023: Final Acts*, Geneva, 2024. https://www.itu.int/dms_pub/itu-r/opb/act/R-ACT-WRC.16-2024-PDF-E.pdf

[2] *Results of the first session of the Conference Preparatory Meeting for WRC-27 (CPM27-1)*, ITU Radiocommunication Bureau (BR) Administrative Circular CA/270, Geneva, 26 January 2024, Resolution 813, p. 668.

The RFI filter of the Argentinian Meteorological Radar: Data quality recovery analysis after real-time automatic filtering

Federico P. Renolfi* [(1)], Daniel Vela Diaz[(1)], Victor A. Bravo[(1)], Roberto Costantini[(1)]
[(1)] INVAP S.E., Bariloche, Argentina
* frenolfi@invap.com.ar

1. Introduction

Most C-band weather radars operate in the same frequency band (5600~5650 MHz) [1] as many RF Local Area Networks (LAN), such as IEEE 802.11-based [2] Radio LANs and Wireless LANs; therefore a considerable amount of radars are threatened by RFI contamination [3, 4]. Unfortunately, Argentina's weather radar network (SINARAME: Sistema Nacional de Radares Meteorológicos) is no exception.

Keeping the band used by weather radars free requires the government to discover, locate, and control the sources of interference. The constant expansion of wireless networks and the enormous effort necessary to control them means that, in practice, it is impossible to eradicate all sources of interference.

Therefore, to alleviate this situation, a digital RFI filter capable of operating in real time was developed for the Argentine Meteorological Radar (RMA).

This research is a continuation of previous works [5, 6, 7] with the aim of comparing data quality before and after applying the RFI filter.

2. Methodology

Two different types of data were used (I/Q time series). The first set, see Figure 1, includes regions with clear air and meteorological data recorded at a virtually interference-free RMA site. The second set, see Figure 2, contains only interference and system background noise, recorded by configuring the RMA radar in receive-only mode at a site heavily contaminated by RFI.

Both sets were combined mathematically, see Figure 3, thus generating a new artificial set of actual meteorological data contaminated with real-world RFI signals.

By filtering the artificially contaminated dataset and comparing the results with the original (RFI-free) dataset, it is possible to evaluate data quality loss due to contamination and quality improvement due to filtering.

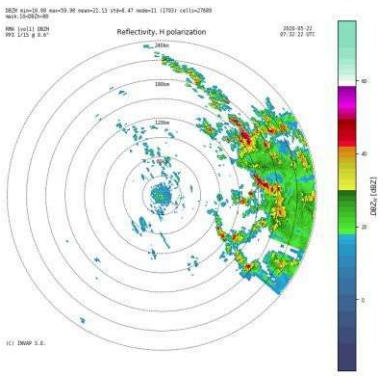

Figure 1. Weather data (RFI-free).

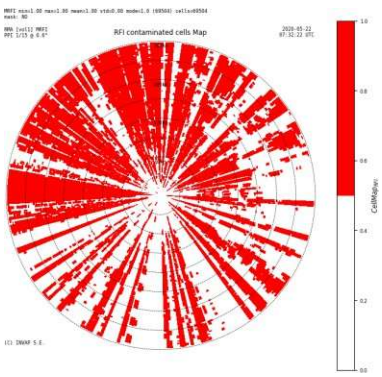

Figure 2. Real world RFI data

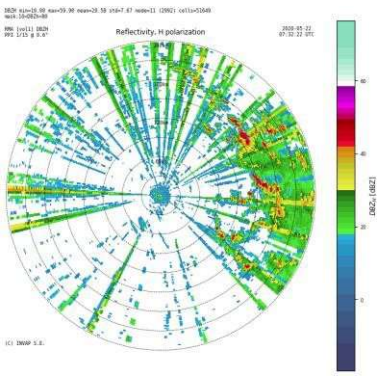

Figure 3. Weather data contaminated with RFI

3. Results

The results of this research, which will be presented in the extended summary, will show a comparison of data quality before and after applying the RFI filter.

4. Remarks and Conclusions

After the activation of RFI filtering in all RMA radars of the SINARAME network by the end of 2023, qualitatively an improvement can already be observed in the radar data shown on the web portal of the National Weather Service of Argentina.

The level of RFI contamination was significantly reduced in every site, while weather echoes stayed mostly unaffected.

This research supplements the previous works [5, 6, 7] on the RFI filter of the RMA radar signal processor.

5. Acknowledgments

This work is part of a joint project to improve the overall quality of the SINARAME data and has been executed by INVAP S.E. in close collaboration with the following institutions:

- Sub-secretaría de Recursos Hídricos, the institution that manages and provides funds for the SINARAME project.
- Servicio Meteorológico Nacional de Argentina, the National Weather Service and principal user of the radar's data.
- Facultad de Matemática, Astronomía, Física y Computación from Universidad Nacional de Córdoba.

The following open source projects/tools/libraries were used in this work:

- Van Rossum, G., & Drake Jr, F. L. (1995). "Python reference manual". Centrum voor Wiskunde en Informatica Amsterdam.
- Harris, C.R., Millman, K.J., van der Walt, S.J. et al. (2020). "Array programming with NumPy". Nature 585, 357–362. DOI: 10.1038/s41586-020-2649-2.
- J. D. Hunter (2007). "Matplotlib: A 2D Graphics Environment", Computing in Science & Engineering, vol. 9, no. 3, pp. 90-95. DOI: 10.1109/MCSE.2007.55

6. References

[1] IEEE Standard 802.11. Wireless LAN Medium Access Control (MAC) and Physical Layer (PHY) Specifications (2016)

[2] EUMETNET. Recommendation on C-Band Meteorological radars design to ensure global and long-term coexistence with 5 GHz RLAN. Available online: https://www.eumetnet.eu/wp-content/uploads/2017/01/OPERA_2008_12_Recommendation_RLAN.pdf

[3] Tristant, Philipe. "RLAN 5 GHz interference to weather radars in Europe." In ITU/WMO Seminar on Use of Radio Spectrum for Meteorology: Weather, Water and Climate Monitoring and Prediction; WMO/OMM: Genevea, Switzerland, Sep 2009.

[4] Saltikoff, Elena, John Y. N. Cho, Philippe Tristant, Asko Huuskonen, Lynn Allmon, Russell Cook, Erik Becker, and Paul Joe. "The Threat to Weather Radars by Wireless Technology", Bulletin of the American Meteorological Society 97, Jul. 2016. doi: 10.1175/BAMS-D-15-00048.1

[5] F. Renolfi, D. Vela Diaz, V. Bravo and R. Costantini, "Performance analysis of the Argentinian Meteorological Radar Radio Frequency Interference filter", presented at the 11th European Conference on Radar in Meteorology and Hydrology (ERAD 2022), Locarno, Switzerland, Sep. 2022. doi: 10.5281/zenodo.8381417.

[6] F. Renolfi, D. Vela Diaz, V. Bravo and R. Costantini, "The Argentinian Meteorological radar RF interference Filter Performance evaluation", presented at the 14th Argentine Congress on Meteorology (CONGREMET XIV), Buenos Aires, Argentina, Nov. 09, 2022. doi: 10.5281/zenodo.8381448.

[7] F. P. Renolfi, R. Costantini, D. Vela Diaz and V. Bravo, "The Argentinian Meteorological Radar, real time RFI digital filter operational data quality impact analysis", presented at the Fourth Calibration and Monitoring Workshop (WXRCalMon 2023), Met Office, Exeter, UK, Nov. 2023. doi: 10.5281/zenodo.12761083.

Prediction of radio frequency occupancy at Inyarrimanha Ilgari Bundara, CSIRO's Murchison Radio-astronomy Observatory

Mohamed Manoufali
Commonwealth Industrial Research Organisation (CSIRO), Perth, Australia, mohamed.manoufali@csiro.au

1. Introduction

The Australian Radio Quiet Zone Western Australia (ARQZWA) was established in the Mid-West region in Australia to host radio telescopes with strict power spectral density (PSD) threshold to protect sensitive telescopes from radio frequency interference (RFI). ARQZWA currently hosts three operational telescopes, along with ongoing constructions of SKA-L telescopes, the largest radio telescope project ever undertaken in the history of radio astronomy. The RFI is detected through a dedicated RFI monitor across 20 to 3000 MHz at the Observatory [1]. The monitor consists of two receiver chains, one is configured for faster scanning, whilst the other one is tailored towards detecting low level signals with a slower scanning rate. There are different data products from the RFI monitor, mainly the raw received signal levels, spectrum occupancy, normalized spectrum and charts for each receiver chain.

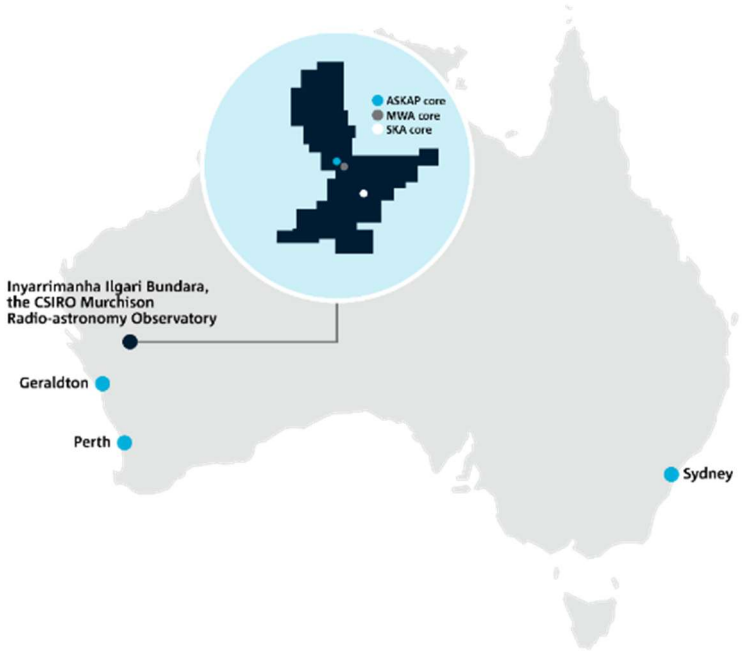

Figure 1. The location of the ARQZWA of Inyarrimanha Ilgari Bundara, CSIRO's Murchison Radio-astronomy Observatory in the Mid-West region of Australia

2. Problem Statement

The occupancy data for the sensitive RFI receiver chain is calculated by taking the average of the received signal across one day and if it's more than two standard deviations, which is known as the threshold, then the frequency is considered occupied. The occupancy data is archived from April 2019 till present. The Australian SKA Pathfinder (ASKAP) is one of the three operational telescope that operates between 700 to 1800 MHz. Despite the site being considered as one of the most prominent radio quiet sites on the globe, it suffers from atmospheric ducting that acts as waveguide to enable rf signals, especially, cellular network onsite, which is not case during normal conditions. The spectrum occupancy (SO) of each frequency channel is calculated using the following equation [2]

$$SO = \frac{No}{N} \times 100\% \quad (1).$$

Where: *No* is the number of samples taken through a certain time on any channel above threshold and *N* is the total number of samples taken through a certain time.

2. Proposed Solution

A lot of science observations have been subjected to strong ducting, which affects the data quality of observation [3],[4]. The observation schedule of ASKAP telescope is automated and would benefit from predicting spectrum occupancy as indicator for ducting of cellular signals to alert science teams about ducting likelihood. Hence, in this work, we explore using machine learning models to predict spectrum occupancy using the recorded data from the sensitive RFI monitor to build a decision-based criteria for scheduling. Different artificial models will be utilized for time-series prediction starting with random forest model. The preliminary results suggest that the model can achieve low mean absolute error for predicting spectrum occupancy, which will be used to build the criteria for indicating ducting events onsite.

[1] C. Wilson *et al.,* "The Australia Radio Quiet Zone – Western Australia: objectives, implementation and early measurements", Radio Frequency Interference Conference, October 2016 pp 922-923.

[2] ITU, "Spectrum Occupancy Measurements and Evaluation," *Reports ITU-R SM. 2256-1*, August 2016, Accessed on Spectrum occupancy measurements and evaluation (itu.int)

[3] B. Indermuehle *et al.*, "The ASKAP RFI environment as seen through BETA," Radio Frequency Interference Conference, October 2016 pp 43-48.

[4] L. Lourenco *et al.,* "Survey and Monitoring of ASKAP's RFI Environment and Trends I: Flagging Statistcs", *Publications of the Astronomical Society of Australia,* 2023. pp 1-14.